THE ASTROPHYSICAL JOURNAL SUPPLEMENT SERIES, 62:109–145, 1986 September

COMPREHENSIVE MODELS OF DIFFUSE INTERSTELLAR CLOUDS: PHYSICAL CONDITIONS AND MOLECULAR ABUNDANCES

EWINE F. VAN DISHOECK[1]
Sterrewacht Leiden and Harvard-Smithsonian Center for Astrophysics
AND
JOHN H. BLACK
Steward Observatory, Tucson
Received 1985 October 17; accepted 1986 February 26

ABSTRACT

Comprehensive models are constructed which reproduce a wide variety of observations for the principal interstellar clouds in front of the stars ζ Per, ζ Oph, χ Oph, and o Per. The models describe accurately the fractions of atomic and molecular hydrogen as functions of depth into the clouds by a simultaneous treatment of the formation of H_2 on grains, its excitation by ultraviolet pumping and inelastic and reactive collisions, and its destruction by photodissociation. The main improvements over previous models are twofold. First, a corrected description of radiative transfer in the H_2 lines is used; second, the clouds are in hydrostatic equilibrium and have continuous gradients of temperature and density. The thermal balance is not solved explicitly; rather, the gas is taken to satisfy a polytropic equation of state, and the estimated heating and cooling rates are checked for approximate consistency. Previous models of the clouds in front of the stars ζ Oph and ζ Per, which underestimated the shielding in the H_2 lines by an order of magnitude, are shown to be inconsistent with observations. The new models of these clouds are designed to reproduce the observed H/H_2 column density ratio and the rotational populations of H_2. The extents of the warm zone and of the H–H_2 transition region are reduced in the new models. Compared with earlier models, the new models generally have lower central densities and more intense ultraviolet radiation fields. The central density in the models is uncertain by a factor of 2 owing to uncertainties in the formation processes of H_2 on grains and the turbulence in the clouds. The strength of the interstellar ultraviolet radiation field is also not well determined, because of uncertainties in the grain scattering properties and the population distribution of H_2 upon formation. The central temperature is better constrained in the models. The temperature and density in the outer parts of the clouds may have been overestimated. The physical parameters have been compared with those inferred from the C_2 and CO rotational excitation and the atomic fine-structure excitation. For the ζ Per and χ Oph clouds, good agreement is found between the various diagnostics. For the ζ Oph and o Per clouds, the C_2 and CO excitations indicate lower central densities than the H/H_2 abundance ratio. Several possible explanations for this discrepancy, including the possibility of a shocked region along the line of sight, are discussed. The models incorporate a large chemical network describing the abundances of about 100 molecules containing H, C, O, N and Cl atoms and their isotopes. As a result of the more intense ultraviolet radiation, improved photodissociation rates, and the smaller warm zone, the abundances of oxygen-bearing molecules are significantly reduced in the new models. Calculations of the OH abundance suggest that a modest increase in the cosmic-ray ionization rate to $\zeta_0 \approx 7\times10^{-17}$ s^{-1} is needed to bring the models into harmony with observations, provided that the H_3^+ dissociative recombination rate is very low at interstellar temperatures. The abundance of the HD molecule is consistent for all four clouds with a deuterium abundance of $(1.5\pm0.5)\times10^{-5}$. The observed abundances of other simple molecules such as CH, C_2, and HCl can be reproduced by reasonable ad hoc adjustments in the molecular reaction rates, although the uncertainties in the rates do not permit the use of these abundances as constraints on the physical conditions. The abundance determination of CO is complicated by the fact that its photodissociation processes through line absorption are still not well known. With the current best estimate of the CO photodissociation rate, the models produce too little CO by factors of 2–10. The reactions leading to the formation of the nitrogen-bearing molecules are still very uncertain, and it is difficult to satisfy the observational constraints on both the NH and CN abundances. Some critical observational tests of the models are suggested.

Subject headings: interstellar: abundances — interstellar: matter — interstellar: molecules — molecular processes

[1]Junior Fellow, Harvard Society of Fellows.

I. INTRODUCTION

The elucidation of the internal structure and composition of diffuse interstellar clouds is an important step toward a better understanding of the interstellar medium in our Galaxy.

The directly observable properties of a diffuse cloud are line intensities and profiles, and they are related to atomic and molecular concentrations by integration over the extent of the cloud. In many cases, these concentrations are expected to vary significantly with depth; consequently, observations can be interpreted properly in terms of local physical conditions and internal cloud structures only through the use of theoretical models which include the depth-dependent structure and reproduce or predict *observable* properties.

Although high-resolution absorption-line observations toward bright background stars have been available for some time, the structure of the diffuse interstellar clouds they probe still remains elusive. The recent expansion of interstellar absorption-line measurements and of our knowledge of certain microscopic processes, as well as prospects for further observational advances in the ultraviolet (through the use of Space Telescope) and infrared, justify a new discussion of diffuse cloud models. In this study, procedures for constructing comprehensive models of diffuse clouds are discussed and their inherent limitations are evaluated. The goals of such an investigation are, first, to reproduce the widest variety of observational data in a way that reveals useful information about densities, temperatures, abundances, and microscopic processes, and, second, to predict further observable properties that can be used to test and refine the theory. Finally, atoms and molecules in diffuse clouds can be used as remote sensors of important parameters such as the Galactic cosmic-ray ionization rate and the brightness temperature of the cosmic background radiation near its peak wavelength.

In general, a steady state cloud model should consist of a specification of the pressure, temperature, and density of the gas, the intensity of the interstellar radiation field, and the abundances of the atoms, ions, and molecules as functions of position in the cloud, such that the equations of hydrostatic equilibrium, thermal balance, radiative transfer, and chemical steady state are satisfied. Most studies have focused only on specific aspects of a complete model. Many people have tried to predict the abundances of interstellar molecules through complicated networks of chemical reactions (e.g., Solomon and Klemperer 1972; Herbst and Klemperer 1973; Iglesias 1977; Mitchell, Ginsburg, and Kuntz 1978; Prasad and Huntress 1980; Henning 1981; Graedel, Langer, and Frerking 1982; Watt 1983; Millar and Freeman 1984*a*, *b*). Such studies have typically ignored either the effects of dissociating and ionizing ultraviolet photons or the depth dependences of the molecular concentrations. Although these models may be appropriate for the description of the chemistry in the cores of dense clouds, they are less valid for diffuse clouds with total visual extinctions $A_V^{\rm tot} \leq 2$ mag. Detailed chemical steady state models, including radiative processes and integration over depth scale, but neglecting the thermal and pressure equilibria, have been constructed by Black and Dalgarno (1973*a*, *b*; 1977, hereafter BD) and Black, Hartquist, and Dalgarno (1978, hereafter BHD) for diffuse clouds, and, with a less extensive chemistry, by Viala and Walmsley (1976) for denser clouds. Other workers (Glassgold and Langer 1974, 1976; Barsuhn and Walmsley 1977; Clavel, Viala, and Bel 1978; Federman and Glassgold 1980) have studied in detail the thermal balance in isobaric or uniform density models, based on a limited description of the chemistry and an approximate treatment of the radiative transfer in line and continuum. Recently, Mann and Williams (1985) have considered the chemistry in models which take the thermal balance into account. Federman, Glassgold, and Kwan (1979) treated accurately the radiative transfer, but did not consider the chemistry, heating, and cooling in the clouds. Hydrostatic models, which are in thermal balance and are supported by turbulent pressure, and which include a detailed chemistry with the radiative transfer solved approximately, have been constructed by de Jong (1980), de Jong, Dalgarno, and Boland (1980), and Boland and de Jong (1984). These last models have been applied mainly to denser molecular clouds with $A_V^{\rm tot} \approx 16$ mag. Tielens and Hollenbach (1985*a*, *b*) have similarly treated the structure of the outer parts of molecular clouds subjected to intense radiation. Roberge (1981) has developed methods for calculating models which are in hydrostatic, thermal, and chemical equilibrium, and which incorporate a full numerical treatment of the radiative transfer, but has considered only limited applications to diffuse clouds.

Most of the studies mentioned above deal with general trends in the observations, while only a few have attempted to reproduce a wide variety of observed features in specific clouds. It is our opinion that comprehensive models of individual clouds are of great value and that successful interpretation of individual clouds is a prerequisite for any trust in general models. Even if the resulting models are not unique, it is important to investigate whether the whole array of observed features for a particular cloud *can* be reproduced in *one* model.

The first step in modeling a *specific* interstellar cloud is to constrain the basic physical parameters by observations of species with great diagnostic value. The abundance and rotational excitation of the H_2 molecule are related to the temperature, density, and strength of the interstellar radiation field (Spitzer and Jenkins 1975; Black and Dalgarno 1973*a*; BD; Jura 1975). The abundance of the molecule is determined by the balance between its formation, which is thought to take place on grains (van de Hulst 1949; Hollenbach and Salpeter 1970, 1971, and references therein), and its destruction by photodissociation through discrete absorptions in the Lyman and Werner systems (Solomon 1965, cited in Field, Somerville, and Dressler 1966; Stecher and Williams 1967; Nishimura and Takayanagi 1969; Dalgarno and Stephens 1970; Hollenbach, Werner, and Salpeter 1971). Since the destruction rate is sensitive to the rotational level population distribution of H_2, the excitation of the molecule needs to be treated simultaneously. Important excitation mechanisms include ultraviolet pumping (again through absorptions in the Lyman and Werner systems) followed by infrared cascade, the formation process, inelastic collisions with H and H_2, and reactive collisions with protons (Spitzer and Cochran 1973; Spitzer and Zweibel 1974; Black and Dalgarno 1973*a*, 1976; Jura 1975).

Because both the abundance and the excitation of H_2 are determined largely by the absorption rate in the Lyman and Werner systems, an accurate treatment of the self-shielding in these lines is very important. Although the BD and BHD models accounted for these processes in detail and were quite successful in reproducing the observations, it has since been shown (Federman, Glassgold, and Kwan 1979) that the description of radiative transfer in these models is incorrect, resulting in an underestimate of the shielding by up to an order of magnitude at the cloud center. We discuss here in detail the adjustments in derived parameters necessary to bring theory into harmony with the observations when a corrected description of the radiative transfer in the H_2 lines is used. Roberge (1981) has previously shown this to some extent for the BD model of the cloud toward ζ Oph.

The physical parameters may also be inferred from observations of other species. In particular, the rotational excitation of the C_2 molecule is sensitive to the density and temperature in the cloud as well (Chaffee *et al.* 1980; van Dishoeck and Black 1982), and accurate absorption-line observations of C_2 for various lines of sight have recently become available (Hobbs 1981; Chaffee *et al.* 1980; Danks and Lambert 1983; van Dishoeck and de Zeeuw 1984). A model cloud structure that closely reproduces the observed distributions of H_2 and C_2 should also account for the populations of atomic ground-state fine-structure levels in C, C^+, and O and for the rotational excitation of CO. The various diagnostic probes, however, have often given conflicting results. In the extreme example of the ζ Oph cloud, temperatures between 20 and 110 K and hydrogen densities between 200 and 2500 cm^{-3} have been inferred (BD; Crutcher and Watson 1981). As long as such uncertainties exist in the physical parameters, predicted abundances of other species that are sensitive to density and temperature cannot be tested with confidence. The primary goal of this study is therefore to constrain the physical conditions as well as possible, and to resolve the discrepancies resulting from the different diagnostic probes. Once the basic physical structure of a cloud is established, the atomic ionization equilibria and the abundances of simple molecules can be calculated for comparison with observations. The second goal of this study is to understand the chemistry well enough to predict correctly the abundances of several simple molecules, including HD, CO, CH, C_2, CN, and OH, for the same models that reproduce the data on the abundance and excitation of H_2.

The models described here assume that diffuse clouds are stable structures in chemical steady state and in hydrostatic equilibrium. The internal structures are calculated and are presented together with an extensive description of molecular abundance and excitation in an internally consistent manner. Observable properties are calculated for comparison with observations, and, where necessary, the available observational data are critically reviewed. These models fall short of complete self-consistency only in that the temperature-density relations are determined by empirical fitting of diagnostic observations rather than by an explicit treatment of the balance of heating and cooling rates.

Nature is manifestly more complex than the theoretical models described here. The principal goal of this work is to explore the limitations of steady state models of interstellar clouds by comparison with the most extensive sets of observational data.

In the following sections the construction of hydrostatic, barytropic models is discussed (§ II); and the problem of the abundance and excitation of H_2 is reiterated, indicating the differences with the BD and BHD models (§ III); and the excitation of other diagnostic species is outlined (§ IV), before the results of the calculations for several lines of sight are presented (§ V). Details of the chemical network are summarized in § VI, and the abundances of the species are discussed in § VII.

II. CLOUD STRUCTURE

The cloud is assumed to have a plane-parallel geometry. For diffuse clouds this may often be a realistic assumption, since the thickness of the cloud, as suggested by ultraviolet absorption-line studies (Spitzer and Jenkins 1975), is usually much smaller than the lateral extent determined by radio observations (e.g., Sancisi *et al.* 1974).

The gas is assumed to be barytropic, i.e., the pressure is assumed to be a function of density only, and to have a polytropic equation of state

$$P/k \propto \rho^{(\Gamma+1)/\Gamma} \text{ cm}^{-3} \text{ K}, \tag{1}$$

where P is the pressure, k is Boltzmann's constant, ρ is the mass density, and Γ is the polytropic index, which will be a free parameter. Although the assumption that the interstellar clouds are barytropic may not be valid, calculations of the equations of state by solving the thermal balance (Shu *et al.* 1972; de Jong, Dalgarno, and Boland 1980) indicate that the polytropic models are reasonable approximations for a range of negative values of Γ. The properties of negative-index polytropes were first considered by Viala (1972) and Shu *et al.* (1972).

For any given value of Γ, the pressure P and density ρ must satisfy the equation of hydrostatic equilibrium

$$\frac{dP}{dz} = \rho \frac{d\phi}{dz}, \tag{2}$$

where ϕ is the gravitational potential obeying Poisson's equation,

$$\frac{d^2\phi}{dz^2} = -4\pi G\rho, \tag{3}$$

with G the gravitational constant and z the linear distance (in centimeters) into the cloud.

For any plane-symmetric geometry, equations (2) and (3) can be solved readily (Spitzer 1942; Harrison and Lake 1972), and they have a particularly simple analytic form when column density,

$$\mu_z = 2\int_0^z \rho \, dz \text{ g cm}^{-2}, \tag{4}$$

rather than z is used as the depth scale. The total column

density is finite and is equal to

$$\mu_{\rm tot} = 2\int_0^\infty \rho\, dz = (2P_0/\pi G)^{1/2}, \quad (5)$$

where the subscript zero refers to the value at the center of the cloud at $z = 0$. Following de Jong, Dalgarno, and Boland (1980), the pressure P_z in terms of the depth variable μ_z can be written

$$P_z/P_0 = 1-(\mu_z/\mu_{\rm tot})^2. \quad (6)$$

The cloud is taken to be bounded at $z = z_1$ by some external pressure P_1, which limits its total size to

$$\mu_1 = \mu_{\rm tot}(1-P_1/P_0)^{1/2}. \quad (7)$$

Thus the clouds are not fully self-gravitating. This outer boundary condition can also be written in terms of a visual extinction in magnitudes which is assumed to be related by (Savage *et al.* 1977)

$$A_V^{\rm tot} = \mu_1/(1.59\times10^{21}\bar{m}) = 289.6\mu_1, \quad (8)$$

where $\mu_1/\bar{m}$ is the total column density of hydrogen nuclei in the cloud and $\bar{m}$ is the average mass of the nuclei, including He.

The pressure at each position in the cloud has contributions from thermal gas pressure as well as from turbulence

$$P/k = \sum_i n_i T + (\delta v)^2\rho/2k \text{ cm}^{-3}\text{ K}, \quad (9)$$

where $\delta v = 10^5 b$ is the Gaussian velocity dispersion in cm s^{-1}, which may be chosen to be the same as the dispersion b in km s^{-1} characterizing the observed line widths. The contributions of radiation pressure and magnetic pressure are generally much smaller for the clouds considered in this work, and have been neglected. The summation in equation (9) is over the constituents of the gas with densities n_i in cm^{-3}, which are mainly H, H_2, and He. If $n_{\rm H} \equiv n({\rm H}) + 2n(H_2)$, $f \equiv 2n(H_2)/n_{\rm H}$, and $n({\rm He}) = 0.075 n_{\rm H}$, then

$$\sum_i n_i T = (1.075-0.5f)\, n_{\rm H} T, \quad (10)$$

so that

$$P/k = \left[(1.075-0.5f)\,T + 78.662b^2\right] n_{\rm H}. \quad (11)$$

At the outer boundary, $f_1 \approx 0$.

The density and temperature at each depth step are found from

$$(n_{\rm H})_z/(n_{\rm H})_0 = \rho_z/\rho_0 = (P_z/P_0)^{\Gamma/(\Gamma+1)}, \quad (12)$$

$$T_z = \left[P_z/(n_{\rm H})_z k - 78.662b^2\right]/(1.075-0.5f_z). \quad (13)$$

TABLE 1

OUTER BOUNDARY VALUES OF THE TEMPERATURE T_1 (K) AND DENSITY $(n_{\rm H})_1$ (cm^{-3}) FOR VARIOUS CLOUD MODELS[a]

A. $b = 3.0$ km s^{-1}, $A_V^{\rm tot} = 1.0$

			$\Gamma = -1.10$		$\Gamma = -1.25$		$\Gamma = -1.50$	
$(n_{\rm H})_0$	T_0	P_1/P_0	$(n_{\rm H})_1$	T_1	$(n_{\rm H})_1$	T_1	$(n_{\rm H})_1$	T_1
100...	20	0.87	23	1911	51	488	67	217
	50	0.88	24	1885	52	500	68	232
250...	20	0.95	142	463	193	164	214	84
	50	0.95	144	476	194	180	215	99
500...	20	0.98	378	205	440	83	464	51
1000...	20	0.99	870	101	939	46	963	28

B. $b = 1.0$ km s^{-1}, $A_V^{\rm tot} = 1.0$

			$\Gamma = -1.30$		$\Gamma = -1.50$		$\Gamma = -2.00$	
$(n_{\rm H})_0$	T_0	P_1/P_0	$(n_{\rm H})_1$	T_1	$(n_{\rm H})_1$	T_1	$(n_{\rm H})_1$	T_1
250...	20	0.60	27	392	54	161	90	67
	50	0.66	42	320	73	154	110	78
500...	20	0.80	189	104	255	58	319	32
	50	0.83	225	112	287	71	346	47
1000...	20	0.90	632	46	728	31	809	20

[a] Obtained from eqs. (5)–(13) assuming $f_1 = 0$ and $f_0 = 1$.

Since $T_0 \le T_1$, this implies that $\Gamma < -1$ (Viala and Horedt 1974*a*, *b*).

A model is specified by values of b and Γ, together with the values of $(n_{\rm H})_0$ and T_0 at the center. Table 1 illustrates some typical outer boundary values P_1, $(n_{\rm H})_1$, and T_1 for given b, Γ, $(n_{\rm H})_0$, T_0, and $A_V^{\rm tot}$ obtained assuming $f_1 \approx 0$ and $f_0 \approx 1$ as a first approximation. In practice, the model is computed on a depth scale of H_2 column density from the outer boundary inward, with the total column density of H_2 fixed, and P_0 and $A_V^{\rm tot}$ are computed results. Moreover, f_z depends on the density, temperature, and chemistry at each position in the cloud. Equations (6), (12), and (13) therefore need to be solved iteratively. Since the models are assumed to be symmetric, they are computed from one boundary to the center, and the resulting column densities are doubled at the end of the calculation.

III. ABUNDANCE AND EXCITATION OF H_2

a) Formation and Destruction Processes of H_2

The H_2 molecule is assumed to be formed on the surfaces of the grains in the interstellar clouds at a rate

$$k^f = 3\times10^{-18} T^{1/2} n_{\rm H} n({\rm H})\, y_f \text{ cm}^{-3}\text{ s}^{-1}, \quad (14)$$

where the constant incorporates the mean size and the relative abundance of the grains, and y_f is a scaling factor that incorporates the sticking probability and formation efficiency (BD). The formation is in balance with the destruction of H_2 by cosmic rays and by photodissociation. Cosmic rays destroy H_2 at a rate (Cravens and Dalgarno 1978)

$$k^p = 1.051\zeta_0 \text{ s}^{-1}, \quad (15)$$

where ζ_0 is the atomic hydrogen cosmic-ray ionizing frequency. Photodissociation of H_2 proceeds by absorption of ultraviolet photons from the interstellar radiation field in the Lyman, $B\,^1\Sigma_u^+ - X\,^1\Sigma_g^+$, and Werner, $C\,^1\Pi_u - X\,^1\Sigma_g^+$, systems in the 912–1100 Å range, followed by fluorescence to the vibrational continuum of the ground state (Solomon 1965, cited in Field, Somerville, and Dressler 1966; Stecher and Williams 1967; Dalgarno and Stephens 1970) at a rate

$$\bar{k}^d = \sum_{J''} k^d_{J''} x_{J''} = \sum_{B,C} \sum_{v'} \sum_{J'} \sum_{J''} \eta_{v'J'} R_{v'J',0J''} x_{J''} \ \mathrm{s}^{-1}. \quad (16)$$

For diffuse interstellar clouds, $\bar{k}^d \gg k^p$. Here $R_{v'J',0J''}$ is the rate of absorption in the $v'J' \leftarrow 0J''$ line, $x_{J''} = n_{J''}(H_2)/n(H_2)$ is the fractional population in level $v''=0, J''$, and $\eta_{v'J'}$ is the relative probability that the upper level decays into the continuum. The values for $\eta_{v'J'}$ were taken from Stephens and Dalgarno (1972). Dissociations out of levels $J''=0$–15 are considered in this work, whereas BD took only dissociations out of $J''=0$ and $J''=1$ into account. As discussed by Federman, Glassgold, and Kwan (1979), the higher levels may contribute significantly to the total rate at those depths where the self-shielding for lines originating from $J''=0$ and $J''=1$ starts to become significant.

The absorption rate $R_{v'J',0J''}$ is evaluated at each depth step into the cloud through a detailed treatment of the radiative transfer in the Lyman and Werner lines. We assume that the attenuation in the lines and in the continuum are separable, so that the absorption rate may be written

$$R_{v'J',0J''} = \theta_{v'J',0J''}(N_{J''})\,\theta_c(\tau_V)\left(\frac{\pi e^2}{mc} f_{v'J',0J''}\right) I_{\mathrm{UV}} \phi_\nu \ \mathrm{s}^{-1}, \quad (17)$$

where $N_{J''}$ is the H_2 column density in level J'', $f_{v'J',0J''}$ is the oscillator strength of the transition as calculated by Allison and Dalgarno (1970), and ϕ_ν is the unattenuated intensity of the interstellar radiation field in $\mathrm{cm}^{-2}\ \mathrm{s}^{-1}\ \mathrm{Hz}^{-1}$, which was taken from Draine (1978) for wavelengths smaller than 2000 Å and from van Dishoeck and Black (1982) for $\lambda > 2000$ Å. In the models, half the intensity is incident on each side of the plane-parallel cloud, so that in the absence of the cloud the unattenuated field is recovered. A scaling factor I_{UV} has been introduced to allow for variations in the strength of the ultraviolet radiation field in a particular location with respect to the average ultraviolet radiation field.

The line attenuation function $\theta_{v'J',0J''}(N_{J''})$ can be expressed (Federman, Glassgold, and Kwan 1979)

$$\theta_{v'J',0J''}(N_{J''}) = \frac{dW_{v'J',0J''}}{dN_{J''}} \left(\frac{\pi e^2}{mc} f_{v'J',0J''}\right)^{-1}, \quad (18)$$

where $W_{v'J',0J''}$ is the equivalent width of the absorption line in frequency units. This expression replaces the formula

$$\theta^{\mathrm{BD}}_{v'J',0J''}(N_{J''}) = \frac{W_{v'J',0J''}}{N_{J''}} \left(\frac{\pi e^2}{mc} f_{v'J',0J''}\right)^{-1} \quad (19)$$

used in the BD and BHD models. The equivalent width for each line as a function of column density may be generated rapidly through the construction of a curve of growth (BD) for the specified value of b, the velocity dispersion. The differentiation in equation (18) was performed numerically by calculating equivalent widths for two closely spaced values of the column density. The contributions of the radiation field from the two sides of the cloud were taken into account separately. Because A_V^{tot} and the column densities of H_2 in each of the J levels are computed results, the evaluation of the far-side contribution is an iterative procedure as well. The additional attenuation due to overlapping lines employed by BD, which was shown to be negligible for diffuse clouds (Roberge 1981), has been discarded.

The continuum attenuation function $\theta_c(\tau_V)$ in the absence of a line has been obtained from the asymptotic form of the solution of the radiative transfer equation (Flannery, Roberge, and Rybicki 1980), and has been averaged over the wavelength dependence of the extinction curve between 912 and 1100 Å. The function depends on the scattering properties of the grains, which are highly uncertain (Roberge, Dalgarno, and Flannery 1981). The grain models 2 and 3 of Roberge, Dalgarno, and Flannery (1981) were employed in this work. For grain model 2, which has an albedo $\omega \approx 0.6$ and a scattering asymmetry parameter $g = 0.5$ at $\lambda \approx 1000$ Å, the attenuation function from each side of a two-sided cloud model is of the form

$$\theta_c(\tau_V) = 0.684 \exp(-3.011\tau_V)[1 - \exp(-1.463\tau_V)]/\tau_V, \quad (20a)$$

where the optical depth $\tau_V \equiv A_V/1.086$. Grain model 3 is highly forward-scattering at ultraviolet wavelengths and has $\omega \approx 0.8$ and $g = 1.0$ at $\lambda \approx 1000$ Å,

$$\theta_c(\tau_V) = 2.519 \exp(-0.818\tau_V)[1 - \exp(-0.397\tau_V)]/\tau_V. \quad (20b)$$

These expressions are strictly valid for describing the continuum attenuation of the photoionization of carbon, and are good approximations for the attenuation of the photodissociation and excitation of H_2. Models for which the full wavelength dependence of the extinction is retained in the continuum attenuation at 912–1100 Å differ from the adopted models by only a few percent in the calculated column densities. Chlewicki and Greenberg (1984*a*, *b*) have recently discussed available observational constraints on the mean ultraviolet scattering properties of interstellar grains and favor an albedo $\omega < 0.4$ and an asymmetry parameter $g \approx 0.7$–0.9. Of the grain models considered by Roberge, Dalgarno, and Flannery (1981), model 2 best satisfies these constraints.

Similar scattering properties were found by Draine and Lee (1984).

The above assumption of separability of line and continuum attenuation implies the neglect of resonant scattering in the H_2 lines. This is a good approximation because the large number of possible fluorescent channels ensures that most of the ultraviolet fluorescence in H_2 occurs outside the range 912–1100 Å, where the initial absorption occurs. The effects of angle-dependent scattering are included approximately in the continuum function $\theta_c(\tau_V)$.

b) *Rotational Population of* H_2

The relative populations $x_{J''}$ in equation (16) are determined by the competition between the formation and destruction processes, ultraviolet absorption, and fluorescence in the Lyman and Werner systems, followed by infrared cascade, quadrupole transitions, and inelastic collision processes (Spitzer and Zweibel 1974; Black and Dalgarno 1973*a*, 1977; Jura 1975). The populations of the $X\ ^1\Sigma_g^+$ levels $v''=0$, $J''=0$–15, $v''=1$, $J''=0$–5, and $v''=2$, $J''=0$–5 were treated explicitly in this work. To this end, 470 levels of the H_2 molecule were considered, and the rates of more than 16,000 radiative transitions were computed at each depth in the model.

The ultraviolet pumping process is initiated by absorptions out of level $v''=0$, $J''=J_i$ into the B and C states at a rate

$$k_{J_i}^{\rm ex} = \sum_{B,C} \sum_{v'} \sum_{J'} (1-\eta_{v'J'}) R_{v'J',0J_i}\ {\rm s}^{-1}, \qquad (21)$$

where the fraction of absorptions that lead to dissociation has been accounted for in equation (16). If $x^{\beta}_{v'J',J_i}$ is the fraction of molecules in the vibration-rotation level $v'J'$ of an excited electronic state $\beta = B$ or $\beta = C$ due to absorptions out of level $v''=0, J_i$,

$$x^{\beta}_{v'J',J_i} = R_{v'J',0J_i}/A^{\beta}_{v'J'}, \qquad (22)$$

the rate of fluorescence from the excited states into level vJ of the ground $X\ ^1\Sigma_g^+$ state due to absorptions out of $v''=0, J_i$ is

$$k^{\rm fl}_{vJ,J_i} = \sum_{\beta=B,C} \sum_{v'} \sum_{J'} x^{\beta}_{v'J',J_i} A_{v'J',vJ}\ {\rm s}^{-1}, \qquad (23)$$

where $A_{v'J',vJ}$ is the probability in s^{-1} for spontaneous emission from $v'J'$ into vJ, and $A^{\beta}_{v'J'}$ is the summed transition probability or inverse lifetime of level $v'J'$ of electronic state β. The excited vibration-rotation levels vJ of the ground electronic state may decay through quadrupole transitions to the $v''=v_f$, $J''=J_f$ level with a cascade probability $C(vJ, v_fJ_f)$, which has been calculated explicitly for $v_f=0$, $J_f=0$–15 and $v_f=1,2$, $J_f=0$–5, using the transition probabilities of Turner, Kirby-Docken, and Dalgarno (1977) in the manner devised by Black and Dalgarno (1976). By summing over the intermediate states vJ,

$$k^{\rm flc}_{v_fJ_f,J_i} = \sum_{v} \sum_{J} k^{\rm fl}_{vJ,J_i} C(vJ, v_fJ_f)\ {\rm s}^{-1}, \qquad (24)$$

the rate at which absorption out of level $v''=0, J_i$ leads to level $v''=v_f, J_f$ through fluorescence and cascade is obtained.

The rotational populations within the $X\ ^1\Sigma_g^+$ $v=0$ state are also affected by inelastic collisions of H_2 with H and H_2, which will cause $\Delta J=\pm 2$ transitions. The rates for the H_2+H processes were obtained from Green and Truhlar (1979). From their rates for the upward $\Delta J=2$ transitions at 100 K, the downward rates were computed by the principle of detailed balance. By taking the downward rates to be independent of temperature, the upward rates at different temperatures could be derived. The rates are smaller than those of Allison and Dalgarno (1967) and Wolken, Miller, and Karplus (1972) used by BD. The rates for the H_2 with H_2 collisions involving the lowest levels have been calculated by Allison and Dalgarno (1967) and have been extended to transitions between higher levels as described by BD. Recently, very accurate cross sections involving the lowest four rotational levels of the H_2 molecules have been obtained by Schaefer (1985). Schaefer has provided cross sections for processes such as the simultaneous excitation $J=0\rightarrow 2$ and de-excitation $J=3\rightarrow 1$ which, if included, would require that the H_2 abundance and excitation be described by a system of nonlinear equations. Test calculations show that the use of rate coefficients based on Schaefer's cross sections have the effect of increasing the column densities in $J=2$ and $J=3$ by 20%–40% compared with identical low-density [$(n_{\rm H})_0 < 500\ {\rm cm}^{-3}$] models using the rates of Allison and Dalgarno. The column densities in other levels of H_2 are affected at the level of 1% or less. The older rates were therefore retained in the present calculations, in order to avoid dealing with nonlinear rate equations. The rates for collisions with $\Delta J=\pm 4, \pm 6, \ldots$ and with $\Delta v=\pm 1, \pm 2, \ldots$ are orders of magnitude smaller and were neglected.

Transitions with $\Delta J=\pm 1$ within the $v=0$ state can be induced by reactive collisions of H_2 with H^+ (Dalgarno, Black, and Weisheit 1973). The cross sections for these collisions are not well known. Experiments (Gerlich and Bohli 1981) indicate a rate for $J=1$ to $J=0$ of approximately $\frac{1}{12}$ of the Langevin rate of 2×10^{-9} cm^3 s^{-1} (Villinger, Henchman, and Lindinger 1982). BD employed a rate of 10^{-10} cm^3 s^{-1} for the $J=1$ to $J=0$ transition, which is consistent with the experiments. The same rate is used in this work. The rates for the higher downward transitions were scaled to this rate by the statistical weights of the levels involved, and were assumed to be independent of temperature. The upward rates were again obtained through the requirement of detailed balance.

The excited rotational levels J of the $X\ ^1\Sigma_g^+$ $v=0$ state of H_2 may also decay radiatively via electric quadrupole transitions which obey the $\Delta J=2$ selection rule. The rates $A_{vJ,vJ-2}$ for these processes were taken from Turner, Kirby-Docken, and Dalgarno (1977).

The H_2 molecules are expected to be formed on the grains in highly excited levels, since 4.5 eV energy is liberated at each formation, but it is not yet clear how the energy is distributed among the rotational, vibrational, and translational degrees of freedom of the molecule, and between the molecule and the dust grain. Hollenbach and Salpeter (1970) and Hunter and Watson (1978) suggest that the molecules

leave the surface in high vibrational ($v \approx 12$) and high rotational ($J \approx 8$) states, whereas the calculations of Allen and Robinson (1976) indicate that the molecules are formed only rotationally hot, but not vibrationally. These conclusions have been questioned by Leonas and Pjarnpuu (1981), whose more extensive calculations show a high vibrational excitation of the newly formed molecule ($v \approx 14$), but not a high rotational excitation ($J \leq 3$). In harmony with this latter work, we assume that 25% of the formations originate in $v = 14$, $J_i = 0$ and 75% in $v = 14$, $J_i = 1$. Since the ultraviolet absorption plus fluorescence process is a factor between 5 and 10 times more rapid than the formation process in populating the rotational levels in the interstellar clouds considered, the results for the lower levels are not very sensitive to this assumption. The excited levels subsequently cascade down to the $v_f J_f$ levels with probabilities given by the cascade matrix elements $C(14J_i, v_f J_f)$, so that the specific formation rate can be written in terms of

$$k^f = n_{\rm H} n({\rm H}) \sum_{v''} \sum_{J''} k^f_{v''J''}, \tag{25}$$

where

$$k^f_{v''J''} = 3.0 \times 10^{-18} T^{1/2} y_f g_{J''} C(14J_i, v''J''), \tag{26}$$

with $g_{J''} = 0.25$ for $J_i = 0$ and J'' even, and $g_{J''} = 0.75$ for $J_i = 1$ and J'' odd.

The steady state concentration n_J in level $v = 0, J$ of the $X\,{}^1\Sigma_g^+$ state is then determined by the competition between the above-mentioned processes and may be obtained from a set of linear equations

$$n_J \left[A_{0J,0J-2} + \left(k_J^{\rm ex} - k^{\rm flc}_{0J,J} \right) + \sum_i \sum_{J' \neq J} n_i q_i(J, J') + k_J^d + 1.051 \zeta_0 \right] = n_{\rm H} n({\rm H})\, k^f_{0J} + \sum_{J' \neq J} n_{J'} \left[k^{\rm flc}_{0J,J'} + A_{0J',0J} + \sum_i n_i q_i(J', J) \right], \tag{27}$$

where $q_i(J, J')$ is the collisional rate coefficient in cm^3 s^{-1} for transitions from J to J' involving collision partner i with density n_i. All other terms have been explained in the previous paragraphs.

The concentrations n_{vJ} in levels J of the excited vibrational levels $v = 1$ and $v = 2$ are found from the simpler expression

$$n_{vJ} A^X_{vJ} = n_{\rm H} n({\rm H})\, k^f_{vJ} + \sum_{v=0, J'} n_{J'} k^{\rm flc}_{vJ,J'}. \tag{28}$$

This equation assumes that the rates of ultraviolet absorption out of vibrationally excited levels are negligible, both with respect to the populations of these levels and with respect to their contributions to the overall dissociation and excitation rates. This is a valid approximation, provided that the scaling factor of the radiation field is $I_{\rm UV} < 1000$. In more intense radiation fields, the treatment becomes more complicated (Shull 1978). The neglect of collisional excitation and de-excitation of the vibrationally excited levels is valid for temperatures less than 1000 K and densities less than 10^4 cm^{-3}.

The ultraviolet absorption rates and rotational excitation of HD can be calculated analogously to the above treatment of H_2. Compared with H_2, the self-shielding in HD is smaller because of its lower abundance. The small permanent dipole moment of HD allows dipole rotational transitions that reduce the lifetimes of excited levels compared with those of H_2; therefore, the excited levels $J \geq 2$ in HD are relatively less populated than those in H_2. The present cloud models include an explicit treatment of the abundance of HD in levels $v = 0$, $J = 0$, 1 and 2, and $v = 1$, $J = 1$.

IV. EXCITATION OF OTHER DIAGNOSTIC SPECIES

a) *Atomic Fine-Structure Excitation*

The steady-state populations of the ground-state fine-structure levels of the $C^+(^2P_J)$, $C(^3P_J)$ and $O(^3P_J)$ atoms have been computed as functions of depth into the cloud.

The fine-structure excitation of C^+ is governed by collisions with electrons (Hayes and Nussbaumer 1984*a*), protons (Hayes and Nussbaumer 1984*b*), H atoms (Launay and Roueff 1977*b*), and H_2 molecules (Flower and Launay 1977). The collisional processes compete with spontaneous radiative transitions between the fine-structure levels (Nussbaumer and Storey 1981). Excitation through absorption and fluorescence in the ultraviolet resonance lines of C^+ has also been taken into account. The oscillator strengths of Nussbaumer and Storey (1981) have been used, and the depth dependences of the absorption rates have been treated in the same way as for the H_2 and HD lines.

The fine-structure excitation of C is governed by similar processes. Sources of atomic data are Nussbaumer and Rusca (1979) for the radiative transition probabilities between the fine-structure levels, and Launay and Roueff (1977*a*) for H-impact excitation rates. Collisions with H_2 were assumed to occur at one-half the rate of the corresponding collisions with H. Electron and proton collisions and ultraviolet radiative excitation have been ignored for C.

For atomic oxygen, collisions with electrons (Le Dourneuf and Nesbet 1976), collisions with H (Launay and Roueff 1977*a*), collisions with H_2 at one-half the corresponding H rates, and collisions with protons (Chambaud *et al.* 1980; Roueff 1981) were considered. Ultraviolet radiative processes have been included as for C^+, and their rates were based on the oscillator strengths of Pradhan and Saraph (1977). Radiative fine-structure transition probabilities were obtained from Mendoza and Zeippen (1983, preliminary results cited in Mendoza 1983). The effects of ultraviolet pumping on the fine-structure populations in C^+ and O are negligible in the clouds considered in this work.

b) C_2 *Excitation*

The C_2 molecule is, like the H_2 molecule, a particularly sensitive diagnostic, because it is a symmetric molecule with no permanent dipole moment. The excited rotational levels

are therefore long-lived and may be populated significantly by the radiative and collisional processes in the cloud. The main difference between the excitation of the two molecules is that the C_2 excitation is initiated primarily by absorptions in the far-red part of the spectrum, whereas the H_2 excitation is sensitive to the strength of the ultraviolet interstellar radiation field. Also, at interstellar temperatures the collisional processes for C_2 compete effectively with the radiative processes for many rotational levels, so that the population distribution of C_2 is sensitive to the density in the cloud.

The theory of the C_2 rotational excitation has been discussed by van Dishoeck and Black (1982). The calculated rotational populations can be characterized by the kinetic temperature T in the cloud and the combination of parameters $n_c\sigma_0/I_R$, where n_c is the density of collision partners in the cloud, $n_c = n(\mathrm{H}) + n(\mathrm{H_2}) = n_\mathrm{H} - n(\mathrm{H_2})$, σ_0 is the cross section for collisional de-excitation, and I_R is a scaling factor for the radiation field in the far-red part of the spectrum. The radiation field adopted by van Dishoeck and Black (1982) with $I_R \approx 1$ is consistent with that calculated recently by Mathis, Mezger, and Panagia (1983) at the relevant wavelengths. Unfortunately, the cross section σ_0 is not well known from laboratory experiments or theoretical calculations. Its value lies most likely in the range $\sigma_0 \approx (1\text{–}5)\times10^{-16}$ cm^2.

c) CO *Excitation*

The excitation of the CO molecule in diffuse clouds is governed by collisions with H and H_2, and by spontaneous transitions and stimulated emission and absorption in the background radiation field. The present calculations include the lowest 10 rotational levels of CO, and use the collisional rates of Green and Chapman (1978). More recent determinations of the H_2–CO collisional rate coefficients differ very little from those of Green and Chapman at low temperatures, $T \leq 100$ K (Flower and Launay 1985; Schinke *et al.* 1985). The excitation will be discussed in more detail in a subsequent paper (van Dishoeck and Black 1986*b*).

V. RESULTS OF CLOUD MODELS

a) *Comparison with Previous Models*

As a test of the program for the calculation of the H_2 excitation and dissociation, the BD model for the ζ Oph cloud was recalculated, and the results were compared with those of Roberge (1981) for the same model. Roberge used a direct numerical treatment of the radiative transfer in line and continuum, and his results are taken as a critical test of the accuracy of our approximate treatment. In this calculation, the temperature and density distributions used by Roberge (1981) were specified *a priori*, without the requirement of hydrostatic equilibrium. The model has a warm envelope with $T = 110$ K and $n_\mathrm{H} = 500$ cm^{-3}, and a cold core with $T = 22$ K and $n_\mathrm{H} = 2500$ cm^{-3}. The other parameters characterizing the model are indicated in Table 2. In order to be consistent with the previous calculations, the H–H_2 collision rates of Allison and Dalgarno (1967) were used, and the radiation field and attenuation factors of BD were employed. The resulting H_2 rotational population distribution is presented in Table 2, together with those obtained by BD and by Roberge. A total H_2 column density of 6.3×10^{20} cm^{-2} was used to compare with the results of Roberge, since in his calculations the total column density of hydrogen nuclei, instead of that of H_2, is fixed. To compare with BD, the model was run with $N(\mathrm{H_2}) = 4.2\times10^{20}$ cm^{-2}.

The calculated column densities of H and H_2 in the various rotational levels are generally in good agreement with those obtained by Roberge. The small discrepancies for the higher J levels result in part from the different assumptions about the relation between extinction and total column density in the two calculations. Furthermore, Roberge did not consider $J = 7$, used a different initial distribution of newly formed molecules, and employed a somewhat different reaction network to describe the ion chemistry. Since the H^+ abundance can affect the J = even/J = odd population ratio in H_2, the value of ζ_0 was increased slightly in this work from 1.6×10^{-17} to 2.5×10^{-17} s^{-1} to reproduce the H^+ densities of Roberge. The dissociation rate $\bar{k}^d$ of H_2 as a function of depth obtained in this work was found to agree well with the rate computed by Roberge, apart from a slightly less steep decrease in the outer layers of the cloud. This difference is caused by the different treatment of the continuum radiative transfer in the two calculations. The excitation temperature characterizing the populations in $J = 0$ and $J = 1$ showed the same large non-thermal behavior in the outer layers of the cloud as found by Roberge. With these considerations taken into account, it appears that the self-shielding in the Lyman and Werner lines of H_2 is described satisfactorily through equation (18) in the present calculations.

The column densities of atomic hydrogen obtained by Roberge and in this work differ considerably from the ones found in the original BD model. Because of the enhanced shielding in the H_2 lines, the H column density is reduced by a factor of 5. The improved radiative transfer also influences the rotational population of H_2. The lower rotational levels are relatively more populated in the new calculations, whereas the populations of the higher levels $J \geq 4$ are diminished by factors of up to 10. The agreement with the observed column densities toward ζ Oph is clearly not as good for the present calculations as for the work of BD, and adjustments in the temperature and density distribution and in the radiation field in the model are necessary to bring the calculations again into harmony with the observations. New models for the ζ Oph cloud are discussed in § V*d* below.

b) *General Considerations*

The above evidence suggests that the observed column densities of H and $H_2(J)$ toward ζ Oph and ζ Per cannot be reproduced with the temperature and density structure of the BD and BHD models. We present here results of more adequate hydrostatic models for these two clouds, as well as for the cloud toward o Per, for which physical parameters have been suggested (Hartquist, Black, and Dalgarno 1978) but not discussed in detail, and for the cloud toward χ Oph, which has not been analyzed before. As may be seen from Tables 4, 5, 7, and 8, the four clouds have, within the observational errors, almost the same column density of H_2,

TABLE 2

CALCULATED COLUMN DENSITIES (cm^{-2}) OF H AND $H_2(v, J)$ FOR THE BD MODEL OF CLOUD IN FRONT OF ζ OPH

Species	This Work I[a]	Roberge[b]	This Work II[a]	BD[c]	Observed[d]
H	1.03(20)	1.10(20)	0.93(20)	5.37(20)	(5.2±0.2)(20)
H_2	6.30(20)	6.31(20)	4.20(20)	4.20(20)	(4.2±0.3)(20)
H_2, v=0:					
J=0	3.68(20)	3.72(20)	2.40(20)	2.95(20)	(2.9±0.3)(20)
J=1	2.56(20)	2.51(20)	1.77(20)	1.17(20)	(1.3±0.2)(20)
J=2	5.06(18)	5.13(18)	3.42(18)	2.95(18)	(4.0±1.6)(18)
J=3	9.77(16)	7.94(16)	6.93(16)	8.71(16)	(1.7±1.2)(17)
J=4	6.82(14)	5.75(14)	6.17(14)	1.55(15)	(5.3±2.2)(15)
J=5	1.50(14)	1.91(14)	1.36(14)	5.62(14)	(4.3±0.5)(14)
J=6	1.46(13)	2.57(13)	1.35(13)	6.76(13)	(4.9±0.5)(13)
J=7	3.44(12)	...	3.14(12)	3.80(13)	(3.6±0.4)(13)
C	2.56(15)	1.58(15)	0.95(15)	3.98(15)	(3.2±0.6)(15)
C^+	1.23(17)	1.26(17)	0.85(17)	1.20(17)	(9.3±4.5)(16)
O	2.38(17)	2.40(17)	1.62(17)	2.40(17)	(7.1±0.5)(17)
HD	1.85(14)	...	1.08(14)	1.78(14)	(2.1±0.2)(14)
OH	4.41(12)	4.47(12)	3.29(12)	4.89(13)	(4.8±0.5)(13)
CO	3.25(13)	1.32(13)	1.63(13)	1.05(15)	(2.0±0.3)(15)
O_2	1.23(10)	2.95(10)	0.90(10)	1.41(11)	...
H_2O	1.68(11)	8.51(11)	1.31(11)	1.07(12)	≤2.2(13)
CH	5.87(13)	...	3.74(13)	3.72(13)	(2.5±0.1)(13)
CH^+	4.51(10)	...	3.22(10)	2.45(11)	(2.9±0.1)(13)
C_2	4.06(13)	...	2.31(13)	1.38(13)	(1.5±0.2)(13)
HCℓ	8.07(11)	...	5.72(11)	2.63(13)	<4.5(11)
H_2O^+	1.71(10)	...	1.42(10)	...	<1.5(13)

NOTE.—In this and subsequent tables, the notation 1.03(20) means 1.03×10^{20}.

[a] Obtained using $I_{UV}=2.5$, $y_f=1.532$, $b=2.0$ km s^{-1}, $\zeta_0=5\times10^{-17}$ s^{-1}, $\delta_C=0.198$, $\delta_O=0.210$, $k_{33}\approx10^{-6}$ cm^3 s^{-1}, and $k_{34}=5\times10^{-16}$ cm^3 s^{-1}. I: calculation with total $N(H_2)=6.3\times10^{20}$ cm^{-2}; II: calculation with total $N(H_2)=4.2\times10^{20}$ cm^{-2}.

[b] Roberge 1981.

[c] Black and Dalgarno 1977.

[d] For references see Tables 5 and 12.

$N(H_2)\approx4.2\times10^{20}$ cm^{-2}, but the column density of H is considerably larger toward χ Oph compared with that toward ζ Per, ζ Oph, and o Per. The degree of excitation in the higher rotational levels $J\geq5$ is observed to be largest toward χ Oph, intermediate toward ζ Oph and o Per, and lowest toward ζ Per. The observed column densities in the $J=3$ and $J=4$ levels are an order of magnitude larger toward o Per than toward the other three clouds, even taking into account the fact that the uncertainties in the measured column densities are particularly large for $J=2$–4, for which the lines lie on the flat part of the curve of growth. For $J=0$ and $J=1$ and for $J\geq5$, the lines lie on the square-root part and on the linear part, respectively, so the errors are considerably smaller.

The procedure for fitting the observed column densities of H and $H_2(J)$ has been outlined by BD. It may be illustrated by considering a number of models which have constant values for the temperature and density with depth. The models are presented in Table 3 for a range of temperatures, densities, and other parameters. From the table we observe the following.

1. The population of none of the rotational levels J of H_2 is, at a certain temperature, particularly sensitive to the density in the cloud; the differences between the various models are smaller than the current uncertainties in the observations.

2. The population of the lower levels $J\leq3$ is sensitive mainly to the temperature in the cloud.

3. The population of the higher levels $J>4$ is sensitive primarily to the strength of the interstellar radiation field in the ultraviolet part of the spectrum, which initiates the pumping process; they are much less sensitive than the lower levels to the temperature and density in the cloud. The strength of the radiation field is determined in the models both by the scaling factor I_{UV} and by the adopted grain scattering parameters (compare models C14 and C16 with model C4).

4. The population of the levels is rather insensitive to the employed b-value (compare models C13 and C4).

5. The population of the levels is not very sensitive to the employed value of the cosmic-ray ionizing frequency ζ_0 (compare models C15 and C4).

6. The use of an alternative set of H–H_2 cross sections affects mainly the population in the levels $J=2$ and $J=3$ (compare models C17 and C4).

7. The column density of atomic hydrogen, N(H), is very sensitive to the combination of parameters $n_H y_f/I_{UV}$. Figure 1 illustrates the relationship.

8. None of these uniform models fits the observed values of N(H) and $N_J(H_2)$ for the four clouds, and this fact cannot be remedied by reasonable variations of the molecular data and

TABLE 3

CALCULATED COLUMN DENSITIES (cm^{-2}) OF H, $H_2(v, J)$, AND SEVERAL ATOMS AND MOLECULES IN MODELS WHICH HAVE CONSTANT TEMPERATURE (K) AND DENSITY (cm^{-3})

Parameters and Species	Model[a]																		
	C1	C2	C3	C4	C5	C6	C7	C8	C9	C10	C11	C12	C13[b]	C14[c]	C15[d]	C16[e]	C17[f]	C18[g]	C19[h]
n_H	250	500	1000	250	500	1000	250	500	1000	250	500	1000	250	250	250	250	250	250	500
T	20	20	20	40	40	40	60	60	60	100	100	100	40	40	40	40	40	40	40
H	7.7(20)	4.1(20)	2.1(20)	6.6(20)	3.5(20)	1.8(20)	6.2(20)	3.3(20)	1.7(20)	5.3(20)	2.8(20)	1.5(20)	6.5(20)	2.5(21)	7.0(20)	4.4(20)	6.6(20)	6.8(20)	6.7(20)
H_2, v=0:																			
J=0	4.1(20)	4.1(20)	4.1(20)	3.7(20)	3.7(20)	3.7(20)	2.7(20)	2.7(20)	2.7(20)	1.6(20)	1.6(20)	1.6(20)	3.7(20)	3.7(20)	3.7(20)	3.7(20)	3.7(20)	3.7(20)	3.7(20)
J=1	5.5(18)	6.5(18)	7.7(18)	5.0(19)	5.0(19)	5.1(19)	1.5(20)	1.5(20)	1.5(20)	2.6(20)	2.6(20)	2.6(20)	5.0(19)	5.5(19)	4.8(19)	4.9(19)	5.0(19)	5.0(19)	5.0(19)
J=2	1.9(17)	1.2(17)	6.8(16)	1.8(17)	1.2(17)	6.8(16)	3.1(17)	3.0(17)	2.9(17)	2.8(18)	3.6(18)	4.1(18)	1.8(17)	7.3(17)	1.7(17)	1.2(17)	6.6(16)	1.8(17)	1.3(17)
J=3	4.3(15)	4.2(15)	3.6(15)	8.9(15)	8.3(15)	6.8(15)	1.4(16)	1.3(16)	1.1(16)	3.5(16)	4.9(16)	6.7(16)	9.0(15)	3.4(16)	8.9(15)	5.8(15)	6.8(15)	1.0(16)	8.0(15)
J=4	1.4(15)	1.5(15)	1.4(15)	1.4(15)	1.4(15)	1.4(15)	1.3(15)	1.3(15)	1.2(15)	1.2(15)	1.2(15)	1.2(15)	1.4(15)	5.1(15)	1.4(15)	9.1(14)	1.3(15)	1.5(15)	1.4(15)
J=5	7.5(13)	8.1(13)	8.5(13)	1.4(14)	1.5(14)	1.5(14)	2.1(14)	2.2(14)	2.3(14)	2.8(14)	2.9(14)	2.9(14)	1.4(14)	5.3(14)	1.4(14)	9.5(13)	1.4(14)	2.9(14)	1.4(14)
J=6	2.9(13)	3.1(13)	3.2(13)	2.9(13)	3.0(13)	3.1(13)	2.6(13)	2.8(13)	2.8(13)	2.5(13)	2.6(13)	2.7(13)	2.8(13)	1.1(14)	2.9(13)	1.9(13)	2.8(13)	4.5(13)	2.9(13)
J=7[i]	2.0(12)	2.1(12)	2.3(12)	3.5(12)	3.7(12)	3.8(12)	5.2(12)	5.5(12)	5.6(12)	6.6(12)	6.9(12)	7.1(12)	3.4(12)	1.4(13)	3.5(12)	2.3(12)	3.5(12)	2.7(13)	3.5(12)
H_2, v=1:																			
J=0	2.5(12)	2.7(12)	2.8(12)	2.4(12)	2.6(12)	2.6(12)	2.2(12)	2.3(12)	2.4(12)	1.9(12)	2.0(12)	2.1(12)	2.4(12)	8.9(12)	2.4(12)	1.6(12)	2.4(12)	2.3(12)	2.4(12)
J=1	1.7(12)	1.9(12)	2.0(12)	3.6(12)	3.8(12)	3.9(12)	5.5(12)	5.8(12)	6.0(12)	7.2(12)	7.6(12)	7.8(12)	3.5(12)	1.4(13)	3.5(12)	2.3(12)	3.5(12)	2.8(12)	3.5(12)
J=2	6.5(12)	6.9(12)	7.1(12)	6.3(12)	6.7(12)	6.8(12)	5.7(12)	6.0(12)	6.2(12)	5.1(12)	5.4(12)	5.6(12)	6.2(12)	2.3(13)	6.3(12)	4.1(12)	6.2(12)	6.0(12)	6.3(12)
H_2, v=2:																			
J=0	1.1(12)	1.1(12)	1.2(12)	1.0(12)	1.1(12)	1.1(12)	9.2(11)	9.7(11)	1.0(12)	8.0(11)	8.5(11)	8.8(11)	1.0(12)	3.8(12)	1.0(12)	6.7(11)	1.0(12)	9.9(11)	1.0(12)
J=1	7.3(11)	8.0(11)	8.7(11)	1.5(12)	1.6(12)	1.6(12)	2.3(12)	2.4(12)	2.5(12)	3.0(12)	3.2(12)	3.2(12)	1.5(12)	5.8(12)	1.5(12)	9.7(11)	1.5(12)	1.1(12)	1.5(12)
J=2	2.6(12)	2.8(12)	2.9(12)	2.6(12)	2.7(12)	2.8(12)	2.3(12)	2.4(12)	2.5(12)	2.1(12)	2.2(12)	2.3(12)	2.5(12)	9.4(12)	2.6(12)	1.7(12)	2.5(12)	2.4(12)	2.6(12)
O	1.0(18)	7.8(17)	6.6(17)	9.4(17)	7.4(17)	6.3(17)	9.1(17)	7.3(17)	6.3(17)	8.6(17)	7.0(17)	6.1(17)	9.2(17)	2.1(18)	9.5(17)	7.9(17)	9.3(17)	9.4(17)	9.3(17)
OH	1.9(13)	1.7(13)	1.3(13)	2.2(13)	1.9(13)	1.4(13)	3.1(13)	2.5(13)	1.7(13)	5.0(13)	3.6(13)	2.4(13)	2.2(13)	6.8(12)	1.2(14)	3.2(13)	2.2(13)	2.2(13)	1.7(13)
H_2O	1.4(11)	1.5(11)	1.4(11)	2.3(11)	2.3(11)	2.0(11)	3.7(11)	3.5(11)	2.8(11)	7.4(11)	6.2(11)	4.7(11)	2.2(11)	4.3(10)	1.0(12)	3.9(11)	2.2(11)	2.3(11)	1.8(11)
H_2O^+	2.8(10)	1.6(10)	9.0(09)	4.6(10)	2.5(10)	1.3(10)	7.7(10)	3.9(10)	1.9(10)	1.5(11)	6.7(10)	3.1(10)	4.6(10)	3.1(10)	2.4(11)	5.0(10)	4.6(10)	4.6(10)	2.3(10)
H_3^+	9.2(13)	5.2(13)	2.8(13)	1.0(14)	5.6(13)	3.0(13)	1.0(14)	5.7(13)	3.0(13)	1.1(14)	5.9(13)	3.1(13)	1.0(14)	6.8(13)	5.7(14)	1.1(14)	1.0(14)	1.0(14)	5.0(13)
HD	3.1(13)	2.7(13)	2.4(13)	2.0(14)	1.5(14)	1.1(14)	3.8(14)	2.6(14)	1.9(14)	2.4(14)	1.8(14)	1.5(14)	6.5(14)	5.1(13)	6.3(15)	5.0(14)	2.0(14)	2.0(14)	1.9(14)
C	4.2(15)	6.0(15)	9.6(15)	2.9(15)	4.3(15)	7.0(15)	2.5(15)	3.7(15)	6.2(15)	1.9(15)	3.0(15)	5.2(15)	2.8(15)	1.9(15)	3.4(15)	4.7(15)	2.9(15)	2.9(15)	5.7(15)
C^+	5.6(17)	4.3(17)	3.6(17)	5.2(17)	4.1(17)	3.5(17)	5.1(17)	4.1(17)	3.5(17)	4.8(17)	3.9(17)	3.4(17)	5.2(17)	1.2(18)	5.3(17)	4.4(17)	5.2(17)	5.2(17)	5.2(17)
CH	1.8(13)	3.2(13)	5.7(13)	1.8(13)	3.2(13)	5.6(13)	1.7(13)	3.2(13)	5.5(13)	1.7(13)	3.1(13)	5.4(13)	1.8(13)	6.6(12)	1.7(13)	2.5(13)	1.8(13)	1.8(13)	3.3(13)
C_2	8.0(12)	2.9(13)	9.3(13)	1.0(13)	3.7(13)	1.2(14)	1.1(13)	4.2(13)	1.3(14)	1.4(13)	4.9(13)	1.5(14)	1.0(13)	9.7(11)	6.7(12)	2.8(13)	1.0(13)	1.0(13)	3.3(13)
CO	4.0(13)	7.3(13)	1.4(14)	5.0(13)	9.4(13)	1.9(14)	7.6(13)	1.3(14)	2.6(14)	1.3(14)	2.1(14)	4.1(14)	5.0(13)	4.4(12)	3.5(14)	1.9(14)	5.0(13)	5.0(13)	9.2(13)
NH	2.7(11)	2.3(11)	1.6(11)	3.1(11)	2.6(11)	1.8(11)	3.2(11)	2.6(11)	1.8(11)	3.4(11)	2.7(11)	1.8(11)	3.1(11)	9.4(10)	1.7(12)	4.4(11)	3.1(11)	3.1(11)	2.3(11)
CN	6.0(11)	1.1(12)	2.3(12)	7.5(11)	1.5(12)	3.1(12)	8.3(11)	1.7(12)	3.7(12)	9.5(11)	1.9(12)	4.6(12)	7.5(11)	7.6(10)	3.7(12)	2.0(12)	7.5(11)	7.5(11)	1.4(12)
HCℓ	1.8(11)	1.6(11)	1.3(11)	2.3(11)	2.0(11)	1.6(11)	2.6(11)	2.2(11)	1.7(11)	2.9(11)	2.4(11)	1.9(11)	2.3(11)	2.4(11)	2.5(11)	1.6(11)	2.3(11)	2.3(11)	2.1(11)
A_V^{tot}	1.01	0.79	0.66	0.95	0.75	0.64	0.92	0.73	0.63	0.86	0.71	0.62	0.93	2.12	0.96	0.80	0.94	0.95	0.94

[a] All models have $N(H_2) = 4.2\times10^{20}$ cm^{-2}, $\zeta_0 = 5\times10^{-17}$ s^{-1}, $y_f = 1.0$, $b = 2$ km s^{-1}, $I_{UV} = 2$, $\delta_C = \delta_O = \delta_N = 0.75$, $\delta_D = 1.0$, $\delta_{Cl} = 0.6$, $\delta_M = 0.4$, $k_{33} = 1\times10^{-10}$ cm^3 s^{-1}, $k_{34} = 7\times10^{-16}$ cm^3 s^{-1}, $k_{36} = 2\times10^{-10}$ cm^3 s^{-1}, assume that the H_2 molecules are formed rotationally cold, employ grain model 3, and use the H–H_2 collisional rates of Green and Truhlar 1979, unless otherwise indicated. If grain model 2 were employed, the results would be similar if I_{UV} were increased from 2 to 3.5.

[b] Same as model C4, but with $b = 0.8$ km s^{-1}.

[c] Same as model C4, but with $I_{UV} = 10$.

[d] Same as model C4, but with $\zeta_0 = 3\times10^{-16}$ s^{-1}.

[e] Same as model C4, but with grain model 2.

[f] Same as model C4, but with the H–H_2 cross sections of Allison and Dalgarno 1967.

[g] Same as model C4, but with the assumption that the newly formed H_2 molecules have 1.5 eV of internal energy distributed over all levels.

[h] Same as model C5, but with $y_f = 0.5$.

[i] The column density in $J = 8$ is 6×10^{11} cm^{-2} within 20% in models C1–C12. The column densities in higher J levels are less than 10^{11} cm^{-2}. The column densities in $J = 3$, $v = 1$ and $v = 2$, are close to those in $J = 1$, $v = 1$ and $v = 2$, respectively.

physical parameters entering the models: the observed populations of the $J = 0$ and $J = 1$ levels generally indicate a lower temperature than the populations of the $J = 2$ and $J = 3$ levels.

As suggested by BD, the observations require models in which the temperature, and thus also the density, vary with depth into the cloud: such models must have a hot outer layer in order to populate the $J = 1$–3 levels, and a cold core to explain the $J = 0$ to $J = 1$ population ratio. The populations of the higher levels are not very sensitive to the temperature and density gradients in the cloud. As follows from observation 3 above, the scaling factor for the radiation field I_{UV} may thus be fixed from the observed populations of the higher levels for a given unattenuated interstellar radiation field and model for the scattering properties of the grains. The density is the most uncertain parameter in the models. Since the H_2 rotational population is not very sensitive to it, except at very low temperatures, the density is mainly constrained by the observed $N(H)/N(H_2)$ column density ratio. As shown in Figure 1, $N(H)$ depends on the combination of parameters $n_H y_f / I_{UV}$. If the scaling factor I_{UV} is inferred from the observed populations of the high-J levels of H_2, and if the scaling factor for the H_2 formation rate is assumed to be $y_f = 1.0$, a value for the average density in the cloud may be derived.

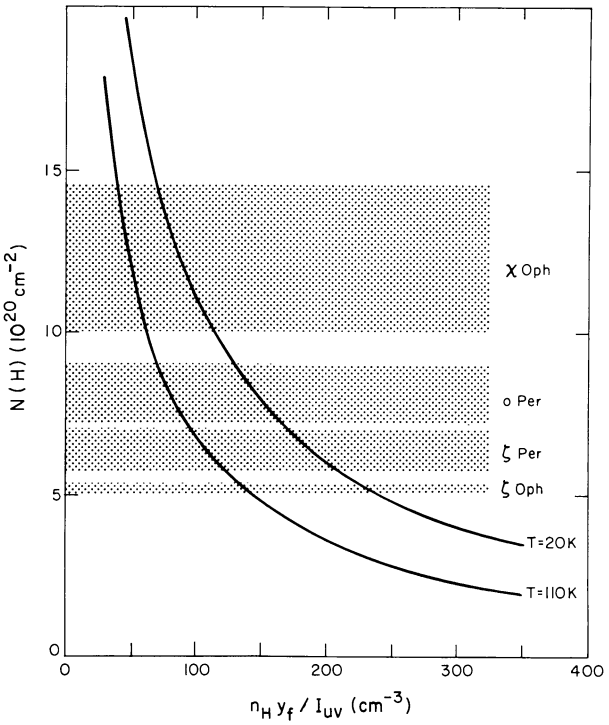

FIG. 1.—The variation of the atomic hydrogen column density $N(H)$ with the density n_H, scaling factor for the H_2 grain formation rate y_f, and scaling factor for the ultraviolet radiation field I_{UV} in the models of Table 3, which have a fixed total H_2 column density $N(H_2) = 4.2 \times 10^{20}$ cm^{-2}. Grain model 3 was employed in the calculations. The observed ranges of $N(H)$ for the molecular components of the clouds in front of ζ Per, ζ Oph, χ Oph, and o Per are indicated by the shaded areas.

The gradients of the temperature and density with depth into the cloud are determined by the employed Doppler parameter b and the polytropic index Γ (cf. Table 1). The values of b inferred from the observations of various species differ considerably. They may be as high as 6–8 km s^{-1} for atomic ions (Spitzer and Jenkins 1975), are generally about 3–5 km s^{-1} for the $J = 2$–4 lines of H_2 (Morton 1975; Snow 1977; Frisch 1980), and are smaller than 1 km s^{-1} for the neutral species (Snow 1977; de Boer 1979, 1981; Liszt 1979) in the clouds studied in this work. This range of b-values may reflect the contributions of minor, unresolved cloud components to highly saturated lines of atomic ions, as well as possible gradients of the velocity dispersion within the principal cloud. We have not considered any depth dependence of b in the present models, but we have constructed models both with a constant $b \approx 3$ km s^{-1} and with a constant $b \approx 1$ km s^{-1} in order to investigate its influence. For a given b-value, the polytropic index Γ has then been chosen so that the temperature at the boundary T_1 is high enough to populate the $J = 1$–3 levels of H_2.

c) *The ζ Per Cloud*

Most of our efforts have been devoted to constructing new models for the diffuse cloud toward ζ Per. Of the four clouds considered, the cloud toward ζ Per is to be favored as a test case for the models, since it lies in the central portion of the Perseus OB2 region but is not thought to be closely associated with the star ζ Per itself or with any other nebulae or condensations in the Perseus region (Snow 1977). In Table 4 the results are presented for several models with b lying between 3.0 and 0.8 km s^{-1}, keeping y_f fixed initially at 1.0 (see models A–C). The temperature and density structure in the models is illustrated in Figure 2*a*. It appears that the observed column densities of H and $H_2(J)$ toward ζ Per are well reproduced in models which have $T_0 \approx 30$ K, $(n_H)_0 \approx 250$–500 cm^{-3}, and $I_{UV} \approx 2$ if grain model 3 is employed. As Figure 2*a* shows, models with a smaller b-value allow a stronger variation of the density in the cloud. They thus require a higher central density in order to provide an average density consistent with the observed $N(H)$. The central temperature is well constrained in the models by the observed column densities of the lower rotational levels of H_2 to be $T_0 \approx 30$ K, although variations of the order of 10 K are possible. The scaling factor I_{UV} is reasonably well determined in the models by the higher rotational levels of H_2, $I_{UV} = 1.6$–2.2 if grain model 3 is employed. If grain model 2 is used, I_{UV} needs to be increased by a factor of about 1.5, but otherwise the inferred physical parameters are the same, as models F and B in Table 4 demonstrate. The observed populations in levels $J = 2$ and $J = 3$ seem to require a boundary temperature $T_1 \approx 100$–200 K, although the uncertainties in the observations allow considerable variance. This results in boundary densities $(n_H)_1 \approx 70$–200 cm^{-3} for models with $b = 0.8$–3.0 km s^{-1}. Calculations of the thermal balance in diffuse clouds (Glassgold and Langer 1974; Barsuhn and Walmsley 1977; Roberge 1981) suggest that high temperatures, $T_1 > 60$ K, can be maintained only for low densities, $n_1 < 50$ cm^{-3}, so that models with small b-values and/or more negative polytropic indices are preferable. The value of

TABLE 4

CALCULATED COLUMN DENSITIES (cm^{-2}) OF H AND $H_2(v, J)$ AND RELATIVE POPULATIONS OF HD(J), $C^+(J)$, C(J), AND O(J) IN MODELS OF CLOUD IN FRONT OF ζ PER

Parameters and Species	Model[a] A	B	C	D	E	F	G[b]	Observed
$(n_H)_0$ (cm^{-3}) ..	250	325	500	500	150	325	225	
T_0 (K)	30	30	25	30	30	30	30	
b (km s^{-1})	3.0	1.2	0.8	3.0	2.0	1.2	1.2	
I_{UV}	2.0	2.0	1.9	1.9	2.0	3.5	2.2	
y_f	1.0	1.0	1.0	0.5	2.0	1.0	1.0	
Γ	-1.37	-1.30	-1.18	-1.20	-1.55	-1.26	-1.36	
Grain model	3	3	3	3	3	2	2	
H	6.5(20)	6.7(20)	5.9(20)	6.3(20)	6.0(20)	6.7(20)	6.9(20)	(6.5±0.7)(20)[c]
H_2	4.8(20)	4.8(20)	4.8(20)	4.8(20)	4.8(20)	4.8(20)	4.8(20)	(4.8±1.0)(20)[d]
H_2, v=0:								
J=0	3.2(20)	3.2(20)	3.3(20)	3.3(20)	3.1(20)	3.3(20)	3.2(20)	(3.2±1.3)(20)[d]
J=1	1.6(20)	1.5(20)	1.4(20)	1.5(20)	1.7(20)	1.5(20)	1.5(20)	(1.5±0.6)(20)[d]
J=2	1.1(18)	1.2(18)	1.5(18)	1.0(18)	1.2(18)	1.0(18)	1.0(18)	(1.1±0.1)(18)[c]
J=3	2.3(16)	2.9(16)	5.1(16)	2.0(16)	2.7(16)	2.7(16)	2.4(16)	(2.0±0.7)(16)[c]
J=4	1.4(15)	1.3(15)	1.3(15)	1.3(15)	1.4(15)	1.2(15)	0.9(15)	(1.0±0.1)(15)[c]
J=5	2.3(14)	2.2(14)	2.1(14)	2.1(14)	2.4(14)	2.3(14)	2.6(14)	(2.3±0.2)(14)[c]
J=6	2.9(13)	2.8(13)	2.7(13)	2.8(13)	2.8(13)	2.5(13)	3.0(13)	...
J=7	5.7(12)	5.3(12)	4.9(12)	5.2(12)	5.7(12)	5.4(12)	2.1(13)	...
J=8	6.2(11)	5.8(11)	5.6(11)	5.9(11)	5.9(11)	5.3(11)	2.6(12)	...
J=9	1.0(11)	9.7(10)	9.1(10)	9.7(10)	1.0(11)	1.0(11)	3.5(12)	...
H_2, v=1:								
J=0	2.5(12)	2.3(12)	2.2(12)	2.2(12)	2.3(12)	2.0(12)	1.3(12)	...
J=1	5.9(12)	5.7(12)	5.3(12)	5.5(12)	6.0(12)	5.8(12)	3.4(12)	...
J=2	6.2(12)	5.9(12)	5.8(12)	6.0(12)	6.0(12)	5.3(12)	3.4(12)	...
J=3	5.6(12)	5.3(12)	5.0(12)	5.2(12)	5.7(12)	5.5(12)	3.2(12)	...
H_2, v=2:								
J=0	9.7(11)	9.6(11)	9.3(11)	9.6(11)	9.7(11)	8.5(11)	5.4(11)	...
J=1	2.5(12)	2.4(12)	2.2(12)	2.3(12)	2.5(12)	2.4(12)	1.4(12)	...
J=2	2.5(12)	2.4(12)	2.3(12)	2.4(12)	2.4(12)	2.1(12)	1.4(12)	...
J=3	2.2(12)	2.1(12)	2.0(12)	2.1(12)	2.3(12)	2.2(12)	1.2(12)	...
HD:								
J=0	0.94	0.96	0.96	0.93	0.97	0.97	0.98	...
J=1	5.8(-2)	3.5(-2)	3.6(-2)	7.2(-2)	3.4(-2)	2.6(-2)	1.9(-2)	...
J=2	1.7(-4)	6.4(-5)	6.1(-5)	1.8(-4)	1.0(-4)	4.7(-5)	2.8(-5)	...
C^+:								
$J=\frac{1}{2}$	0.97	0.97	0.97	0.95	0.98	0.97	0.98	...
$J=\frac{3}{2}$	0.03	0.03	0.03	0.05	0.02	0.03	0.02	...
C:								
J=0	0.63	0.62	0.61	0.50	0.73	0.66	0.73	(0.91±0.10)[e]
J=1	0.31	0.32	0.33	0.40	0.23	0.29	0.23	(0.05±0.04)[e]
J=2	0.06	0.06	0.06	0.10	0.04	0.05	0.04	(0.04±0.02)[e]
O:								
J=2	1.0	1.0	1.0	1.0	1.0	1.0	1.0	1.0
J=1	5.5(-6)	6.9(-6)	9.5(-6)	8.6(-6)	3.8(-6)	8.7(-6)	6.5(-6)	(1.6±0.5)(-5)[c]
J=0	1.6(-6)	2.4(-6)	3.9(-6)	2.3(-6)	1.2(-6)	3.3(-6)	2.6(-6)	...
A_V^{tot}	1.01	1.02	0.97	0.99	0.98	1.02	1.03	1.0

[a] All models have $\zeta_0 = 5\times10^{-17}$ s^{-1} and use the H–H_2 collisional rates of Green and Truhlar 1979. See Table 11 for total column densities of HD, C^+, C, and O.

[b] Model assumes that the H_2 molecules are formed rotationally hot with 1.5 eV of internal energy distributed statistically over all levels.

[c] Snow 1977; the errors for $H_2(J = 2–4)$ may be underestimated.

[d] Savage *et al.* 1977.

[e] Jenkins and Shava 1979.

the polytropic index Γ in the models lies in the range -1.2 to -1.5, and is roughly consistent with the equations of state in the centers of such clouds calculated, e.g., by de Jong, Dalgarno, and Boland (1980).

In the above models, the scaling factor for the H_2 formation rate was assumed to be $y_f = 1.0$. Since the parameter y_f incorporates several ill-determined properties of the grains, it is uncertain by a factor of 2. If we allow y_f to be smaller than unity in the models by a certain factor, the density needs to be increased by the same factor in order to reproduce the observed N(H). An example of such a model is included in Table 4 (compare models D and A). On the other hand, the H_2 formation rate in the ζ Per cloud may also be larger than average, since the ultraviolet extinction curve suggests an overabundance of small grains in the cloud (Snow 1977) and hence a larger ratio of surface area to grain mass (Snow 1983).

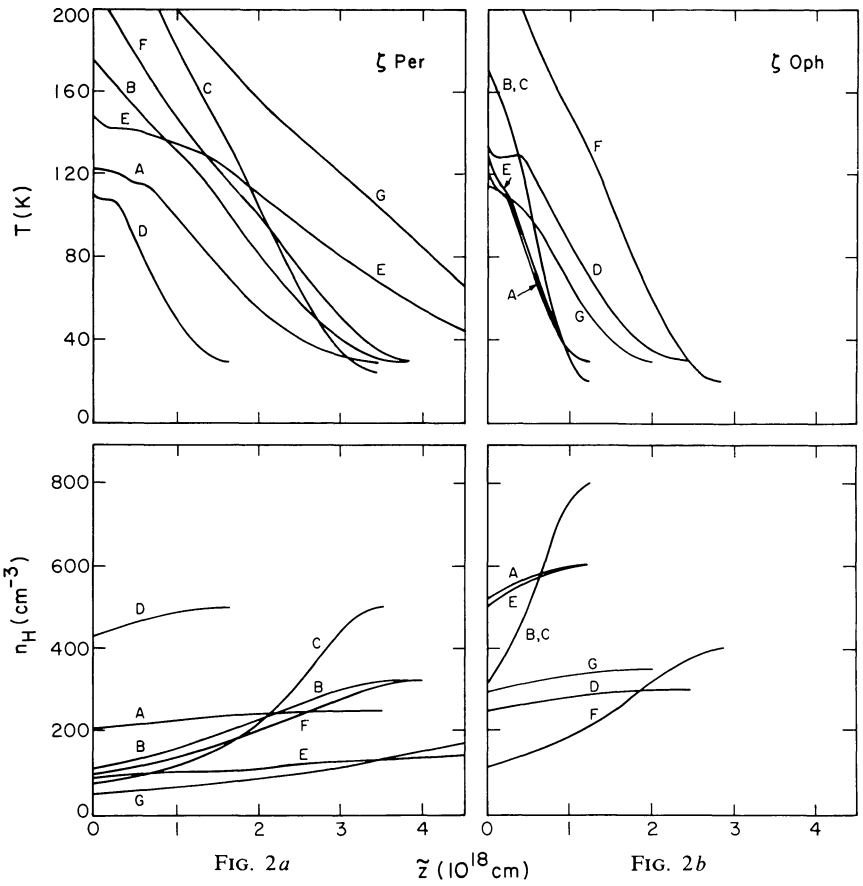

FIG. 2a FIG. 2b

FIG. 2.—The temperature T and total density n_H as functions of depth in the models of the cloud toward (*a*) ζ Per, (*b*) ζ Oph, (*c*) χ Oph, and (*d*) o Per. The edge of the cloud is at $\tilde{z} = 0$. Models E and G of the ζ Per cloud extend to 6.2×10^{18} cm. Model F of the χ Oph cloud extends to 5.7×10^{18} cm.

A model with $y_f = 2.0$, and consequently a low density $n_H \approx 150$ cm^{-3}, is also presented in the table (see model E).

Although the populations of the lower rotational levels $J \leq 4$ are not sensitive to the assumptions about the initial distribution of the newly formed H_2 molecules on grains, the populations of the higher levels $J \geq 5$ show some dependence. Model G in Table 4 assumes that 1.5 eV of the binding energy liberated on formation of H_2 is distributed statistically over all vibration-rotation levels. In this model the H_2 molecules are thus formed not only vibrationally hot, but also rotationally. If the same physical parameters as in model F were employed, the populations of the vibrationally excited levels would vary by less than 10%, but the resulting column density in $v = 0$, $J = 5$ would be increased by 60%, and in $v = 0$, $J = 6$ and $J = 7$ by as much as factors of 2 and 6, respectively (compare also models C18 and C4 in Table 3). Model G therefore allows a less intense ultraviolet radiation field, $I_{UV} \approx 2.2$ instead of $I_{UV} = 3.5$ for grain model 2 (1.1 instead of 2.0 for grain model 3), and consequently a somewhat lower central density, $(n_H)_0 \approx 225$ cm^{-3} instead of 325 cm^{-3}, to be consistent with the observed column densities.

The inferred central temperature and density in the new models for the ζ Per cloud do not differ significantly from the values obtained by BHD. However, the scaling factor for the radiation field is about 2–3 times as large as in the BHD model. Also, the thickness of the warm envelope is generally reduced in the new models. Both these differences will have important effects on the chemistry of certain species, notably the oxygen-bearing molecules such as OH, H_2O, and CO, whose formation results in part from the temperature-sensitive $H^+ + O$ charge-transfer reaction.

The physical parameters in the cloud may also be derived from other atomic and molecular observations. From considerations of the ionization equilibria in atoms, Snow (1977) finds $n_H \approx 270$–760 cm^{-3}, where his inferred electron density $n_e \approx 0.12$ cm^{-3} is slightly larger than the density $n_e \approx 0.10$ cm^{-3} obtained in the present models. His analysis of the measured CO rotational temperature gives $n_H \approx 100$–910 cm^{-3} (cf. BHD). Our reanalysis of the CO excitation indicates that densities $n(H_2) = 100$–200 cm^{-3}, corresponding to $n_H = 200$–500 cm^{-3}, are consistent with the observed excitation temperature $T_{ex} \approx 4$ K.

The fine-structure populations of the neutral carbon atom C have been interpreted with a much lower density, $n_H \approx 30$ cm^{-3} for $T = 45$ K (Jenkins, Jura, and Loewenstein 1983). The inferred low density stems mainly from the fact that the observed column density of C in $J = 1$ is anomalously small in the ζ Per cloud. The fine-structure excitation of C is calculated as a function of depth in our models, and the resulting column density ratios are included in Table 4. They are in reasonable agreement with observations for $J = 0$ and $J = 2$. The large calculated column density in $J = 1$ compared

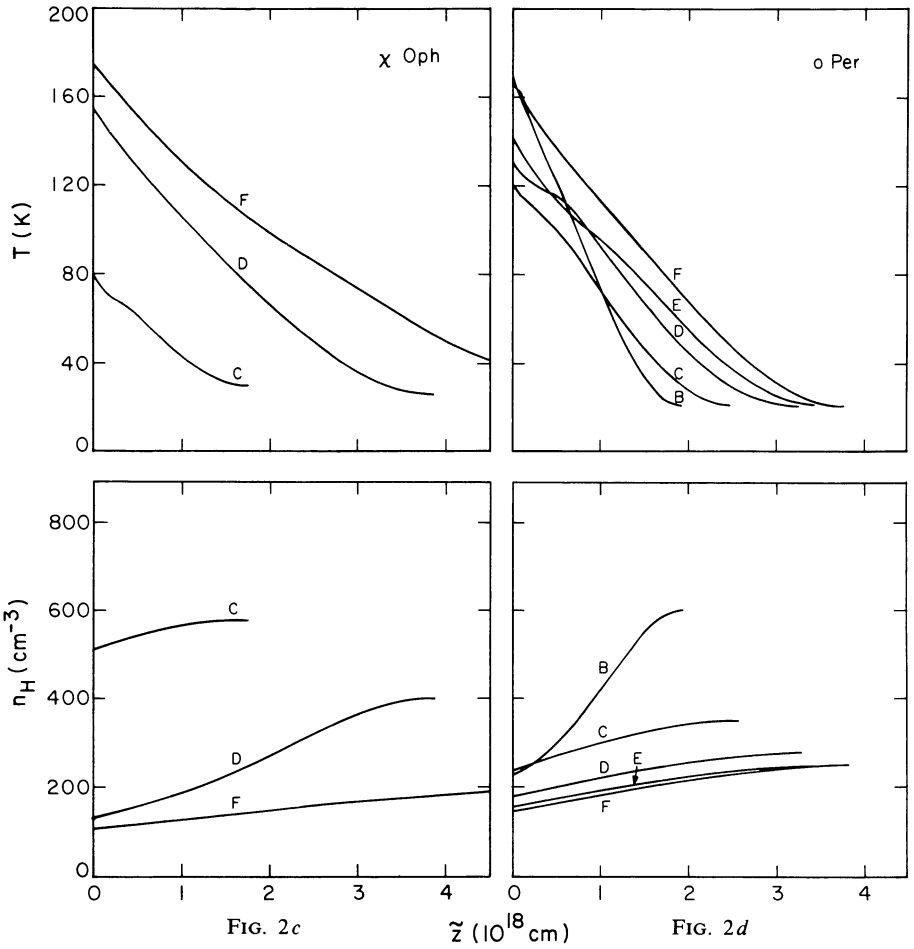

FIG. 2c FIG. 2d

FIG. 2—*Continued*

with observations indicates that—unless the observed value is in error—the temperature and the density in the outer region of the cloud are too high. The computed fine-structure populations of the O and C^+ atoms in the models are in reasonable agreement with the (uncertain) observations, as Table 4 shows.

The rotational population of the C_2 molecule may provide a more powerful probe of the physical conditions in the ζ Per cloud. Observations of absorption lines of interstellar C_2 toward ζ Per arising from rotational levels up to $J=12$ have been presented by Hobbs (1979) and Chaffee *et al.* (1980). The measured populations have been interpreted by van Dishoeck and Black (1982) and van Dishoeck (1984) with an excitation parameter $n_c\sigma_0/I_R \approx (4\pm2)\times10^{-14}$ cm^{-1} and a temperature $T \approx 30$–40 K. It is plausible that $I_R \approx 1$ in the far-red, since there is generally no indication of strong infrared sources near the diffuse clouds. Since σ_0 is not well known, van Dishoeck and Black (1982) assumed $n_c \approx 200$ cm^{-3} and $I_R \approx 1$ for the ζ Per cloud, and calibrated $\sigma_0 \approx 2\times10^{-16}$ cm^2 from the astronomical observations, a value which was used in all subsequent analyses of C_2 observations in other directions. Alternatively, it is reasonable to assume that the cross section lies in the range $\sigma_0 \approx (1$–$5)\times10^{-16}$ cm^2, which, together with $I_R \approx 1$, implies $n_H \approx 150$–500 cm^{-3}.

It is thus concluded that the density in the ζ Per cloud, as derived from the H/H_2 column density ratio, is uncertain by a factor of at least 2 because of uncertainties in the H_2 formation rate, the population distribution of H_2 upon formation, and the Doppler parameter. The strength of the ultraviolet radiation field is somewhat better determined, given the grain scattering and H_2 formation properties. The central temperature in the cloud seems well constrained by the observations, although the temperature in the outer region may have been overestimated in the models. The observed C_2 and CO rotational excitations, and the atomic fine-structure excitations, are consistent with the density $n_H \approx 150$–500 cm^{-3} inferred from the H_2 observations, but the uncertainties both in the molecular parameters entering the analyses and in the observations do not permit more accurate constraints on the density in the ζ Per cloud.

d) The ζ Oph Cloud

Following the same procedure as described for the ζ Per cloud, we constructed new models which reproduce the observed column densities of H and $H_2(J)$ toward ζ Oph. They are listed in Table 5 for various values of the parameters. The temperature and density structure in the models is illustrated in Figure 2*b*. Since the higher rotational levels are more populated toward ζ Oph than toward ζ Per, the value of the scaling factor for the radiation field I_{UV} is considerably larger in this case. Since the observed N(H) values are similar in the two directions, the H_2/H abundance ratio suggests that the density must be significantly higher in the ζ Oph cloud than

in the ζ Per cloud. Similar results were obtained by BD and BHD. The derived central densities in this work, $n_H \approx 600$–800 cm^{-3} assuming $y_f = 1$ (models A–C), however, are a factor of 3 lower than the central density $n_H = 2500$ cm^{-3} found by BD with an even larger H_2 formation rate. The extent of the warm envelope is again substantially reduced in this work compared with that found by BD. Similarly to the case of the ζ Per cloud, models with higher central densities may be constructed if $y_f < 1$, and models with lower densities if $y_f > 1$. Some models with $y_f = 2$ are included in Table 5 (see models D and F).

The agreement between the models and the observations is not as good for the ζ Oph cloud as for the ζ Per cloud, especially for the levels $J = 2$, $J = 4$, and $J = 7$. The column

TABLE 5

CALCULATED COLUMN DENSITIES (cm^{-2}) OF H AND $H_2(v, J)$ AND RELATIVE POPULATIONS OF HD(J), $C^+(J)$, C(J), AND O(J) IN MODELS OF CLOUD IN FRONT OF ζ OPH

Parameters and Species	Model[a] A	B	C	D	E	F	G[b]	H[b]	Observed
$(n_H)_0$ (cm^{-3})	600	800	800	300	600	400	350	225	
T_0 (K)	30	20	20	30	30	20	30	30	
b (km s^{-1})	3.0	1.2	1.2	3.0	3.0	1.2	3.0	3.0	
I_{UV}	4.0	4.0	4.0	4.0	6.5	6.5	3.5	2.2	
y_f	1.0	1.0	1.0	2.0	1.0	2.0	1.0	1.0	
Γ	-1.12	-1.08	-1.08	-1.20	-1.10	-1.14	-1.18	-1.27	
Grain model	3	3	3	3	2	2	2	2	
Collisional rates[c]	GT	GT	AD	GT	GT	GT	GT	GT	
H	5.4(20)	5.3(20)	5.4(20)	5.3(20)	5.2(20)	5.6(20)	5.1(20)	5.0(20)	(5.2±0.2)(20)[d]
H_2	4.2(20)	4.2(20)	4.2(20)	4.2(20)	4.2(20)	4.2(20)	4.2(20)	4.2(20)	(4.2±0.3)(20)[e]
H_2, v=0:									
J=0	2.8(20)	2.9(20)	2.9(20)	2.7(20)	2.8(20)	2.9(20)	2.9(20)	2.9(20)	(2.9±0.3)(20)[e]
J=1	1.4(20)	1.3(20)	1.3(20)	1.5(20)	1.4(20)	1.2(20)	1.3(20)	1.3(20)	(1.3±0.2)(20)[e]
J=2	1.3(18)	1.9(18)	2.5(18)	1.7(18)	1.3(18)	2.6(18)	8.3(17)	7.5(17)	(4.0±1.6)(18)[e]
J=3	3.6(16)	6.7(16)	1.4(17)	5.1(16)	3.9(16)	1.5(17)	2.2(16)	1.6(16)	(1.7±1.2)(17)[e]
J=4	2.6(15)	2.7(15)	2.6(15)	2.6(15)	2.4(15)	2.6(15)	1.5(15)	1.0(15)	(5.3±2.2)(15)[e]
J=5	4.4(14)	4.2(14)	4.1(14)	4.6(14)	4.7(14)	4.4(14)	4.5(14)	2.9(14)	(4.3±0.5)(14)[e]
J=6	5.7(13)	5.6(13)	5.6(13)	5.7(13)	5.7(13)	5.2(13)	5.3(13)	3.4(13)	(4.9±0.5)(13)[e]
J=7	1.1(13)	1.0(13)	1.0(13)	1.2(13)	1.2(13)	1.1(13)	3.8(13)	2.4(13)	(3.6±0.4)(13)[e]
J=8	1.3(12)	1.2(12)	1.2(12)	1.3(12)	1.3(12)	1.2(12)	4.7(12)	3.0(12)	...
J=9	2.1(11)	2.0(11)	2.0(11)	2.2(11)	2.3(11)	2.1(11)	6.5(12)	4.1(12)	...
H_2, v=1:									
J=0	4.6(12)	4.6(12)	4.7(12)	4.6(12)	4.4(12)	4.1(12)	2.3(12)	1.4(12)	<7.0(12)[d]
J=1	1.2(13)	1.1(13)	1.1(13)	1.2(13)	1.2(13)	1.1(13)	5.5(12)	3.5(12)	<1.2(13)[d]
J=2	1.2(13)	1.2(13)	1.2(13)	1.2(13)	1.2(13)	1.1(13)	6.0(12)	3.7(12)	<1.0(13)[d]
J=3	1.1(13)	1.0(13)	1.0(13)	1.2(13)	1.2(13)	1.1(13)	5.2(12)	3.3(12)	...
H_2, v=2:									
J=0	2.0(12)	2.0(12)	2.0(12)	1.9(12)	1.9(12)	1.7(12)	9.5(11)	6.0(11)	<4.4(12)[d]
J=1	4.8(12)	4.6(12)	4.6(12)	5.1(12)	5.1(12)	4.7(12)	2.2(12)	1.4(12)	...
J=2	4.7(12)	4.9(12)	5.0(12)	4.9(12)	4.8(12)	4.5(12)	2.4(12)	1.5(12)	...
J=3	4.4(12)	4.1(12)	4.2(12)	4.6(12)	4.7(12)	4.3(12)	2.0(12)	1.3(12)	...
HD:									
J=0	0.86	0.87	0.87	0.89	0.89	0.93	0.92	0.95	0.88:[f]
J=1	1.4(-1)	1.3(-1)	1.3(-1)	1.1(-1)	1.1(-1)	6.6(-2)	7.5(-2)	5.5(-2)	1.3(-1):[f]
J=2	1.1(-3)	8.0(-4)	7.7(-4)	8.5(-4)	7.3(-4)	4.0(-4)	3.5(-4)	2.0(-4)	<1.2(-1)[f]
C^+:									
$J=\frac{1}{2}$	0.94	0.94	0.94	0.96	0.93	0.96	0.96	0.97	(0.99±0.1)[d]
$J=\frac{3}{2}$	0.06	0.06	0.06	0.04	0.07	0.04	0.04	0.03	(0.01±0.1)[d]
C:									
J=0	0.47	0.52	0.52	0.58	0.50	0.68	0.60	0.68	(0.63±0.06)[g]
J=1	0.41	0.39	0.39	0.34	0.40	0.28	0.33	0.27	(0.31±0.09)[g]
J=2	0.12	0.09	0.09	0.08	0.10	0.04	0.07	0.05	(0.06±0.02)[g]
O:									
J=2	1.0	1.0	1.0	1.0	1.0	1.0	1.0	1.0	1.0
J=1	1.1(-5)	1.7(-5)	1.8(-5)	8.6(-6)	1.6(-5)	1.3(-5)	7.2(-6)	4.9(-6)	<1(-5)[d]
J=0	3.2(-6)	6.2(-6)	6.3(-6)	2.7(-6)	4.6(-6)	5.4(-6)	2.0(-6)	1.4(-6)	...
A_V^{tot}	0.87	0.86	0.87	0.86	0.86	0.88	0.84	0.83	1.0

[a] All models have $\zeta_0 = 5 \times 10^{-17}$ s^{-1}. See Table 12 for total column densities of HD, C^+, C, and O.
[b] See footnote *b* to Table 4.
[c] Employed H–H_2 collisional rates; GT: Green and Truhlar 1979; AD: Allison and Dalgarno 1967.
[d] Morton 1975.
[e] Spitzer, Cochran, and Hirschfeld 1974; Spitzer and Morton 1976; and Savage *et al.* 1977.
[f] Wright and Morton 1979; see text.
[g] de Boer and Morton 1979.

density for $J = 2$ is sensitive to the employed collisional rates, and the high observed value is more easily reproduced with the H–H_2 collisional rates of Allison and Dalgarno (1967) than with the smaller rates of Green and Truhlar (1979), as models B and C demonstrate. All models in Table 5 have a rather low column density in $J = 4$. Moreover, as may be concluded from Table 3, it may not be possible to construct *any* reasonable model, even with a constant $T = 100$ K, with a column density in $J = 4$ as high as 5×10^{15} cm^{-2}. Although the observed $J = 7$ column density is based only upon a single line, the factor of 2–3 disagreement with the theoretical value is significant. The discrepancy for this level is probably caused by the assumption about the initial distribution of the newly formed H_2 molecules on grains, as discussed in § V*c*. As model G shows, the calculated column density in $J = 7$ may be consistent with observations if the molecules are formed with a significant amount of rotational excitation. The ultraviolet radiation field can be reduced to $I_{UV} \approx 3.5$ for grain model 2 ($I_{UV} \approx 2.2$ for grain model 3), and the central density from 600 to 350 cm^{-3} in this model, in order to reproduce the observed column densities in $J = 5$, $J = 6$, and $J = 7$. The calculated column densities in vibrationally excited levels are consistent with, but close to, the observed upper limits for all models, indicating that the scaling factor for the ultraviolet radiation field is unlikely to be larger than $I_{UV} \approx 4$ for grain model 3. Further searches for lines arising from $J > 7$ or from vibrationally excited levels would provide significant tests of the present calculations.

There have been numerous other attempts to determine the physical conditions in the cloud toward ζ Oph, which are summarized in Table 6. Herbig (1968), in his classic paper on the spectrum of ζ Oph, inferred a density $n_H \approx 500$–900 cm^{-3} from the Na/H abundance ratio, under the assumption that Na is undepleted from the gas. Morton (1975) derived a high density $n_H \approx 10^4$ cm^{-3} at $T = 56$ K from the ionization equilibria in atoms. His inferred electron density $n_e \approx 0.7$ cm^{-3} was obtained using large Doppler parameters $b \approx 6$ km s^{-1} in the conversion of equivalent widths to column densities. It has been argued (de Boer 1979) that a smaller ion velocity dispersion is appropriate for the principal cloud component. Therefore, the column densities of Morton for many atomic ions may be too small, and the densities inferred from the resulting ionization balance too large.

De Jong (1980) constructed a model which is in thermal balance and in pressure equilibrium, and obtained a temperature varying from $T = 105$ K at the edge to $T = 40$ K at the center of the cloud, with a density ranging between 400 and 1900 cm^{-3}. The (constant) pressure in his model was fixed by reproducing the observed C column density, although his assumed carbon depletion factor, $\delta_C = 0.25$, has since been shown to be too low (see §§ VI and VII), resulting again in too large densities.

The fine-structure populations of C were originally interpreted with $n_H \approx 220$–660 cm^{-3} (de Boer and Morton 1974), whereas more recent data (Jenkins, Jura, and Loewenstein 1983) yield a thermal pressure $n_H T = 5 \times 10^3 - 2 \times 10^4$ cm^{-3} K for $10 < T < 300$ K. At $T = 80$ K, this pressure implies $n_H \approx 100$ cm^{-3}, while at $T = 20$ K, $n_H \approx 800$ cm^{-3} is obtained. Our calculations of the C fine-structure excitation are included in Table 5 and are reasonably consistent with observations. The C^+ fine-structure excitation has been measured by Morton (1975). A proper treatment of the curve of growth for the 1335.7 Å blend of $C^+(^2P_{3/2})$ lines suggests that the $C^+(J = \frac{3}{2})$ column density should be significantly larger than Morton's tabulated value, in harmony with the calculated results of the present models. Morton (1975) also listed an upper limit on the $O(J = 1)$ column density. As Table 5 shows, our calculated column density in $J = 1$ is in somewhat better agreement with the models of lowest density, although the uncertainties in the excitation calculation do not allow the higher density models to be excluded.

Jura (1975) obtained $n_H \approx 700$ cm^{-3} at $T = 75$ K from the $H_2(J = 4)$/H column density ratio, but noted that the ratio $H_2(J = 6)$/H would give a factor of 3 smaller density (Jenkins,

TABLE 6

PHYSICAL CONDITIONS IN THE ζ OPH CLOUD AS DERIVED FROM VARIOUS OBSERVATIONS

CORE		ENVELOPE			
n_H (cm^{-3})	T (K)	n_H (cm^{-3})	T (K)	REFERENCE	METHOD[a]
500–900	...	...	...	Herbig 1968	Na/H
10000	56	...	...	Morton 1975	Electron density
220–660	...	...	...	de Boer and Morton 1974	$C(J)$
700	75	...	...	Jura 1975	$H_2(J = 4)$/H
2500	22	500	110	Black and Dalgarno 1977	$H_2(J)$, H_2/H
1900	40	400	105	de Jong 1980	Thermal + hydrostatic balance, C/(H + H_2)
< 400	60[b]	...	...	Liszt 1979	$CO(J)$
				Smith, Krishna Swamy, and Stecher 1978	
200	65	200	150	Crutcher and Watson 1981	$^{12}CO/^{13}CO$
100–1000	100–20[c]	...	...	Jenkins, Jura, and Loewenstein 1983	$C(J)$
250	75	...	...	Jenkins, Jura, and Loewenstein 1983	$H_2(J = 6)$/H
300–800	25	100–500	100–200	This work	H_2(J), H_2/H
200–500	25	...	...	This work	$C_2(J)$

[a] See text for a discussion of the methods.
[b] $T = 60$ K is assumed; only an upper limit to the product $n(H_2)T$ is given.
[c] Only the pressure $n_H T$ is given.

Jura, and Loewenstein 1983). Our more extensive treatment of the H_2/H abundance equilibrium gives similar results if Jura's larger H_2 formation rate is employed.

The pressure in the ζ Oph cloud may also be inferred from the observed CO rotational population. Smith, Krishna Swamy, and Stecher (1978) derived $n(H_2)T \approx 3 \times 10^3$ cm^{-3} K, whereas Liszt (1979) obtained a conservative upper limit $n(H_2)T < 8 \times 10^3$ cm^{-3} K for the region of the cloud where the CO is predominant. If we take $T \approx 60$ K and $n(H) \approx n(H_2)$ for this region, as the models suggest, we find $n_H < 400$ cm^{-3}. As for the ζ Per cloud, the observed excitation temperature $T_{ex} \approx 4$ K implies $n(H_2) \approx 100$–200 cm^{-3} in our new analysis, corresponding to $n_H \approx 200$–500 cm^{-3}.

Finally, the temperature and density may be derived from the observed rotational population of C_2. Observations of interstellar C_2 toward ζ Oph have been performed most recently by Hobbs and Campbell (1982) and Danks and Lambert (1983). The relative populations derived from the two sets of observations agree rather well, except for $J = 0$ and $J = 4$. The fact that the observations show a scatter in the $J = 0/J = 2$ C_2 column density ratio is unfortunate, because this ratio provides the principal constraint on the inferred temperature in the cloud. The C_2 data of Hobbs and Campbell imply a high temperature, $T \approx 50$ K, although their observed column densities are rather uncertain. On the contrary, the measured ratio of Danks and Lambert implies $T \approx 25$ K, in harmony with the central temperature derived from the H_2 excitation. A strong argument in favor of this low temperature is given by the fact that *all* individual sets of observations by Danks and Lambert, obtained on three different nights, indicate $T \approx 25$ K within a very narrow range. Unless the continuum for one of their lines is systematically misplaced, the data clearly indicate a low temperature in the region where the C_2 exists. Recent observations of C_2 in the (3, 0) band of the Phillips system confirm the low temperature (van Dishoeck and Black 1984, 1986*a*). Since in the models the C_2 molecules are concentrated in the center of the cloud, as Figure 3 demonstrates (see § VII), the C_2 column-averaged temperature is close to the central temperature.

With $T \approx 25$ K, the C_2 excitation in the ζ Oph cloud is very similar to that for the ζ Per cloud, and the best fit is obtained for $n_c\sigma_0/I_R \approx (3 \pm 1) \times 10^{-14}$ cm^{-1} (van Dishoeck and Black 1986*a*). If $I_R \approx 1$ and $\sigma_0 \approx 2 \times 10^{-16}$ cm^2 is assumed, i.e., the parameters for which the C_2 analysis is consistent with the H_2 analysis for the ζ Per cloud, a density $n_c \approx 100$–200 cm^{-3}, corresponding to $n_H \approx 200$–350 cm^{-3}, is inferred for the ζ Oph cloud. This density is significantly smaller than $n_H \approx 600$–800 cm^{-3} found from the H_2 analysis with $y_f \approx 1$.

Crutcher and Watson (1981, hereafter CW) suggested a uniform temperature $T \approx 65$ K and density $n_H \approx 200$ cm^{-3} for the ζ Oph cloud based on upper limits on the observed $^{13}CO/^{12}CO$ abundance ratio, together with a reinterpretation of the CO and HD rotational excitations and the C fine-structure excitation. The main argument in favor of a high central temperature was based on their treatment of the $^{13}CO/^{12}CO$ isotope fractionation. In arguing against a $T = 20$ K central temperature, however, they misrepresented the BD model by incorrectly attributing all of the CO in it to the coldest zone at $T = 22$ K, whereas the BD model would actually predict a weighted, column-averaged temperature,

$$T_{CO} = \int n(CO)\, T\, dz \Big/ \int n(CO)\, dz \approx 60 \text{ K}, \qquad (29)$$

that is consistent with their results. In our models as well, the CO is broadly distributed in the cloud, with an average temperature $T_{CO} \approx 60$ K (cf. Fig. 3). CW also did not consider the depth dependences of the species, and they neglected the possibility of isotope-selective photodissociation of CO (Bally and Langer 1982; Chu and Watson 1983). The observed $^{13}CO/^{12}CO$ abundance ratio therefore does not appear to be in conflict with the present models, which have $T_0 \approx 25$–30 K. Because of uncertainties in the ^{12}CO and ^{13}CO photodissociation rates, it is not yet possible to obtain conclusive results from our models. The low density $n_H \approx 200$ cm^{-3} obtained by CW is not in conflict with our interpretations of the CO, C, and C_2 excitations. As shown in Table 5 and discussed in § VII*d*, the HD excitation is also well reproduced in our models.

It is thus concluded that the $H_2(J)$ and H observations yield densities in the ζ Oph cloud which are generally somewhat higher than the densities inferred from other observations, in particular those of C_2. Several possible explanations for this discrepancy will be discussed in § V*g*.

e) The χ Oph Cloud

Table 7 lists the models that were constructed to reproduce the observed H and $H_2(J)$ data toward χ Oph. The uncertainties in the observed column densities for $J = 2$ and $J = 3$ of H_2 are so large in this case that the data can already be fitted with a model which has a constant density and temperature as a function of depth, $T \approx 45$ K and $n_H \approx 325$–650 cm^{-3} for $y_f = 1$ (models A, B, and E). The high $J = 5$ level is even more populous toward χ Oph than toward ζ Oph and suggests an intense radiation field with a scaling factor $I_{UV} > 5$ for grain model 3. Since, in addition, the observed $N(H)$ is much larger toward χ Oph than toward ζ Oph, the density does not need to be increased by the same amount. The models predict a column density in $J = 2$ comparable to that for ζ Oph and ζ Per. A model with a lower density and $y_f \approx 2$ is also presented in the table (see model F).

We have also constructed models with an additional warm envelope, although not required by the observations (models C–D). The temperature and density structure in these models is illustrated in Figure 2*c*. However, the low excitation temperature characterizing the $J = 0$ and $J = 1$ population ratios precludes a large warm zone, so that the results of the polytropic models do not differ significantly from those of the constant models.

Although the total H_2 column density toward χ Oph listed by Savage *et al.* (1977) is close to that measured for the other three clouds, the uncertainties allow a 50% larger H_2 column density. Model G in Table 7 has been constructed to match the upper limit.

A detailed discussion of the physical conditions in the χ Oph cloud as derived from observations of other species has

TABLE 7

CALCULATED COLUMN DENSITIES (cm^{-2}) OF H AND $H_2(v, J)$ AND RELATIVE POPULATIONS OF HD(J), $C^+(J)$, C(J), AND O(J) IN MODELS OF CLOUD IN FRONT OF χ OPH

Parameters and Species	Model[a] A	B	C	D	E	F	G[b]	Observed
$(n_H)_0$ (cm^{-3}) ..	325	520	575	400	520	200	300	
T_0 (K)	45	45	30	25	45	30	45	
b (km s^{-1})	3.0	3.0	3.0	1.2	3.0	2.0	3.0	
I_{UV}	5.0	8.0	8.0	5.0	12.0	10.0	9.0	
y_f	1.0	1.0	1.0	1.0	1.0	2.0	1.0	
Γ	[c]	[c]	-1.40	-1.45	[c]	-1.50	[c]	
Grain model	3	3	3	3	2	2	2	
H	1.2(21)	1.2(21)	1.1(21)	1.2(21)	1.1(21)	1.0(21)	1.2(21)	(1.2±0.2)(21)[d]
H_2	4.2(20)	4.2(20)	4.2(20)	4.2(20)	4.2(20)	4.2(20)	6.0(20)	(4.2±1.5)(20)[e]
H_2, v=0:								
J=0	3.4(20)	3.4(20)	3.5(20)	3.4(20)	3.4(20)	3.2(20)	4.9(20)	(3.4±1.5)(20)[e]
J=1	7.5(19)	7.8(19)	7.3(19)	7.9(19)	7.7(19)	1.0(20)	1.1(20)	(8.0±3.4)(19)[e]
J=2	3.8(17)	4.7(17)	4.8(17)	5.3(17)	3.7(17)	6.2(17)	3.2(17)	...
J=3	2.3(16)	3.5(16)	3.6(16)	2.7(16)	2.8(16)	3.4(16)	2.2(16)	(1.4±1.2)(17)[d]
J=4	3.1(15)	4.8(15)	4.9(15)	3.0(15)	3.9(15)	2.8(15)	2.8(15)	(3.7±1.8)(15)[d]
J=5	3.8(14)	6.0(14)	6.2(14)	3.9(14)	5.3(14)	4.9(14)	6.5(14)	(7.6±1.7)(14)[d]
J=6	6.7(13)	1.1(14)	1.1(14)	6.1(13)	9.2(13)	6.1(13)	9.5(13)	<2.1(14)[d]
J=7	9.9(12)	1.6(13)	1.7(13)	9.6(12)	1.5(13)	1.3(13)	6.1(13)	...
J=8	1.5(12)	2.4(12)	2.5(12)	1.3(12)	2.1(12)	1.4(12)	8.0(12)	...
J=9	1.9(11)	3.3(11)	3.4(11)	1.8(11)	3.0(11)	2.4(11)	1.1(13)	...
H_2, v=1:								
J=0	5.6(12)	8.9(12)	9.0(12)	5.2(12)	7.3(12)	4.8(12)	4.4(12)	...
J=1	9.8(12)	1.6(13)	1.6(13)	1.0(13)	1.4(13)	1.3(13)	7.0(12)	...
J=2	1.5(13)	2.3(13)	2.4(13)	1.4(13)	1.9(13)	1.3(13)	1.2(13)	...
J=3	9.5(12)	1.5(13)	1.6(13)	9.5(12)	1.4(13)	1.2(13)	6.9(12)	...
H_2, v=2:								
J=0	2.3(12)	3.8(12)	3.8(12)	2.2(12)	3.1(12)	2.0(12)	1.8(12)	...
J=1	4.1(12)	6.7(12)	6.9(12)	4.2(12)	5.8(12)	5.3(12)	2.8(12)	...
J=2	5.9(12)	9.5(12)	9.6(12)	5.5(12)	7.8(12)	5.2(12)	4.6(12)	...
J=3	3.8(12)	6.2(12)	6.4(12)	3.8(12)	5.5(12)	4.9(12)	2.6(12)	...
HD:								
J=0	0.96	0.94	0.92	0.97	0.96	0.97	0.98	...
J=1	4.0(-2)	5.8(-2)	7.6(-2)	3.4(-2)	4.3(-2)	3.1(-2)	2.4(-2)	...
J=2	4.9(-4)	1.1(-3)	1.3(-3)	1.8(-4)	3.1(-4)	2.5(-4)	5.8(-5)	...
C^+:								
$J=\frac{1}{2}$	0.97	0.96	0.95	0.97	0.96	0.97	0.98	0.50:[d]
$J=\frac{3}{2}$	0.03	0.04	0.05	0.03	0.04	0.03	0.02	0.50:[d]
C:								
J=0	0.53	0.46	0.47	0.58	0.48	0.69	0.61	(0.73±0.10)[f]
J=1	0.38	0.42	0.41	0.35	0.42	0.27	0.33	(0.18±0.10)[f]
J=2	0.09	0.12	0.12	0.07	0.10	0.04	0.06	(0.09±0.05)[f]
O:								
J=2	1.0	1.0	1.0	1.0	1.0	1.0	1.0	1.0
J=1	6.8(-7)	1.1(-6)	3.3(-6)	5.5(-6)	1.0(-6)	6.1(-6)	5.5(-7)	...
J=0	8.9(-8)	1.4(-7)	6.5(-7)	1.7(-6)	1.4(-7)	2.1(-6)	7.1(-8)	...
A_V^{tot}	1.29	1.30	1.22	1.30	1.21	1.17	1.50	1.5

[a] All models have $\zeta_0 = 5\times10^{-17}$ s^{-1}, and use the H–H_2 collisional rates of Green and Truhlar 1979. See Table 13 for total column densities of HD, C^+, C, and O.

[b] See footnote *b* to Table 4.

[c] These models have a constant temperature and density structure.

[d] Frisch 1979, 1980.

[e] Savage *et al.* 1977.

[f] Jenkins, Jura, and Loewenstein 1983.

been given by van Dishoeck and de Zeeuw (1984). The best additional constraints on the temperature and density were obtained from observations of the C_2 molecule. The C_2 rotational excitation toward χ Oph, as measured by van Dishoeck and de Zeeuw (1984) and Danks and Lambert (1983), is again very similar to that observed for the ζ Per and ζ Oph clouds, implying $T \approx 40$ K and $n_c\sigma_0/I_R \approx 3.5\times10^{-14}$ cm^{-1}. For $I_R \approx 1$ and $\sigma_0 \approx 2\times10^{-16}$ cm^2, this results in $n_c \approx 150$–270 cm^{-3} or $n_H \approx 225$–400 cm^{-3}, consistent with the lower density models obtained from the H_2 data.

f) *The o Per Cloud*

Models of the o Per cloud based on the observations of H and $H_2(J)$ are presented in Table 8. The observed column density in the high $J = 5$ level toward o Per is close to that observed toward ζ Oph, so that the same enhancement of the

TABLE 8

CALCULATED COLUMN DENSITIES (cm^{-2}) OF H AND $H_2(v, J)$ AND RELATIVE POPULATIONS OF HD(J), $C^+(J)$, C(J), AND O(J) IN MODELS OF CLOUD IN FRONT OF o PER

Parameters and Species	Model[a]						
	A	B	C	D	E	F[b]	Observed
$(n_H)_0$ (cm^{-3})	530	600	350	275	250	250	
T_0 (K)	48	20	20	20	20	20	
b (km s^{-1})	1.2	1.2	2.0	2.0	2.0	2.0	
I_{UV}	5.0	4.5	3.0	4.5	7.0	4.0	
y_f	1.0	1.0	1.0	2.0	2.0	1.0	
Γ	c	-1.15	-1.26	-1.30	-1.30	-1.28	
Grain model	3	3	3	3	2	2	
Collisional rates[d] ...	GT	AD	AD	GT	GT	GT	
H	7.4(20)	7.8(20)	7.4(20)	7.1(20)	6.9(20)	7.7(20)	(7.4±1.1)(20)[e]
H_2	4.1(20)	4.1(20)	4.1(20)	4.1(20)	4.1(20)	4.1(20)	(4.1±0.2)(20)[f]
H_2, v=0:							
J=0	3.2(20)	3.1(20)	3.1(20)	3.1(20)	3.2(20)	3.1(20)	(3.2±0.2)(20)[f]
J=1	8.8(19)	1.0(20)	9.6(19)	1.0(20)	8.8(19)	9.7(19)	(8.5±0.4)(19)[f]
J=2	3.1(17)	1.4(18)	8.4(17)	8.8(17)	5.9(17)	6.2(17)	(1.0±0.2)(18)[e]
J=3	2.5(16)	5.9(16)	2.2(16)	3.3(16)	2.7(16)	2.1(16)	(3.9±0.4)(17)[e]
J=4	3.2(15)	2.6(15)	1.8(15)	2.9(15)	2.5(15)	1.5(15)	(3.7±2.5)(16)[e]
J=5	4.2(14)	4.1(14)	2.7(14)	4.3(14)	4.0(14)	4.1(14)	(4.1±1.5)(14)[e]
J=6	6.6(13)	5.9(13)	4.1(13)	6.1(13)	5.3(13)	5.0(13)	≤1(14)[e]
J=7	1.0(13)	1.0(13)	6.9(12)	1.1(13)	1.0(13)	3.5(13)	...
J=8	1.4(12)	1.3(12)	8.8(11)	1.3(12)	1.2(12)	4.4(12)	...
J=9	2.0(11)	2.0(11)	1.3(11)	2.1(11)	2.0(11)	6.0(12)	...
H_2, v=1:							
J=0	5.7(12)	5.0(12)	3.4(12)	5.1(12)	4.3(12)	2.2(12)	...
J=1	1.1(13)	1.1(13)	7.2(12)	1.1(13)	1.0(13)	5.0(12)	...
J=2	1.5(13)	1.3(13)	8.9(12)	1.3(13)	1.1(13)	5.7(12)	...
J=3	1.0(13)	1.0(13)	6.8(12)	1.1(13)	9.9(12)	4.7(12)	...
H_2, v=2:							
J=0	2.4(12)	2.1(12)	1.4(12)	2.1(12)	1.8(12)	9.1(11)	...
J=1	4.6(12)	4.5(12)	3.0(12)	4.7(12)	4.3(12)	2.0(12)	...
J=2	6.0(12)	5.3(12)	3.6(12)	5.4(12)	4.6(12)	2.3(12)	...
J=3	4.2(12)	4.1(12)	2.7(12)	4.3(12)	4.0(12)	1.8(12)	...
HD:							
J=0	0.95	0.95	0.96	0.96	0.98	0.98	...
J=1	5.4(-2)	4.8(-2)	4.0(-2)	4.0(-2)	2.0(-2)	2.2(-2)	...
J=2	8.8(-5)	1.5(-4)	1.2(-4)	1.6(-4)	9.3(-5)	5.3(-5)	...
C^+:							
$J=\frac{1}{2}$	0.96	0.95	0.97	0.97	0.97	0.97	0.96:[e]
$J=\frac{3}{2}$	0.04	0.05	0.03	0.03	0.03	0.03	0.04:[e]
C:							
J=0	0.46	0.56	0.62	0.65	0.72	0.71	(0.84±0.05)[e]
J=1	0.42	0.36	0.32	0.30	0.24	0.25	(0.11±0.05)[e]
J=2	0.12	0.08	0.06	0.05	0.04	0.04	(0.05±0.03)[e]
O:							
J=2	1.0	1.0	1.0	1.0	1.0	1.0	1.0
J=1	1.3(-6)	1.2(-5)	5.4(-6)	5.0(-6)	4.9(-6)	7.2(-6)	<1.6(-5)[e]
J=0	1.8(-7)	4.0(-6)	1.5(-6)	1.4(-6)	1.4(-6)	2.4(-6)	...
A_V^{tot}	0.98	1.00	0.98	0.96	0.95	0.99	1.0

[a]All models have $\zeta_0 = 5\times10^{-17}$ s^{-1}. See Table 14 for total column densities of HD, C^+, C, and O.

[b]See footnote *b* to Table 4.

[c]This model has a constant temperature and density structure.

[d]Employed H–H_2 collisional rates; GT: Green and Truhlar 1979; AD: Allison and Dalgarno 1967.

[e]Snow 1976.

[f]Savage *et al.* 1977.

radiation field, $I_{UV} \approx 3$–5 for grain model 3, is found. Since the observed N(H) is only slightly larger toward o Per than toward ζ Oph, the inferred densities are very similar as well. A model with a constant temperature $T = 48$ K and density $n_H \approx 500$–600 cm^{-3} is listed in the table (model A). Also included are several polytropic models, which have $T_0 \approx 20$ K and $(n_H)_0 \approx 350$–600 cm^{-3} if $y_f = 1$ (models B–C), and a lower density if $y_f = 2$ (models D–E). Since the ultraviolet extinction curve indicates an unusually large proportion of small grains in the line of sight toward o Per, as it did toward ζ Per and ζ Oph, the models with $y_f \approx 2$ may be more appropriate. If the H_2 molecules are formed rotationally hot,

I_{UV} may be decreased to $I_{UV} \approx 4$ for grain model 2, and the density from about 550 to about 250 cm^{-3}, as model F demonstrates.

The agreement between the calculated H_2 rotational populations and the observations is not very good for several levels. Although the polytropic models can reproduce the large column density in $J = 2$, where the constant models fail, they give column densities in $J = 3$ and $J = 4$ which are an order of magnitude below the observed values. The measured column densities in $J = 3$ and $J = 4$ are an order of magnitude larger toward o Per than toward the other three clouds studied in this work. Assuming that the Doppler parameter $b \approx 2$ km s^{-1} employed in the analysis of the H_2 observations (Snow 1976) is not significantly too small, the results indicate the presence of a small, very warm, region, which cannot be included in the present polytropic models.

The physical conditions in the new models differ somewhat from those found in previous models of the o Per cloud. Hartquist, Black, and Dalgarno (1978) mention a model with three components with densities ranging from 120 cm^{-3} at the edge to 800 cm^{-3} at the center, temperatures ranging from 500 to 45 K, and an intense ultraviolet radiation field with $I_{UV} \geq 10$, although no further details of the model have been published. Also in this model, the treatment of the radiative transfer in the H_2 lines was incorrect, so that the differences from the new models are not surprising.

Snow (1976) has discussed the physical conditions in the o Per cloud as inferred from other atomic and molecular observations. His analysis of the low rotational temperature of CO observed in the o Per cloud, $T_{ex} \approx 3$ K, gave $n_H < 1650$ cm^{-3}, whereas his interpretation of the C fine-structure lines resulted in densities of a few hundred cm^{-3}. Jenkins, Jura, and Loewenstein (1983) obtained $n_H T < 2.5 \times 10^3$ cm^{-3} K from the C fine-structure excitation, which for $T \approx 40$ K indicates a low density less than 100 cm^{-3}. In our reanalysis of the C excitation, the computed column densities in $J = 0$ and $J = 2$ are in reasonable accord with observation for most models, while the observed column density in $J = 1$ is best reproduced by the models of lower density. The upper limit on O in $J = 1$ is satisfied by all of the models. If the CO rotational temperature is indeed as low as 3 K, a density $n(H_2) \approx 100$ cm^{-3} corresponding to $n_H < 300$ cm^{-3} is implied in our calculations.

The C_2 rotational excitation toward o Per has been measured by Hobbs (1981). Again, the relative populations are virtually identical with those in the ζ Per, ζ Oph, and χ Oph clouds, implying similar conditions, $T \approx 40$ K and $n_c \sigma_0 / I_R \approx 3.5 \times 10^{-14}$ cm^{-1}. For $I_R \approx 1$ and $\sigma_0 \approx 2 \times 10^{-16}$ cm^2, the observational errors allow the range of densities $n_c \approx 100$–400 cm^{-3}, corresponding to $n_H \approx 150$–500 cm^{-3}.

It thus appears that the H_2 excitation and abundance imply somewhat larger densities in the o Per cloud than the other diagnostic species, as was also found for the ζ Oph cloud.

g) Discussion

The models presented in this work are constructed to reproduce the observed atomic and molecular hydrogen column densities. It is found that the density in the clouds as derived from the $N(H)/N(H_2)$ ratio is uncertain by a factor of at least 2, owing to uncertainties in the H_2 grain formation rate, the initial population distribution of H_2 upon formation, and the Doppler parameter. The strength of the ultraviolet interstellar radiation field is also not well determined because of uncertainties in the grain scattering properties and the H_2 formation population distribution. The central temperature is somewhat better constrained in the models.

Since the $N(H)/N(H_2)$ ratio is an important diagnostic of the density in the models, it is crucial to have accurate column densities of these species from observations. The measured values of $N(H)$ for the principal cloud have been determined from fits of damping profiles to the wings of the interstellar Lyman-alpha absorption. The damping wings are sensitive only to the total column density of atomic hydrogen along the line of sight. Although there might be a contribution to the Lyman-alpha absorption from a more extended diffuse component outside the cloud, this is unlikely in the clouds discussed here because of the relative weakness of all interstellar lines at velocities different from those of the principal cloud components.

The density determination also relies heavily on the assumption that the H/H_2 abundances are in steady state. Although the time scale to reach equilibrium for most of the gas-phase chemical reactions in the models is only 10^3 years, the formation time of H_2 on grains varies from less than 10^3 years at the boundary to 5×10^6 years near the cloud center. The latter time scale is comparable to the expected lifetime, 10^7 years, of such a cloud against cloud-cloud collisions, for example (Spitzer 1978). For the ζ Oph cloud the lifetime may be even shorter. Blaauw (1961) noted that ζ Oph is a runaway star, which left the Sco OB2 association only 10^6 years ago. However, since most of the atomic hydrogen exists in the outer region of the cloud where the time scale is shorter, the assumption that the H/H_2 abundance ratio is in steady state may still be realistic. It is not evident what the effects of time dependence on the H/H_2 abundances will be, since the history of the cloud is unknown. Previous treatments of time-dependent H/H_2 abundances have ignored the effects of ultraviolet photodissociation and of depth structure (Allen and Robinson 1976; Iglesias 1977), and discussions of time-dependent chemistry in general ignore the history of the H and H_2 concentrations (Graedel, Langer, and Frerking 1982). Time-dependent hydrodynamical models suggest that dynamical effects will serve to shorten the approach to chemical equilibrium (Gerola and Glassgold 1978).

The assumption that the models are symmetric is not crucial. Some test runs of models with the flux incident on only one side of the cloud gave only slightly different results.

The physical parameters obtained in the models have been compared with those inferred from other observations, in particular those derived from the C_2 rotational excitation. It is significant that for all four clouds studied in this work the observed C_2 excitation is remarkably uniform, suggesting similar physical conditions in the clouds. In contrast, the observed rotational populations of the higher levels of H_2 differ considerably. Since the H_2 excitation is sensitive to the strength of the ultraviolet radiation field, whereas the C_2 excitation is determined by absorptions in the red part of the spectrum, these findings seem to indicate simply that the ultraviolet flux varies more from one region to another than

the flux in the red, a reasonable result. However, since the density determination from the H/H_2 abundances depends on the ratio n_H/I_{UV}, the intense ultraviolet radiation fields suggested for the ζ Oph and o Per clouds require—for the *same* H_2 grain formation rate and distribution—factors of 2–3 larger densities in these clouds than in the ζ Per cloud, in conflict with the results from the C_2 excitation. For the χ Oph cloud, the observed H column density is much larger, so that, in spite of the intense ultraviolet radiation field, the inferred density is comparatively low and similar to that found for the ζ Per cloud. Unfortunately, there are no other lines of sight besides these four for which both C_2 and H_2 observations are available.

Assuming that the observed H column densities and the H_2 population ratios are not in error, there are several possible explanations for the discrepant densities in the ζ Oph and o Per clouds:

1. Since the C_2 data constrain only the ratio n_c/I_R, they may be consistent with the H_2 observations if the radiation field in the red is also enhanced by a factor of about 3 in the ζ Oph and o Per regions, but not in the ζ Per cloud. The stars themselves could account for such an enhancement only if the clouds were located extremely close to them, in which case the ultraviolet intensities would be expected to be even larger. There are no other indications of strong infrared sources in these regions.

2. The density determination from the H/H_2 abundance ratio depends on the adopted formation rate of H_2 on grains. The discrepancy could be resolved if this rate were twice as large in the ζ Oph and o Per clouds as in the other clouds. Although the H_2 formation rate may be larger than normal in the ζ Oph and o Per clouds, the ultraviolet extinction data do not show a significant difference between the o Per and ζ Per clouds, for example.

3. Other mechanisms apart from the ultraviolet pumping mechanism may contribute to the population of the high-J levels of H_2 in the ζ Oph and o Per clouds. An argument in favor of this suggestion is the fact that the ultraviolet pumping mechanism does not reproduce the observed population ratios as well for these clouds as for the ζ Per cloud. In particular, the large column densities in $J = 3$ and $J = 4$ seem to indicate the presence of an additional small, very warm region. Shock excitation has often been suggested (e.g., Aannestad and Field 1973; Elitzur and Watson 1980) as an alternative mechanism. If a shocked region could produce most of the observed column densities in $J = 2$, $J = 3$, and $J = 4$, and contribute about half of the measured column density in $J = 5$, then the scaling factor for the ultraviolet radiation field could be reduced, and thus also the density. Model H of the ζ Oph cloud in Table 5 is constructed to this end, and is very similar to model G of the ζ Per cloud. Care must be taken, however, in the construction of shocked models of diffuse clouds that they not be in conflict with the observed abundances of other species, such as CH^+, CH, and OH. Recent attempts to construct shock models for the ζ Oph cloud indicate that nonmagnetic or single-fluid shocks fail to reproduce the observed CH^+/OH abundance ratio (Graff and Dalgarno 1986; Draine and Katz 1986*a*, *b*; Draine 1986; Pineau-des-Forêts *et al.* 1986), but that reasonable two-fluid magnetohydrodynamic models can be made, which have a shock speed of about 10 km s^{-1}, a preshock density $n_H \approx 20$ cm^{-3}, and a postshock density $n_H \approx 150$ cm^{-3}, although the employed preshock H_2/H ratio of about unity may be unrealistically large (Draine and Katz 1986*b*; Draine 1986). As Table 2 of Draine (1986) demonstrates, the sum of the column densities produced by collisional excitation in such a shocked region and by ultraviolet pumping in the quiescent region reproduces the observations toward ζ Oph quite well, although the $J = 5$ level is somewhat overpopulated. Slight adjustments both in the shock structure and in the H_2 grain formation distribution may be necessary to improve the comparison with observations. For the o Per cloud, the shock parameters must be somewhat different in order to reproduce the observed larger H_2 column densities in $J = 3$ and $J = 4$, and the smaller CH^+ column density (Draine and Katz 1986*b*; Pineau-des-Forêts *et al.* 1986). Since the shocks are predicted to contribute very little to the column densities in $J > 5$ and in vibrationally excited levels, observations of these higher levels toward o Per would be very useful. Any shock in the ζ Per cloud would have to have a low shock speed such that it produces the comparatively small CH^+ column density in this direction, and has negligible effects on the H_2 rotational populations, which are well reproduced by the ultraviolet pumping mechanism. Additional theoretical and observational work will be needed to confirm the existence of shocked regions in diffuse interstellar clouds, and to investigate the frequency with which they occur.

The models provide explicit predictions of the amounts of vibrationally excited H_2 to be expected in diffuse interstellar clouds. Table 9 lists predicted equivalent widths of selected lines in the two Lyman bands of longest wavelength that arise in $v = 1$ and 2 for the four diffuse clouds analyzed here. All of these lines are expected to have equivalent widths of the order of 1 mÅ, which will correspond approximately to the detection threshold in a spectrum of signal-to-noise ratio $S/N \approx 20$ at the maximum resolving power of the high-resolution spectrograph of the Hubble Space Telescope. The lines of the $B-X$ (0,2) band near 1220 Å lie within the wavelength range of good detector sensitivity of that instrument and should therefore be detectable. Some additional calculations have been performed in which the populations in all levels $v = 1$–6, $J = 0$–7 are computed. The equivalent widths in lines of the $B-X$ (0,3) band near 1275 Å and the (0,4) band near 1334 Å are comparable to, or slightly larger than, those of the lines of the (0,2) band, because the increase in oscillator strengths compensates for the decrease in relative populations in $v = 3$ and $v = 4$. For $v > 4$ the equivalent width in accessible lines is much smaller. The range of values listed for each line and each cloud reflects the full variety of models in Tables 4, 5, 7, and 8. The predicted line strengths in Table 9 result from a population distribution characterized by a vibrational excitation temperature of 6000–7000 K for $v = 1$, $v = 2$ and $v = 3$. Weak shocks in diffuse clouds cannot maintain such a high-temperature distribution; hence the detection of these lines will provide a direct measure of the ultraviolet pumping. Failure to detect these lines at the predicted levels would most likely indicate that the ultraviolet radiation field has been overestimated, thus implying that the observed superthermal populations in $v = 0$, $J > 3$ are maintained by collisions in high-temperature gas. Thick molecular clouds should possess

TABLE 9

PREDICTED EQUIVALENT WIDTHS (mÅ) OF H_2 LINES IN THE LYMAN $B\,^1\Sigma_u^+ - X\,^1\Sigma_g^+$ SYSTEM ARISING IN VIBRATIONALLY EXCITED LEVELS

Band	Line	λ (Å)[a]	f[b]	ζ Per	ζ Oph	χ Oph	o Per
(0,1).....	$R(0)$	1161.689	1.29(−2)	0.2–0.4	0.3–0.7	0.7–1.7	0.3–0.9
	$R(1)$	1162.171	8.57(−3)	0.3–0.6	0.6–1.2	0.7–2.0	0.5–1.1
	$R(2)$	1163.645	7.70(−3)	0.3–0.6	0.5–1.1	1.1–2.7	0.5–1.4
	$R(3)$	1166.112	7.32(−3)	0.3–0.5	0.5–1.1	0.6–1.8	0.4–1.0
(0,2).....	$R(0)$	1217.208	4.42(−2)	0.3–0.6	0.6–1.2	1.0–2.7	0.5–1.4
	$R(1)$	1217.645	2.95(−2)	0.5–1.0	0.9–2.0	1.1–3.3	0.8–1.8
	$R(2)$	1219.090	2.65(−2)	0.5–0.9	0.8–1.7	1.6–4.2	0.8–2.1
	$R(3)$	1221.542	2.52(−2)	0.4–0.8	0.6–1.6	0.9–2.6	0.6–1.4

[a] Dabrowski 1984.

[b] Line oscillator strengths have been determined from the band values of Allison and Dalgarno 1970.

column densities of vibrationally excited H_2 similar to those of diffuse clouds, provided that their boundary layers have comparable densities and are exposed to comparable ultraviolet radiation fields.

Another predictable property of steady state diffuse clouds is the intensity of infrared line emission arising in the vibration-rotation cascade that follows ultraviolet absorption and fluorescence in H_2 (Black and Dalgarno 1976). The specific intensities of the stronger lines of the (1,0), (2,1) and (2,0) bands at wavelengths 1–4 μm are of the order of 10^{-7} ergs s^{-1} cm^{-2} sr^{-1} or more in all four clouds. Such fluorescent infrared line emission has recently been identified in Orion (Hayashi *et al.* 1985) at an intensity level 50–100 times larger than this. Although the infrared line emission from diffuse clouds is probably still undetectably weak, the lines should be widely observable with a suitable infrared spectrometer wherever a molecular cloud surface is exposed to ultraviolet starlight with $I_{UV} \geq 100$. The intensity and diagnostic uses of H_2 fluorescent line emission will be discussed elsewhere (Black and van Dishoeck 1986).

The temperatures in diffuse clouds are thought to be maintained by the balance between heating through the photoelectric effect on grains and cooling primarily by radiative decay following collisional excitation of ground-state fine-structure levels in abundant atoms and ions. Known heating and cooling rates can be readily evaluated in our models where the abundance and excitation of coolants and the penetrating ultraviolet flux are evaluated explicitly as functions of depth. In general, the microscopic heating and cooling rates in these models agree to within a factor of 2 for the empirically constrained temperature profiles in the central zones. However, the photoelectric heating rate tends to fall a factor of 5 below the cooling rate in the outer layers. The observed fact that interstellar line widths almost always exceed thermal Doppler widths suggests that diffuse clouds may have significant macroscopic dynamical sources of heat input into the gas.

VI. CHEMICAL NETWORK

The chemistry in interstellar clouds has been discussed in detail elsewhere (Herbst and Klemperer 1973; Dalgarno and Black 1976; Glassgold and Langer 1976; Watson 1974, 1976, 1978; Huntress 1977; Prasad and Huntress 1980). The chemical scheme used in this work consists of about 500 reactions involving 120 species containing H, D, He, ^{12}C, ^{13}C, ^{16}O, ^{18}O, N, Cl, and metal atoms. It is appropriate both for diffuse and for denser interstellar clouds. The rates for the reactions, with the exception of the photodissociation processes, are mainly derived from the above-mentioned papers and updated, and will not be reiterated here. The networks for the most important species are illustrated in Figures 4–8 (see § VII). Aside from the formation of H_2, this is entirely a gas-phase chemistry. All of the gas-phase processes in which H and H_2 participate are included explicitly in the computation of their steady state abundances, although in diffuse clouds these processes have little effect on the results in comparison with formation of H_2 on grain surfaces and destruction by photodissociation.

a) *Photodissociation Rates*

The rates for the photodissociation processes are improved, compared with the previous BD and BHD models, as a result of recent quantum chemical calculations of the photodissociation cross sections of several molecules, such as CH^+ (Kirby *et al.* 1980), OH (van Dishoeck and Dalgarno 1984), HCl (van Dishoeck, van Hemert, and Dalgarno 1982), and C_2 (Pouilly *et al.* 1983), and also as a result of experimental measurements of the cross sections of species such as CH_4, C_2H_2, NH_3, and HCN (Lee 1984). A detailed discussion of the photodissociation cross sections, and their uncertainties, is given by van Dishoeck (1986). In general, the new rates are substantially larger than those used by BD and BHD.

The depth dependences of the photodissociation rates due to continuum extinction were obtained using the program of Roberge, Dalgarno, and Flannery (1981) for grain models 2 and 3, and various total extinctions ranging between $A_V^{tot} = 1$ and $A_V^{tot} = 10$ mag. For those species for which the photodissociation proceeds mainly through continuous absorption, the rates were fitted to the bi-exponential form used by van Dishoeck and Dalgarno (1984) for each A_V^{tot}, and the resulting coefficients were interpolated for the appropriate A_V^{tot} of the cloud. The same procedure may be used for molecules for which the photodissociation takes place mostly through line

absorption, but whose abundance in diffuse clouds is too small for self-shielding to occur, such as the HCl and N_2 molecules.

As discussed in § III, the photodissociation of HD also proceeds through line absorption in the Lyman and Werner systems, and its abundance in diffuse clouds is large enough so that self-shielding becomes important. Because of the improved formulation of the self-shielding function, equation (18), the photodissociation rate of HD in this work differs substantially from the one used by BD and BHD. An extensive discussion of the HD photodissociation and excitation, and the deuterium chemistry, will be presented in a separate paper (Black and van Dishoeck 1986).

The photodissociation of the important and ubiquitous CO molecule is particularly uncertain. This is due mostly to a lack of basic molecular data. Experimental work has revealed no continuous absorption in CO longward of 1060 Å (Lee and Guest 1981), and it is likely that there is no appreciable continuous dissociation channel longward of 912 Å (Fock, Gürtler, and Koch 1980; Rostas 1985). Then the interstellar photodissociation of CO is dominated by discrete absorptions into excited electronic states, but both the states that participate in the dissociation process and the oscillator strengths for the transitions are not well known. Additional uncertainty arises in the depth dependence of the rate, because the self-shielding in the predissociating lines depends on the assumed line widths, the distribution of lower state populations, and the appropriate Doppler parameter for CO in the cloud (van Dishoeck 1984). An accurate treatment of the depth dependence of the abundance of CO is of great importance for understanding the C, C^+, ^{12}CO, and ^{13}CO abundance ratios in the outer parts of molecular clouds, and a detailed discussion of the CO photodissociation rate will be given in a separate paper which deals with the structure of denser interstellar clouds with $A_V^{\rm tot} \approx 3$ mag (van Dishoeck and Black 1986*b*).

In this work, a small continuum photodissociation of CO shortward of 945 Å, corresponding to an unattenuated rate of about 10^{-12} $I_{\rm UV}$ s^{-1} (Glassgold, Huggins, and Langer 1985), was included. The discrete photodissociation of CO was assumed to proceed through absorptions into the $v' = 0$ level of the $E\,^1\Pi$ state and the $v' = 1$ level of the $C\,^1\Sigma^+$ state at 1076 and 1063 Å, respectively, with a predissociation probability of 10%. The oscillator strengths of these transitions were taken to be 4 times as large as those listed by Lee and Guest (1981) (cf. Rostas 1985). The photodissociation is dominated, however, by absorptions into higher lying states, which are mainly Rydberg in character and have 100% predissociation probabilities. A total integrated absorption cross section of about 2×10^{-15} cm^2 Å has been estimated from experiments (Rostas 1985). The present models use a somewhat smaller total absorption cross section corresponding to an unshielded photodissociation rate of about 5×10^{-11} $I_{\rm UV}$ s^{-1}, which is still an order of magnitude larger than the rate used by BD and, e.g., Glassgold, Huggins, and Langer (1985). The CO photodissociation rate is currently uncertain by a factor of 5. The excitation temperature characterizing the rotational population of the ground state of CO was taken to be $T_{\rm ex} \approx 4$ K, as suggested by the observations (see § V). The Doppler parameter was assumed to be small, $b_{\rm CO} \leq 1$ km s^{-1}, as indicated by high-resolution absorption-line observations both of CO (Wannier, Penzias, and Jenkins 1982) and of other molecular species such as CN (Meyer and Jura 1985), and as indicated by radio emission-line observations (Liszt 1979). The natural width of a predissociated line in CO can be of the order of 0.1 cm^{-1}, which corresponds to a line broadened by $b \approx 2$ km s^{-1} at $\lambda \approx 1000$ Å. Thus, if the high-lying Rydberg states are important in the photodissociation process and if the predissociation widths of the lines are large, the results are insensitive to the values of $b_{\rm CO}$ in quiescent clouds.

The photodissociation of ^{13}CO is complicated by the fact that the lines in the (0,0) bands are shielded by ^{12}CO, but not the generally weaker lines in the (1,0) bands, owing to the larger isotope shift when a nonzero vibrational quantum number is involved (Bally and Langer 1982; Glassgold, Huggins, and Langer 1985). The present calculations assume that most of the photodissociation occurs through the (0,0) bands of the various transitions, so that for diffuse clouds the ^{13}CO photodissociation rate does not differ appreciably from that of ^{12}CO.

The photodissociation rate of the CN molecule is also uncertain. Previous estimates (Solomon and Klemperer 1972; BD) assumed a rather small unshielded rate of about 5×10^{-11} $I_{\rm UV}$ s^{-1}. On the other hand, recent quantum chemical calculations (Lavendy, Gandara, and Robbe 1984) suggest that the CN photodissociation may be very rapid with a rate close to 10^{-9} $I_{\rm UV}$ s^{-1}. However, the limited size of these computations may have resulted in an overestimate of the rate. Recent more extensive calculations (van Dishoeck 1986) suggest a somewhat lower rate, although it is unlikely to be smaller than 10^{-10} $I_{\rm UV}$ s^{-1}, the value employed in this work.

The photoionization rate of carbon was calculated using a cross section of 1.6×10^{-17} cm^2 (Burke and Taylor 1979) between 1110 and 912 Å. The resulting unshielded rate is 3.1×10^{-10} $I_{\rm UV}$ s^{-1}. The depth dependence of the rate was determined by taking into account not only the continuous attenuation but also the effect of shielding by H_2. This was accomplished in an approximate way by calculating the total absorption rate in the H_2 lines at each depth.

The rates of all photoprocesses in this work were obtained using the scaling factor for the ultraviolet radiation field $I_{\rm UV}$ as determined from the H_2 excitation. Since the H_2 absorptions occur only at wavelengths shorter than 1100 Å, the rates of other species depend severely on the assumed variations of the intensity of the radiation field and the grain scattering properties with wavelength. The photodissociation of various hydrides, e.g., OH and CH, occurs mainly at $\lambda \approx 1500$ Å, whereas the photodissociation of metal hydrides such as NaH takes place at even longer wavelengths.

b) *Elemental Abundances*

The molecular abundances depend directly on the assumed atomic abundances. The original abundance determinations of Morton (1974) suggested depletions of factors of about 4 with respect to the solar abundances, and these depletions were used in the models of BD and BHD. Subsequent analyses (de Boer 1979, 1981; Liszt 1979, 1981; Jenkins and Shaya 1979; Jenkins, Jura, and Loewenstein 1983; York *et al.* 1983) have questioned these results and have concluded that ox-

ygen and carbon may be almost undepleted in diffuse interstellar clouds, except toward a few stars in the Scorpius region (Hobbs, York, and Oegerle 1982; Jenkins, Jura, and Loewenstein 1983). In agreement with the latest results, we used in our calculations a carbon abundance $A_C = 4.68 \times 10^{-4} \delta_C n_H$ and an oxygen abundance $A_O = 8.3 \times 10^{-4} \delta_O n_H$ with depletion factors $\delta_C = \delta_O \approx 0.75$, unless otherwise indicated. The employed deuterium, nitrogen, and chlorine abundances were $1.5 \times 10^{-5} \delta_D n_H$, $1.0 \times 10^{-4} \delta_N n_H$, and $1.1 \times 10^{-7} \delta_{Cl} n_H$, respectively, with $\delta_D \approx 1.0$, $\delta_N \approx 0.75$, and $\delta_{Cl} \approx 0.6$. For the metals such as Na and Mg, which may be important in charge-transfer reactions with ions, we assumed a total abundance $A_M = 1.0 \times 10^{-5} \delta_M n_H$ with $\delta_M \approx 0.4$. If other species, such as Si, Fe, and Ca, are substantially depleted with $\delta \leq 0.01$, then the adopted abundances and depletions are consistent with a 1% mass fraction of dust particles.

VII. MOLECULAR ABUNDANCES

a) *General Considerations*

The abundances of several simple molecules for which observational data exist are included in Tables 2 and 3. Table 3 illustrates the dependence of the abundances on the various cloud parameters, such as density, temperature, and cosmic-ray ionization rate. The abundances of the carbon-bearing molecules, such as CH, vary almost linearly with the density in the cloud, whereas that of C_2 depends even quadratically on n_H. On the other hand, the abundances of the oxygen-bearing molecules such as OH and H_2O, and the deuterium-containing molecule HD, are not very sensitive to the density. The abundances of the carbon-bearing molecules CH, CH^+, and C_2 are not sensitive to the cosmic-ray ionization rate ζ_0, whereas those of the oxygen-containing molecules such as OH, O_2, H_2O, and CO are directly proportional to ζ_0, because their formation is initiated by the reactions

$$H^+ + O \rightarrow O^+ + H, \quad (30)$$

$$H_3^+ + O \rightarrow OH^+ + H_2, \quad (31)$$

followed by reactions with H_2. Similarly, the abundance of HD, which depends on the charge-transfer reaction

$$H^+ + D \rightarrow H + D^+, \quad (32)$$

is proportional to ζ_0. Since reactions (30) and (32) are also sensitive to the temperature in the cloud, the abundances of the oxygen- and deuterium-bearing molecules increase with higher temperatures. The abundances of the carbon-containing molecules are rather insensitive to the temperature in the cloud.

The column densities listed in Table 2 were obtained using mainly the same reaction network as in the original BD model, but with the improved estimates for the photodissociation rates. It appears that the column densities of the oxygen-bearing molecules, such as OH, CO, O_2, and H_2O, are substantially lowered in the new computations compared with the BD calculations. As explained by Roberge (1981), this is due in part to the improved treatment of the radiative transfer in the H_2 lines and the corresponding diminished thickness of the $H-H_2$ transition region by an order to magnitude in the new models. Additional factors influencing the column densities are the enhanced photodissociation rates of OH and CO in this work by factors ranging from 3 at the boundary to more than 10 in the center of the cloud. Finally, the rate of reaction (30) was taken from the calculations of Chambaud *et al.* (1980) and is slightly smaller than the value used by BD. If the old rates for photodissociation and for reaction (30) employed by BD are chosen, the calculated column densities of OH and CO in the ζ Oph model are $N(OH) = 1.3 \times 10^{13}$ and $N(CO) = 5.0 \times 10^{14}$ cm^{-2}, respectively, so that the improved rates alone diminish the column densities by factors of 3 and 15, respectively. The column densities of the carbon-bearing molecules, such as CH and C_2, are less affected in the new calculations, although the differences from the observed values may be significant.

The discrepancies for most molecular abundances suggest that the employed parameters in the old models were not correct. In the following, the chemistry in the new models for the ζ Per, ζ Oph, χ Oph, and o Per clouds, and the procedure for fitting the parameters such as the elemental depletion factors and the cosmic-ray ionization rate ζ_0, are discussed. The observed molecular column densities have been critically reviewed to ensure the use of a consistent set of oscillator strengths. The adopted oscillator strengths are summarized in Table 10. The results of the chemistry calculations are summarized in Tables 11–14. The depth dependences of the concentrations of the most important species in one model of the ζ Per cloud are illustrated in Figure 3.

b) *Atomic Abundances*

The carbon depletion factor δ_C was fixed by the observed neutral carbon column density $N(C)$. Although most carbon is present as C^+ in diffuse clouds, the observed value of $N(C^+)$ is usually too uncertain to determine the carbon abundance. For all four clouds, carbon appears to be almost undepleted. The calculated values of $N(C^+)$ are somewhat higher than suggested by the observations, in accordance with the fact that the published values tend to be underestimates (cf. Liszt 1979). The depletion factors of oxygen and nitrogen may similarly be determined from the observed $N(O)$ and $N(N)$. For the ζ Oph, o Per, and ζ Per clouds, some depletion seems necessary. For the χ Oph cloud, the observational errors are too large to make any definite statements, so that $\delta_O = \delta_N = 0.5$ was assumed. In general, δ_O was taken such that the calculated $N(O)$ are somewhat larger than the observed values. Chlorine appears to be only mildly depleted in diffuse clouds, $\delta_{Cl} \approx 0.7$ in the models. The observed Na and Mg abundances require $\delta_M \approx 0.4$–0.6.

c) *Oxygen-bearing Molecules*

Since the formation rates of the oxygen-bearing molecules are directly proportional to the cosmic-ray ionization rate (see Fig. 4), their abundances may be used to infer a value for ζ_0, if all other formation and destruction rates are well understood. The use of the OH abundance as a diagnostic probe for ζ_0 was suggested by Black and Dalgarno (1973*a*), and the method was subsequently applied by Hartquist, Black, and Dalgarno (1978) to the ζ Per, o Per, and ζ Oph clouds after

TABLE 10

ADOPTED MOLECULAR OSCILLATOR STRENGTHS

Species	Transition	Band	λ (Å)	f	Reference
CO.....	$A\,^1\Pi$–$X\,^1\Sigma^+$	(0, 0)	1545	1.56(−2)	Field *et al.* 1983; Albritton 1976
		(1, 0)	1510	3.43(−2)	
		(11, 0)	1264	2.41(−4)	
		(12, 0)	1246	1.08(−4)	
		(13, 0)	1230	4.80(−5)	
	$B\,^1\Sigma^+$–$X\,^1\Sigma^+$	(0, 0)	1151	1.0(−2)	Cooper and Langhoff 1981; Smith 1978
	$C\,^1\Sigma^+$–$X\,^1\Sigma^+$	(0, 0)	1088	8.9(−2)	Cooper and Langhoff 1981; Smith 1978
		(1, 0)	1063	1.8(−3)	
	$E\,^1\Pi$–$X\,^1\Sigma^+$	(0, 0)	1078	1.0(−1)	Smith 1978
CH.....	$A\,^2\Delta$–$X\,^2\Pi$	(0, 0)	4300	5.06(−3)	Larsson and Siegbahn 1983a
		(1, 0)	3850	1.61(−3)	
	$B\,^2\Sigma^-$–$X\,^2\Pi$	(0, 0)	3880	3.1(−3)	Brzozowski *et al.* 1976
	$C\,^2\Sigma^+$–$X\,^2\Pi$	(0, 0)	3143	6.1(−3)	Brzozowski *et al.* 1976
CH^+	$A\,^1\Pi$–$X\,^1\Sigma^+$	(0, 0)	4233	5.45(−3)	Larsson and Siegbahn 1983b
		(1, 0)	3958	3.31(−3)	
C_2.....	$A\,^1\Pi_u$–$X\,^1\Sigma_g^+$	(2, 0)	8750	1.7(−3)	van Dishoeck 1983, and see text
		(3, 0)	7720	7.5(−4)	
CN.....	$B\,^2\Sigma^+$–$X\,^2\Sigma^+$	(0, 0)	3874	3.38(−2)	Larsson, Siegbahn, and Ågren 1983
OH.....	$A\,^2\Sigma^+$–$X\,^2\Pi$	(0, 0)	3080	1.10(−3)	Wang and Huang 1980; Smith and Crosley 1981
	$D\,^2\Sigma^-$–$X\,^2\Pi$	(0, 0)	1222	1.2(−2)	van Dishoeck and Dalgarno 1983
H_2O.....	$\tilde{C}\,^1B_1$–$\tilde{X}\,^1A_1$	(0, 0, 0)–(0, 0, 0)	1240	1.0(−2)	Smith *et al.* 1981
	$\tilde{F}\,^1B_1$–$\tilde{X}\,^1A_1$	(0, 0, 0)–(0, 0, 0)	1114	3.0(−2)	Smith *et al.* 1981
H_2O^+ ...	$\tilde{A}\,^2A_1$–$\tilde{X}\,^2B_1$	(0, 8, 0)–(0, 0, 0)	6147	7.8(−5)	Möhlmann *et al.* 1978; Smith *et al.* 1984
HCl.....	$C\,^1\Pi$–$X\,^1\Sigma^+$	(0, 0)	1290	1.5(−1)	van Dishoeck, van Hemert, and Dalgarno, 1982; Smith *et al.* 1980
NH	$A\,^3\Pi$–$X\,^3\Sigma^-$	(0,0)	3350	7.5(−3)	Fairchild *et al.* 1984; Hofzumahaus and Stuhl 1985
CO^+	$A\,^2\Pi$–$X\,^2\Sigma^+$	(2, 0)	4260	8.6(−4)	Mahan and O'Keefe 1981; Holland and Maier 1972
C_3.....	$\tilde{A}\,^1\Pi_u$–$\tilde{X}\,^1\Sigma_g^+$	(0, 0, 0)–(0, 0, 0)	4050	1.8(−2)	Clegg and Lambert 1982
MgH	$A\,^2\Pi$–$X\,^2\Sigma^+$	(0, 0)	5180	1.6(−1)	Kirby, Saxon, and Liu 1979
MgO	$B\,^1\Sigma^+$–$X\,^1\Sigma^+$	(0, 0)	4998	1.5(−1)	Diffenderfer, Yarkony, and Dagdigian 1983
NaH.....	$A\,^1\Sigma^+$–$X\,^1\Sigma^+$	(8, 0)	3991	2.3(−2)	Kirby and Dalgarno 1978

measurements of the OH column densities became available. Since the previous analysis, some of the main uncertainties in the molecular reactions, such as the rate of equation (30) and the OH photodissociation rate, appear to have been removed by quantum chemical calculations (Chambaud *et al.* 1980; van Dishoeck and Dalgarno 1984). Furthermore, calculations of the OH D–X (0,0) oscillator strength (van Dishoeck and Dalgarno 1983) have confirmed the value $f_{00}=1.1\times10^{-2}$ used in the analysis of the observations of Chaffee and Lutz (1977), so that the observed OH column densities are rather well established. However, a new uncertainty in the reaction scheme has recently become apparent, since the dissociative recombination of H_3^+,

$$H_3^+ + e \rightarrow H_2 + H \text{ or } H + H + H, \qquad (33)$$

previously thought to be fast, has now been shown to be slow

TABLE 11

CALCULATED COLUMN DENSITIES (cm^{-2}) OF SEVERAL ATOMIC AND MOLECULAR SPECIES IN MODELS OF THE ζ PER CLOUD

Parameters and Species	Model[a] A	B	C	D	E	F	G	Observed	References
δ_C	0.80	0.75	0.62	0.52	1.10	0.62	0.58		
δ_D	1.60	1.40	1.30	1.70	1.70	1.10	1.00		
ζ_0 (s^{-1})	7.0(-17)	6.0(-17)	5.5(-17)	6.0(-17)	6.5(-17)	6.0(-17)	4.0(-17)		
O	6.7(17)	6.7(17)	6.4(17)	6.4(17)	6.4(17)	6.7(17)	6.7(17)	(0.2–1.0)(18)	1
OH	4.9(13)	4.7(13)	4.8(13)	4.5(13)	4.5(13)	4.8(13)	5.3(13)	(4.2±0.5)(13)	2
H_2O	5.4(11)	5.3(11)	6.6(11)	6.9(11)	4.0(11)	6.4(11)	7.5(11)	...	
OH^+	3.9(11)	5.1(11)	6.8(11)	1.8(11)	6.3(11)	6.8(11)	8.4(11)	...	
H_2O^+	1.4(11)	1.6(11)	2.0(11)	8.8(10)	1.8(11)	1.9(11)	2.3(11)	<3.6(13)	3
O_2	1.2(11)	1.1(11)	1.3(11)	2.1(11)	6.0(10)	9.8(10)	1.2(11)	...	
H_3^+	2.4(14)	2.0(14)	1.5(14)	1.1(14)	3.9(14)	2.1(14)	2.1(14)	...	
D	3.7(16)	3.1(16)	2.6(16)	3.8(16)	3.8(16)	2.4(16)	2.1(16)	...	
HD	1.4(15)	3.1(15)	3.6(15)	2.0(15)	1.7(15)	3.2(15)	3.4(15)	(3.8±1.4)(15)	4
H_2D^+	6.3(11)	4.1(11)	5.5(11)	3.2(11)	9.6(11)	3.3(11)	2.9(11)	...	
C	3.6(15)	3.3(15)	3.2(15)	3.3(15)	3.4(15)	3.5(15)	3.4(15)	(3.3±0.4)(15)	5
C^+	6.0(17)	5.7(17)	4.4(17)	3.8(17)	8.0(17)	4.7(17)	4.4(17)	(3.0±1.0)(17)	4
CH^+	4.1(10)	3.9(10)	3.3(10)	2.8(10)	5.3(10)	3.0(10)	2.8(10)	(3.5±0.4)(12)	6,7,8
CH	2.0(13)	2.1(13)	2.5(13)	2.7(13)	1.6(13)	1.7(13)	1.7(13)	(2.0±0.1)(13)	9
C_2	1.3(13)	1.6(13)	2.6(13)	2.9(13)	6.8(12)	1.6(13)	1.7(13)	(1.1±0.2)(13)	10
CH_2	2.5(13)	2.8(13)	3.7(13)	4.2(13)	1.7(13)	2.9(13)	3.0(13)	...	
CH_3	2.3(8)	2.9(8)	5.5(8)	5.9(8)	1.1(8)	4.1(8)	4.6(8)	...	
C_2H	1.2(12)	1.5(12)	2.7(12)	3.5(12)	5.5(11)	1.7(12)	1.9(12)	...	
C_3	2.8(7)	4.3(7)	1.1(8)	1.2(8)	9.2(6)	7.7(7)	9.2(7)	<3.7(12)	11
C_2^+	4.5(9)	4.4(9)	4.5(9)	5.3(9)	3.7(9)	3.3(9)	3.4(9)	...	
^{12}CO	1.3(14)	1.2(14)	1.4(14)	2.0(14)	7.6(13)	1.7(14)	2.0(14)	(5.4±2.6)(14)	4
^{13}CO	2.0(12)	1.9(12)	2.4(12)	3.2(12)	1.1(12)	3.1(12)	3.8(12)	...	
HCO^+	4.0(10)	3.9(10)	4.8(10)	4.2(10)	3.5(10)	4.2(10)	4.9(10)	...	
HCO	3.0(8)	3.7(8)	6.5(8)	5.2(8)	2.1(8)	5.4(8)	5.8(8)	...	
CO^+	1.1(10)	1.0(10)	9.7(9)	7.8(9)	1.2(10)	9.3(9)	9.8(9)	<4.2(13)	12
N	1.1(17)	1.1(17)	1.1(17)	1.1(17)	1.1(17)	1.1(17)	1.1(17)	>2.5(17)	1
NH	6.6(11)	5.8(11)	5.7(11)	5.8(11)	6.2(11)	3.3(11)	6.8(11)	<6.3(11)	2
NH_2	1.1(12)	1.0(12)	1.1(12)	1.1(12)	9.7(11)	6.4(11)	1.4(12)	...	
CN	1.6(12)	1.6(12)	2.0(12)	2.3(12)	1.1(12)	9.8(11)	2.0(12)	(3.0±0.1)(12)	13
HCN	3.3(10)	3.3(10)	4.4(10)	5.3(10)	2.0(10)	2.3(10)	4.6(10)	...	
Cℓ	1.2(14)	1.3(14)	1.2(14)	1.2(14)	1.2(14)	1.2(14)	1.2(14)	(0.2–1.4)(14)	14
Cℓ^+	1.8(12)	1.8(12)	1.9(12)	1.2(12)	2.0(12)	4.5(12)	4.9(12)	(1.7–21.)(13)	14
HCℓ	3.3(11)	3.4(11)	3.6(11)	3.9(11)	2.8(11)	2.7(11)	2.8(11)	...	
HCℓ^+	5.2(10)	7.1(10)	8.6(10)	3.0(10)	8.1(10)	1.1(11)	1.2(11)	...	
Na	1.1(14)	1.1(14)	1.3(14)	1.5(14)	8.3(13)	8.5(13)	8.4(13)	9.4(13):	15
Na^+	2.2(15)	2.2(15)	2.1(15)	2.1(15)	2.2(15)	2.3(15)	2.3(15)	...	
NaH	1.7(10)	1.8(10)	2.3(10)	3.5(10)	9.2(9)	1.0(10)	1.1(10)	...	

[a] See Table 4 for the density and temperature structure of the models. All models have $\delta_O = 0.5$, $\delta_N = 0.7$, $\delta_{Cl} = 0.7$, $\delta_M = \delta_{Na} = 0.6$, $k_{33} = 1\times10^{-10}$ cm^3 s^{-1}, $k_{34} = 7\times10^{-16}$ cm^3 s^{-1}, $k_{36} = 2\times10^{-10}$ cm^3 s^{-1}, and assume $[^{12}C/^{13}C] = 90$.

REFERENCES.—(1) York *et al.* 1983; (2) Chaffee and Lutz 1977; (3) Smith, Schempp, and Federman 1984; (4) Snow 1977; (5) Jenkins and Shaya 1979; (6) Hobbs 1973*a*; (7) Chaffee 1974; (8) Federman 1982; (9) Jura and Meyer 1985; (10) van Dishoeck 1984; (11) Clegg and Lambert 1982; (12) Hobbs 1973*b*; (13) Meyer and Jura 1985; (14) Jenkins, Savage, and Spitzer 1986; (15) Hobbs 1978.

for ground-state H_3^+ at interstellar temperatures (Michels and Hobbs 1984; Smith and Adams 1984). If this rate is indeed low, the H_3^+ abundance will be greatly enhanced in the clouds, since its destruction by photodissociation is also very slow (van Dishoeck 1986). Reaction (31) then becomes an important path for the formation of OH. Unfortunately, the rate for reaction (33) is still not well known. The upper limit $k_{33} < 2\times10^{-8}$ cm^3 s^{-1} measured by Smith and Adams (1984) at $T = 95$ K corresponds to $k_{33} < 10^{-7}$ cm^3 s^{-1} at $T = 40$ K, assuming that the rate varies as $T^{-1/2}$. If k_{33} were as large as 10^{-7} cm^3 s^{-1} at low temperatures, the calculated OH column densities would be too small by factors of 5–10 when the previously derived cosmic-ray ionization rate $\zeta_0 \approx 3\times10^{-17}$ s^{-1} (Hartquist, Black, and Dalgarno 1978) is used. For the ζ Per cloud, ζ_0 needs to be increased to $(1–2)\times10^{-16}$ s^{-1} to reproduce the observations, whereas for the ζ Oph and o Per clouds, the rates need to be at least $\zeta_0 \approx 4\times10^{-16}$ s^{-1} and $\zeta_0 \approx 8\times10^{-16}$ s^{-1}, respectively. On the other hand, it is plausible that k_{33} is significantly smaller than the measured upper limit, although it is unlikely to be much smaller than an estimated rate of radiative electron capture by H_3^+, $k_{33} \approx 10^{-10}$ cm^3 s^{-1} at $T \approx 40$ K. Then the OH observations can be

TABLE 12

CALCULATED COLUMN DENSITIES (cm^{-2}) OF SEVERAL ATOMIC AND MOLECULAR SPECIES IN MODELS OF THE ζ OPH CLOUD

Parameters and Species	Model[a] A	B	C	D	E	F	G	H	Observed	References
δ_C	0.77	0.70	0.70	1.10	0.68	0.84	0.67	0.67		
δ_D	0.70	0.80	0.80	1.00	0.70	0.80	0.80	0.80		
ζ_0 (s^{-1})	1.4(-16)	1.3(-16)	1.3(-16)	1.4(-16)	1.6(-16)	1.4(-16)	8.0(-17)	5.5(-17)		
O	7.1(17)	7.1(17)	7.1(17)	7.0(17)	7.0(17)	7.2(17)	6.9(17)	6.8(17)	(7.1±0.5)(17)	1
OH	4.3(13)	4.5(13)	4.5(13)	4.4(13)	5.0(13)	4.9(13)	4.5(13)	5.0(13)	(4.8±0.5)(13)	2
H_2O	5.1(11)	5.5(11)	5.5(11)	4.1(11)	6.6(11)	5.1(11)	6.0(11)	6.7(11)	≤2.2(13)	3
OH^+	2.8(11)	3.9(11)	4.0(11)	5.2(11)	3.7(11)	1.1(12)	3.0(11)	3.2(11)	...	
H_2O^+	1.1(11)	1.4(11)	1.4(11)	1.6(11)	1.4(11)	2.7(11)	1.2(11)	1.3(11)	<1.5(13)	4
O_2	1.5(11)	1.4(11)	1.4(11)	8.2(10)	1.5(11)	6.7(10)	1.4(11)	1.6(11)	...	
H_3^+	1.5(14)	1.3(14)	1.3(14)	2.9(14)	1.8(14)	2.8(14)	1.6(14)	1.7(14)	...	
D	1.4(16)	1.6(16)	1.6(16)	2.0(16)	1.4(16)	1.6(16)	1.6(16)	1.6(16)	...	
HD	1.9(14)	2.9(14)	2.9(14)	2.3(14)	3.1(14)	4.0(14)	3.5(14)	4.0(14)	(2.1±0.2)(14)	5
H_2D^+	1.7(11)	7.6(11)	7.6(11)	4.1(11)	2.0(11)	1.7(12)	2.0(11)	2.1(11)	...	
C	3.2(15)	3.1(15)	3.1(15)	3.0(15)	3.3(15)	3.2(15)	3.3(15)	3.3(15)	(3.2±0.6)(15)	6
C^+	4.9(17)	4.5(17)	4.5(17)	7.0(17)	4.3(17)	5.5(17)	4.2(17)	4.1(17)	(9.3±4.5)(16)	7
CH^+	3.5(10)	3.2(10)	3.2(10)	4.7(10)	2.9(10)	3.3(10)	2.8(10)	2.8(10)	(2.9±0.1)(13)	8
CH	2.0(13)	2.1(13)	2.1(13)	1.5(13)	1.7(13)	1.3(13)	1.8(13)	1.8(13)	(2.5±0.1)(13)	9
C_2	1.5(13)	1.7(13)	1.7(13)	6.5(12)	1.5(13)	7.8(12)	1.7(13)	1.8(13)	(1.5±0.2)(13)	10
CH_2	2.6(13)	2.7(13)	2.7(13)	1.6(13)	2.6(13)	1.7(13)	2.8(13)	2.8(13)	...	
CH_3	2.4(8)	3.2(8)	3.2(8)	1.0(8)	3.1(8)	1.9(8)	3.4(8)	3.5(8)	...	
C_2H	1.5(12)	1.6(12)	1.6(12)	5.5(11)	1.5(12)	6.6(11)	1.7(12)	1.8(12)	...	
C_3	3.6(7)	4.8(7)	4.9(7)	8.6(6)	5.8(7)	2.0(7)	6.8(7)	7.1(7)	<1.5(12)	11
C_2^+	4.4(9)	4.1(9)	4.1(9)	3.5(9)	3.6(9)	2.5(9)	3.7(9)	3.8(9)	...	
^{12}CO	1.3(14)	1.3(14)	1.3(14)	8.9(13)	2.0(14)	1.1(14)	1.9(14)	2.1(14)	(2.0±0.3)(15)	12
^{13}CO	2.0(12)	2.1(12)	2.1(12)	1.1(12)	3.5(12)	2.1(12)	3.4(12)	3.7(12)	(3.6±1.0)(13)	12
HCO^+	3.7(10)	4.1(10)	4.1(10)	3.7(10)	4.5(10)	3.9(10)	4.0(10)	4.5(10)	...	
HCO	3.9(8)	4.6(8)	4.6(8)	2.3(8)	5.0(8)	3.5(8)	5.6(8)	5.8(8)	...	
CO^+	9.7(9)	9.6(9)	9.6(9)	1.2(10)	1.0(10)	1.1(10)	9.2(9)	1.0(10)	<1.4(14)	13
N	8.3(16)	8.2(16)	8.3(16)	8.2(16)	8.2(16)	8.4(16)	8.0(16)	8.0(16)	(5.2±3.3)(16)	14
NH	4.0(11)	3.8(11)	3.8(11)	4.1(11)	4.9(11)	4.6(11)	4.5(11)	4.9(11)	<7.5(12)	15
NH_2	7.0(11)	6.7(11)	6.7(11)	6.5(11)	9.3(11)	8.1(11)	8.6(11)	9.4(11)	...	
CN	1.2(12)	1.2(12)	1.2(12)	7.4(11)	1.5(12)	9.3(11)	1.4(12)	1.6(12)	(2.5±0.1)(12)	16
HCN	2.4(10)	2.4(10)	2.4(10)	1.4(10)	3.2(10)	1.9(10)	3.2(10)	3.5(10)	...	
Cℓ	1.1(14)	1.1(14)	1.1(14)	1.1(14)	1.0(14)	1.1(14)	1.0(14)	1.0(14)	(1.1±0.5)(14)	7
$Cℓ^+$	1.4(12)	1.1(12)	1.1(12)	1.8(12)	2.9(12)	4.1(12)	2.6(12)	2.5(12)	(1.2–4.1)(13)	7
HCℓ	2.9(11)	3.0(11)	3.0(11)	2.5(11)	2.4(11)	2.1(11)	2.4(11)	2.4(11)	<4.5(11)	17
$HCℓ^+$	3.7(10)	4.8(10)	4.9(10)	6.1(10)	4.5(10)	1.3(11)	4.0(10)	4.0(10)	...	
Na	7.2(13)	8.1(13)	8.1(13)	5.1(13)	5.6(13)	4.6(13)	6.0(13)	5.9(13)	6.0(13):	18
Na^+	1.2(15)	1.2(15)	1.2(15)	1.3(15)	1.3(15)	1.3(15)	1.2(15)	1.2(15)	...	
NaH	1.2(10)	1.2(10)	1.2(10)	5.8(9)	7.1(9)	3.8(9)	7.5(9)	7.5(9)	<1.6(11)	19

[a] See Table 5 for the density and temperature structure of the models. All models have $\delta_O = 0.62$, $\delta_N = 0.6$, $\delta_{Cl} = 0.7$, $\delta_M = \delta_{Na} = 0.4$, $k_{33} = 1\times10^{-10}$ cm^3 s^{-1}, $k_{34} = 7\times10^{-16}$ cm^3 s^{-1}, $k_{36} = 2\times10^{-10}$ cm^3 s^{-1}, and assume $[^{12}C/^{13}C] = 90$.

REFERENCES.—(1) de Boer 1981; (2) Chaffee and Lutz 1977; (3) Snow and Smith 1981; (4) Smith, Schempp, and Federman 1984; (5) Wright and Morton 1979 (see text); (6) de Boer and Morton 1979; (7) Morton 1975; (8) Hawkins, Jura, and Meyer 1985; (9) Jura and Meyer 1985; (10) van Dishoeck 1984; (11) Clegg and Lambert 1982; (12) Wannier, Penzias, and Jenkins 1982; (13) Hobbs 1973*b*; (14) Lugger *et al.* 1978; Hibbert, Dufton, and Keenan 1985; (15) Herbig 1968; (16) Meyer and Jura 1985; (17) M. Jura 1980, unpublished measurement; (18) Hobbs 1978; (19) Snow and Smith 1977.

reproduced with much smaller cosmic-ray ionization rates, $\zeta_0 \approx (6\pm2)\times10^{-17}$ s^{-1} for the ζ Per cloud, $\zeta_0 \approx (1.3\pm0.5)\times10^{-16}$ s^{-1} for the ζ Oph cloud, and $\zeta_0 \approx (2.5\pm1.5)\times10^{-16}$ s^{-1} for the o Per cloud. No observational data on OH exist for the cloud toward χ Oph, so $\zeta_0 \approx 2\times10^{-16}$ s^{-1} was assumed. Adams and Smith (1986) have very recently reported an improved upper limit, $k_{33} \leq 10^{-11}$ cm^3 s^{-1}, at $T = 80$ K which supports the low rate used in this work.

The H_3^+ abundance is included in Tables 11–14, and it appears that for $k_{33} \approx 10^{-10}$ cm^3 s^{-1}, the calculated column densities $N(H_3^+) \approx 10^{14}$–10^{15} cm^{-2} are large enough so that its infrared absorption lines (Oka 1981) may be detectable. Any measurement or upper limit on the H_3^+ column density in these clouds would help constrain the dissociative recombination rate of H_3^+ or the cosmic-ray ionization rate.

The above analysis of the cosmic-ray ionization rate assumes that all the OH molecules are formed in the cool, quiescent clouds. If additional shocked or heated regions along the lines of sight were invoked to explain both the populations of the higher rotational levels of H_2 (cf. § Vg)

TABLE 13

CALCULATED COLUMN DENSITIES (cm^{-2}) OF SEVERAL ATOMIC AND MOLECULAR SPECIES IN MODELS OF THE χ OPH CLOUD

Parameters and Species	Model[a] A	B	C	D	E	F	G	Observed	References
δ_C	0.90	0.90	0.90	0.90	0.70	1.10	0.70		
O	1.0(18)	1.0(18)	1.0(18)	1.0(18)	9.6(17)	9.2(17)	1.2(18)	(1.3±0.3)(18)	1
OH	3.5(13)	2.2(13)	2.3(13)	4.3(13)	3.3(13)	4.1(13)	8.1(13)	...	
H_2O	2.5(11)	1.7(11)	1.6(11)	2.7(11)	3.7(11)	2.8(11)	9.4(11)	...	
OH^+	4.1(11)	2.6(11)	2.9(11)	1.1(12)	2.7(11)	1.4(12)	6.3(11)	...	
H_2O^+	9.8(10)	6.4(10)	6.4(10)	1.5(11)	9.5(10)	2.3(11)	2.4(11)	...	
O_2	4.9(10)	3.2(10)	2.9(10)	5.1(10)	5.2(10)	2.7(10)	1.2(11)	...	
H_3^+	3.1(14)	2.0(14)	1.9(14)	3.0(14)	2.3(14)	6.0(14)	6.1(14)	...	
D	3.0(16)	3.1(16)	2.9(16)	3.0(16)	2.8(16)	2.7(16)	3.1(16)	...	
HD	4.4(14)	2.2(14)	1.8(14)	1.3(15)	8.1(14)	8.3(14)	4.5(15)	...	
H_2D^+	5.0(11)	3.1(11)	6.5(11)	2.0(12)	3.0(11)	1.4(12)	6.9(11)	...	
C	3.5(15)	3.4(15)	3.4(15)	3.4(15)	3.5(15)	3.4(15)	5.6(15)	(1–10)(15)	2
C^+	8.6(17)	8.7(17)	8.2(17)	8.6(17)	6.2(17)	9.5(17)	7.7(17)	(0.3–4.0)(17)	3
CH^+	4.5(10)	4.5(10)	4.3(10)	4.4(10)	3.2(10)	4.4(10)	4.3(10)	(1.3±0.1)(13)	4
CH	1.3(13)	1.3(13)	1.3(13)	1.3(13)	1.1(13)	7.4(12)	1.5(13)	(3.4±0.2)(13)	5
C_2	3.7(12)	4.0(12)	4.3(12)	4.2(12)	6.1(12)	2.0(12)	8.6(12)	(2.5±0.3)(13)	6
CH_2	1.0(13)	1.1(13)	1.1(13)	1.1(13)	1.5(13)	7.3(12)	2.2(13)	...	
CH_3	6.8(7)	7.4(7)	8.5(7)	8.6(7)	1.7(8)	5.4(7)	2.5(8)	...	
C_2H	2.6(11)	2.8(11)	2.9(11)	2.8(11)	5.6(11)	1.3(11)	8.2(11)	...	
C_3	3.6(6)	4.0(6)	4.4(6)	4.7(6)	1.7(7)	2.4(6)	3.4(7)	...	
C_2^+	2.7(9)	2.7(9)	2.7(9)	2.7(9)	2.3(9)	1.6(9)	3.2(9)	...	
^{12}CO	5.4(13)	3.4(13)	3.5(13)	6.6(13)	1.1(14)	6.6(13)	3.8(14)	5(14):	3
^{13}CO	8.1(11)	5.1(11)	5.6(11)	1.1(12)	1.9(12)	1.1(12)	6.9(12)	...	
HCO^+	1.4(10)	9.5(9)	8.7(9)	1.4(10)	2.0(10)	1.8(10)	5.1(10)	...	
HCO	1.1(8)	1.1(8)	1.2(8)	1.2(8)	2.3(8)	9.2(7)	4.0(8)	...	
CO^+	7.5(9)	4.9(9)	4.9(9)	9.3(9)	6.4(9)	1.0(10)	1.5(10)	...	
N	1.2(17)	1.2(17)	1.2(17)	1.2(17)	1.2(17)	1.1(17)	1.4(17)	>8(16)	7
NH	4.9(11)	3.1(11)	3.0(11)	4.8(11)	4.4(11)	4.8(11)	1.2(12)	...	
NH_2	6.6(11)	4.3(11)	4.1(11)	6.4(11)	7.9(11)	7.2(11)	2.0(12)	...	
CN	7.0(11)	4.6(11)	4.6(11)	7.4(11)	8.4(11)	5.1(11)	2.1(12)	(1.3±0.2)(12)	8
HCN	1.2(10)	8.0(9)	7.9(9)	1.2(10)	1.8(10)	8.8(9)	4.4(10)	...	
Cℓ	1.5(14)	1.5(14)	1.5(14)	1.5(14)	1.4(14)	1.3(14)	1.7(14)	(0.4–1.4)(14)	9
$Cℓ^+$	7.4(12)	7.6(12)	5.8(12)	6.7(12)	1.4(13)	1.3(13)	1.7(13)	(0.5–1.4)(14)	9
HCℓ	2.7(11)	2.6(11)	2.6(11)	2.6(11)	1.9(11)	1.6(11)	2.4(11)	...	
$HCℓ^+$	8.6(10)	8.6(10)	8.5(10)	1.4(11)	7.2(10)	1.8(11)	8.9(10)	...	
Na	8.0(13)	8.6(13)	8.5(13)	8.0(13)	6.3(13)	3.6(13)	7.0(13)	7.9(13):	10
Na^+	2.1(15)	2.1(15)	2.0(15)	2.1(15)	2.0(15)	2.0(15)	2.5(15)	...	
NaH	1.0(10)	1.1(10)	1.0(10)	9.9(9)	6.3(9)	2.4(9)	6.9(9)	...	

[a] See Table 7 for the density and temperature structure of the models. All models have $\delta_O = 0.6$, $\delta_N = 0.6$, $\delta_D = 1.0$, $\delta_{Cl} = 0.7$, $\delta_M = \delta_{Na} = 0.45$, $\zeta_0 = 2\times10^{-16}$ s^{-1}, $k_{33} = 1\times10^{-10}$ cm^3 s^{-1}, $k_{34} = 7\times10^{-16}$ cm^3 s^{-1}, $k_{36} = 2\times10^{-10}$ cm^3 s^{-1}, and assume $[^{12}C/^{13}C] = 90$.

REFERENCES.—(1) Bohlin *et al.* 1983; (2) Jenkins, Jura, and Loewenstein 1983; (3) Frisch 1980; (4) Lambert and Danks 1986; (5) Danks, Federman, and Lambert 1984; (6) van Dishoeck and de Zeeuw 1984; (7) York *et al.* 1983; (8) Federman, Danks, and Lambert 1984; (9) Jenkins, Savage, and Spitzer 1986; (10) Crutcher 1975.

and the observed high abundance of CH^+ (cf. § VII*e*), a considerable amount of OH might be formed in these regions as well, so that the inferred rates are only upper limits; indeed, the nonmagnetic shock models (Elitzur and Watson 1980; Mitchell and Watt 1985) tend to form most of the observed OH column density in the shocked region. However, high-resolution radio observations of OH in the ζ Oph cloud (Crutcher 1979) suggest that at most 20% of the OH is formed in the shock. Recent magnetohydrodynamic models of the ζ Oph cloud (Draine 1986) also find a low percentage. For the ζ Per cloud, the evidence for a shocked zone is much weaker, so that the fraction of shocked OH is expected to be very small. For the o Per cloud, a significant fraction of the OH molecules may be formed in the shock (Pineau-des-Forêts *et al.* 1986). If these estimated shocked OH fractions are taken into account, the observations for all three lines of sight are consistent with $\zeta_0 \approx (7\pm3)\times10^{-17}$ s^{-1}, and no significant variations in ζ_0 from cloud to cloud are required.

The reaction sequence that forms OH also produces H_2O and H_2O^+; therefore, observational limits on the abundances of these species are useful in constraining some details of the oxygen chemistry. In particular, the low limit on H_2O in its

TABLE 14

CALCULATED COLUMN DENSITIES (cm^{-2}) OF SEVERAL ATOMIC AND MOLECULAR SPECIES IN MODELS OF THE σ PER CLOUD

Parameters and Species	Model[a] A	B	C	D	E	F	Observed	References
δ_G	0.85	0.82	0.82	1.10	0.95	0.70		
δ_D	1.00	1.00	1.20	1.30	1.30	1.20		
ζ_0 (s^{-1})	4.5(-16)	3.0(-16)	2.0(-16)	3.5(-16)	3.0(-16)	1.5(-16)		
O	7.1(17)	7.3(17)	7.1(17)	7.0(17)	6.9(17)	7.2(17)	(5.5±1.6)(17)	1
OH	7.0(13)	7.5(13)	7.0(13)	7.6(13)	7.2(13)	7.5(13)	(7.8±0.5)(13)	2
H_2O	5.9(11)	6.2(11)	5.8(11)	5.0(11)	5.4(11)	7.3(11)	<2.6(13)	3
OH^+	5.6(11)	1.1(12)	7.4(11)	1.4(12)	1.4(12)	1.1(12)	...	
H_2O^+	1.6(11)	2.5(11)	2.0(11)	3.0(11)	3.0(11)	2.8(11)	<3.6(13)	4
O_2	1.4(11)	1.3(11)	1.3(11)	7.7(10)	5.4(10)	1.1(11)	...	
H_3^+	5.0(14)	3.6(14)	3.7(14)	7.9(14)	8.0(14)	4.2(14)	...	
D	1.9(16)	2.1(16)	2.5(16)	2.7(16)	2.6(16)	2.4(16)	...	
HD	4.6(15)	3.0(15)	2.5(15)	2.7(15)	3.7(15)	4.5(15)	(5.9±1.5)(15)	5
H_2D^+	5.4(11)	3.7(12)	4.8(12)	9.9(12)	1.1(13)	5.2(12)	...	
C	3.4(15)	3.6(15)	3.4(15)	3.2(15)	3.3(15)	3.4(15)	(3.3–6.4)(15)	6
C^+	6.2(17)	6.1(17)	5.9(17)	7.8(17)	6.7(17)	5.1(17)	(0.1–2.0)(17)	6
CH^+	3.9(10)	3.7(10)	3.7(10)	4.6(10)	3.8(10)	2.9(10)	(6.0±0.5)(12)	7
CH	1.6(13)	1.7(13)	1.6(13)	1.1(13)	9.5(12)	1.2(13)	(1.9±0.1)(13)	8
C_2	6.7(12)	7.9(12)	7.0(12)	2.9(12)	3.2(12)	6.4(12)	(1.3±0.2)(13)	9
CH_2	1.6(13)	1.6(13)	1.6(13)	9.3(12)	9.7(12)	1.5(13)	...	
CH_3	1.1(8)	1.5(8)	1.4(8)	6.1(7)	9.1(7)	1.8(8)	...	
C_2H	6.0(11)	6.4(11)	5.8(11)	2.0(11)	2.3(11)	5.7(11)	...	
C_3	1.1(7)	1.4(7)	1.1(7)	2.5(6)	4.6(6)	1.6(7)	...	
C_2^+	3.8(9)	3.5(9)	3.4(9)	2.5(9)	1.9(9)	2.5(9)	...	
^{12}CO	1.9(14)	1.8(14)	1.6(14)	1.1(14)	1.4(14)	2.3(14)	(4.9±0.5)(14)	5
^{13}CO	2.9(12)	3.1(12)	2.8(12)	1.7(12)	2.7(12)	4.6(12)	...	
HCO^+	3.3(10)	3.9(10)	3.5(10)	3.5(10)	3.1(10)	4.1(10)	...	
HCO	1.7(8)	1.9(8)	1.7(8)	9.9(7)	1.3(8)	2.1(8)	...	
CO^+	1.5(10)	1.7(10)	1.5(10)	1.9(10)	1.6(10)	1.5(10)	<8.0(13)	10
N	8.6(16)	8.8(16)	8.6(16)	8.4(16)	8.3(16)	8.7(16)	(7.9±3.3)(16)	1
NH	9.5(11)	7.1(11)	7.1(11)	8.4(11)	8.5(11)	7.7(11)	<7.5(11)	11
NH_2	1.5(12)	1.1(12)	1.1(12)	1.1(12)	1.3(12)	1.3(12)	...	
CN	1.9(12)	1.5(12)	1.4(12)	1.1(12)	1.2(12)	1.5(12)	(1.6±0.1)(12)	12
HCN	3.5(10)	2.7(10)	2.6(10)	1.7(10)	2.1(10)	3.0(10)	...	
Cℓ	1.0(14)	1.0(14)	1.0(14)	1.0(14)	9.7(13)	1.0(14)	(2–8)(13)	13
Cℓ^+	1.4(12)	2.0(12)	1.7(12)	2.4(12)	5.0(12)	4.9(12)	(2–10)(13)	13
HCℓ	2.3(11)	2.4(11)	2.4(11)	2.0(11)	1.6(11)	1.9(11)	...	
HCℓ^+	4.2(10)	6.7(10)	5.1(10)	7.6(10)	8.7(10)	7.4(10)	...	
Na	9.2(13)	1.1(14)	1.0(14)	7.4(13)	5.9(13)	7.3(13)	(0.8–1.3)(14)	6
Na^+	2.2(15)	2.2(15)	2.1(15)	2.1(15)	2.1(15)	2.2(15)	...	
NaH	1.5(10)	1.5(10)	1.5(10)	7.6(9)	4.4(9)	7.9(9)	...	

[a] See Table 8 for the density and temperature structure of the models. All models have $\delta_O = 0.55$, $\delta_N = 0.55$, $\delta_{Cl} = 0.6$, $\delta_M = \delta_{Na} = 0.6$, $k_{33} = 1 \times 10^{-10}$ cm^3 s^{-1}, $k_{34} = 7 \times 10^{-16}$ cm^3 s^{-1}, $k_{36} = 2 \times 10^{-10}$ cm^3 s^{-1}, and assume $[^{12}C/^{13}C] = 90$.

REFERENCES.—(1) York *et al.* 1983; (2) Chaffee and Lutz 1977; (3) Smith and Snow 1979; (4) Smith, Schempp, and Federman 1984; (5) Snow 1975; (6) Snow 1976; (7) Federman 1982; (8) Jura and Meyer 1985; (9) van Dishoeck 1984; (10) Hobbs 1973*b*; (11) Crutcher and Watson 1976; (12) Meyer and Jura 1985; (13) Jenkins, Savage, and Spitzer 1986.

lowest 0_{00} level implies a total column density $N(H_2O) < 2.1 \times 10^{13}$ cm^{-2} toward ζ Oph (Snow and Smith 1981), in agreement with the present models.

Although Smith, Schempp, and Federman (1984) have placed very low limits on the equivalent widths of interstellar lines of H_2O^+ toward several stars, the corresponding limits on column densities are quite uncertain, owing to an unresolved order-of-magnitude disagreement in published lifetimes for the observed transitions (Curtis and Erman 1977; Möhlmann *et al.* 1978). Nevertheless, even the more restrictive possible limits are consistent with our calculated column densities.

Molecular oxygen, O_2, is expected to have an unobservably small column density in diffuse clouds owing to its inefficient formation (Black and Smith 1984; Smith *et al.* 1984).

d) *Deuterium-bearing Molecules*

Like the abundances of the oxygen-bearing molecules, the abundance of the HD molecule is sensitive to the cosmic-ray

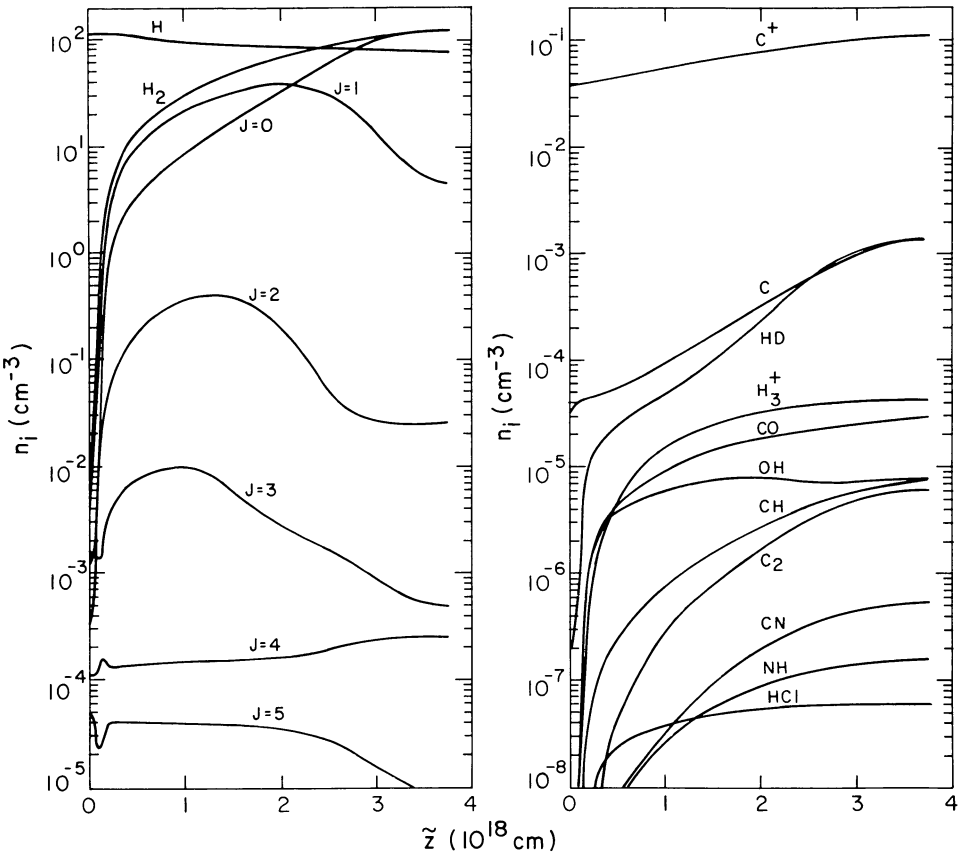

FIG. 3.—Depth dependences of the H and $H_2(J)$ concentrations (*left*), and of some atomic and molecular concentrations (*right*), in model B of the ζ Per cloud. The edge of the cloud is at $\tilde{z} = 0$.

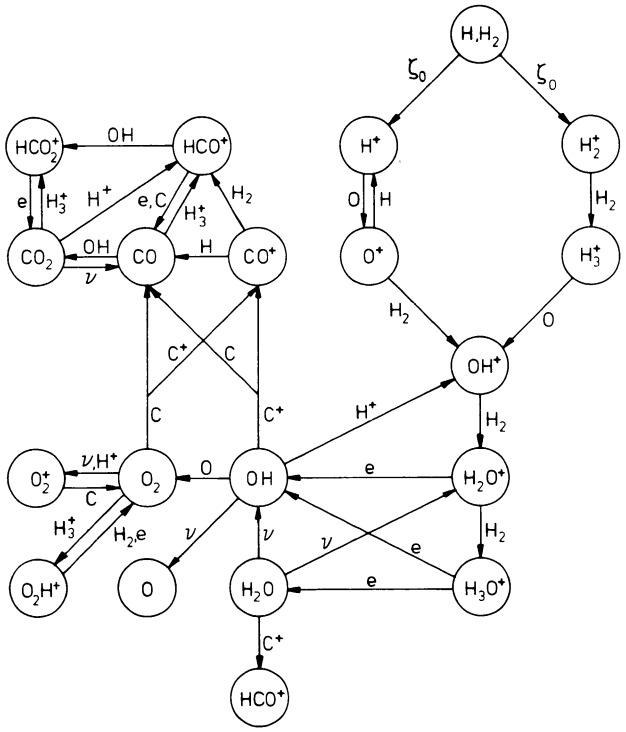

FIG. 4.—The most important reactions for the oxygen-bearing molecules included in the chemical network.

ionization rate (see Fig. 5), but it also depends on the assumed deuterium abundance (Dalgarno, Black, and Weisheit 1973; O'Donnell and Watson 1974; Barsuhn and Walmsley 1977). If the values of ζ_0 derived from the observed OH abundances are used in the models, the [D/H] ratio may be inferred from the observed HD abundances. As Tables 11–14 show, the derived [D/H] ratios are in the range $(1.0–2.0)\times 10^{-5}$ for the various clouds, consistent with previously published values of the deuterium abundance in the interstellar medium, $[D/H] = (1.5 \pm 1.0)\times 10^{-5}$ (Vidal-Madjar and Gry 1984). The models of the ζ Per cloud favor the upper part of

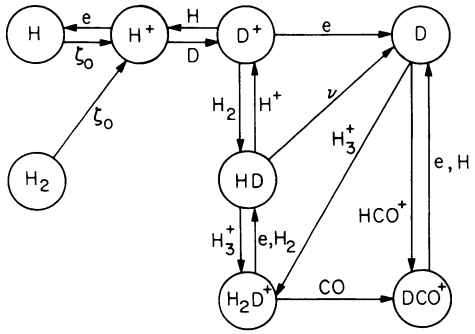

FIG. 5.—Same as Fig. 4, but for the deuterium-bearing molecules

this range, those of the ζ Oph cloud the lower part. The calculated HD column densities are very sensitive to the employed Doppler parameter in the calculation of the photodissociation rate, and the large observed column densities for the ζ Per and o Per clouds are more easily reproduced with a small velocity dispersion, $b \approx 1.2$ km s^{-1}.

The analysis of the deuterium abundance again assumes that no significant fraction of the HD molecules is formed in a shocked region. No information on shocked HD is available from the models by Draine and Katz (1986*b*) and Draine (1986), since the deuterium chemistry has not yet been included. The relative shock contributions to OH and HD will probably be fairly similar. In that case, the inferred [D/H] ratio will not differ significantly.

Tables 4–8 include the rotational populations of HD. Rotationally excited HD has been detected only toward ζ Oph by Wright and Morton (1979), who interpreted their data with a Doppler parameter $b \approx 3.8$ km s^{-1}. Crutcher and Watson (1981) have suggested that a much lower value, $b \approx 1.2$ km s^{-1}, may be more appropriate in the analysis, in which case the $J = 1/J = 0$ population ratio would be lowered by an order of magnitude. However, the line measurements with the smallest uncertainties are better fitted with the larger value of b; therefore we adopt the original results of Wright and Morton (1979). A value $b \approx 2$ km s^{-1} changes the column density ratio by a factor of only 2. The calculated populations in $J = 0$ and $J = 1$ agree well with the observed values within this factor of 2 uncertainty.

As discussed by Croswell and Dalgarno (1985), the OD/OH abundance ratio can exceed the overall deuterium abundance. In our models, where the depth dependence of this fractionation is calculated explicitly, the ratio of column densities is typically $N(\mathrm{OD})/N(\mathrm{OH}) \approx 2 \times 10^{-4} \approx 20$ [D/H], so that OD will not be detectable in such thin clouds. The column density of H_2D^+ is evidently very sensitive to the conditions in the models.

e) *Carbon-bearing Molecules*

The formation of most carbon-containing molecules is initiated by the radiative association reaction

$$C^+ + H_2 \rightarrow CH_2^+ + h\nu. \qquad (34)$$

There have been various theoretical and experimental attempts to determine this rate (Herbst 1979; Fehsenfeld 1980; Herbst 1982), and the latest computations indicate $k_{34} \approx 10^{-16}$ to 10^{-15} cm^3 s^{-1}, whereas the most recently measured upper limit is 1.5×10^{-15} cm^3 s^{-1} (Luine and Dunn 1985). The abundance of the CH molecule is closely related to the radiative association reaction (cf. Fig. 6), and its observed abundances may be used to estimate the rate. However, the uncertainty of a factor of 2 in the CH photodissociation rate (Barsuhn and Nesbet 1978; van Dishoeck 1986) limits the accuracy of the derived value. If the unshielded CH photodissociation rate is assumed to be 10^{-9} I_{UV} s^{-1}, the calculated CH abundance is consistent with the observations of the ζ Per cloud for $k_{34} \approx 7 \times 10^{-16}$ cm^3 s^{-1}. For the ζ Oph and o Per clouds, the calculated CH column densities are consistent with observations for the higher density models, but are somewhat too small in the lower density models. All models of the χ Oph cloud underestimate the CH abundance significantly, suggesting that either the strength of the ultraviolet radiation has been overestimated or the density has been underestimated. Model G with the larger total H_2 column density produces the best results.

One of the few other carbon-bearing molecules that has been detected in diffuse clouds is the C_2 molecule. Its formation is thought to proceed mainly through the reaction of CH

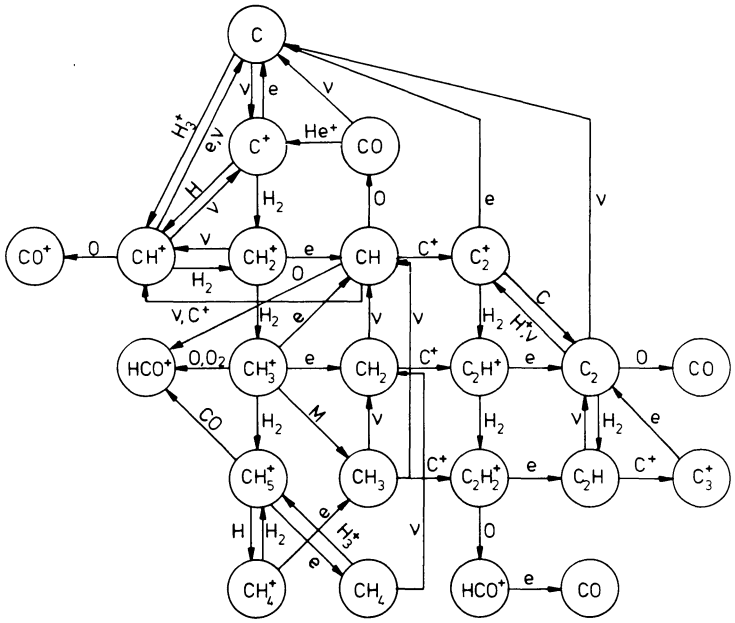

FIG. 6.—Same as Fig. 4, but for the carbon-bearing molecules. M stands for metal. Note that this network is connected to the oxygen network in Fig. 4 through HCO^+ and CO.

with C^+, followed by hydrogen abstraction reactions and dissociative recombination to form either C_2 directly, or to form C_2H, which then photodissociates to C_2 (cf. Fig. 6). The reaction $C_2 + H_2 \rightarrow C_2H + H$, suggested by van Dishoeck and Black (1982) to be important, has since been shown to have a small barrier (Pitts, Pasternack, and McDonald 1982) and is thus negligible at low temperatures. If the previously adopted ion-molecule reaction rates are used, the models produce too little C_2 by a factor of about 2–4. The value of the C_2 $A-X$ oscillator strength remains controversial: the most recent experimental determinations (Davis *et al.* 1984 and Bauer *et al.* 1985) would require a factor of 1.8 increase in all of the observed column densities tabulated here, thus increasing the discrepancy with the models. Since C_2 is destroyed in the diffuse clouds mainly by photodissociation, the simplest way to remove the discrepancy is to assume that the C_2 photodissociation rate has been overestimated by a factor of 2–3. The unshielded photodissociation rate used in this work is about 10^{-10} I_{UV} s^{-1}, based on the calculations by Pouilly *et al.* (1983). Although the uncertainty in the calculated value could be as large as a factor of 2, it is unlikely that the C_2 photodissociation rate is much smaller than 10^{-10} s^{-1} (van Dishoeck 1986). The formation of C_2 may be enhanced in several ways without affecting the CH abundance, for example, by increasing the CH_2 abundance. CH_2 also reacts rapidly with C^+ to form C_2, and its abundance may be increased by either reducing the CH_2^+ dissociative recombination rate by a small factor, or by assuming that the branching ratio to form CH_2 from the dissociative recombination reaction of CH_3^+ is 0.9 instead of 0.1. Both changes in reaction rates are not excluded by the laboratory experiments or calculations. The latter possibility was used in the calculations of the C_2 column densities listed in Tables 11–14, which are reasonably consistent with the observed values. Models with a low density, $(n_H)_0 < 200$ cm^{-3}, appear to be less favored. Measurements or upper limits on the CH_2 and C_2H abundances, which are predicted to be substantial in the clouds, would be of great interest. The C_2H radical is unusual in that it has an electronic transition ($\tilde{A}\ ^2\Pi - \tilde{X}\ ^2\Sigma$) at very long wavelengths, $\lambda \approx 2.5$ μm (Curl, Carrick, and Merer 1985). For expected line oscillator strengths of the order of $f \approx 10^{-5}$ to 10^{-4} (Reimers *et al.* 1985), the predicted column densities $N(C_2H) \approx 10^{12}$ cm^{-2} are a factor of 100 too small to be detected by infrared absorption-line techniques. Observations of thicker clouds with larger C_2H abundances may be fruitful.

The calculated CH^+ column densities are at least 2 orders of magnitude below the observed values for the four clouds, as was found in previous cloud models (BD, BHD). The reaction scheme for the CH^+ formation and destruction, shown in Figure 6, contains several uncertain rates, however. For example, it is still possible that the CH^+ dissociative recombination rate, which has been measured by Mul *et al.* (1981) to be fast at room temperature, is slow at interstellar temperatures. Nevertheless, even with the most favorable rates, the computed CH^+ abundance is still an order of magnitude below the observations.

The CH^+ molecules may be formed in an additional shocked region of the cloud (Elitzur and Watson 1980; Mitchell and Deveau 1983), although improved nonmagnetic or single-fluid shock models also seem to produce too little CH^+ by factors of 2–5 (Graff and Dalgarno 1986; Mitchell and Watt 1985; Pineau-des-Forêts *et al.* 1986). Magnetohydrodynamic models, in which the mean velocities of the ions and neutrals differ, are able to reproduce the observed CH^+ column densities without producing too many other molecules such as OH (see § VII*c*), CH, and C_2 (Draine and Katz 1986*b*; Draine 1986).

f) CO *and Its Isotopic Varieties*

Although CO accounts for only a few percent of the carbon, it is the second or third most abundant molecule in the four clouds studied here. The principal source of CO in these models derives from the reactions of C^+ with OH, and it is difficult to see how an additional, competitive source can be found in a steady state, gas-phase chemistry. CO is destroyed mainly by photodissociation at a poorly determined rate. With the current best estimate of the CO photodissociation rate (see § VI) the calculated column densities, $N(CO) \approx (1-2) \times 10^{14}$ cm^{-2}, lie factors of 2–10 below the observed results. The observed CO abundances can be reproduced only with the ad hoc assumptions that the photodissociation is controlled by the $E-X$ (0,0) line absorptions with small predissociation probabilities and that the strong shorter wavelength transitions do not predissociate. Then the photodissociation rate is decreased by an order of magnitude, and the self-shielding reaches its onset at shallower depths. However, the available experimental data on CO do not support these assumptions, and more likely indicate an even larger CO photodissociation rate than was used in this work. If the photodissociation rate is indeed at least as large as the value used in this work, some other source of CO, e.g., formation in shock-heated gas, must be found. The small inferred velocity dispersions of CO (Wannier, Penzias, and Jenkins 1982; Liszt 1979), however, argue against a large disturbed component of CO.

Our models incorporate a thorough treatment of the ^{13}C and ^{18}O isotope chemistry. The relative abundances of CO, ^{13}CO, $C^{18}O$, and $^{13}C^{18}O$ depend both on various isotope exchange reactions such as

$$^{13}C^+ + CO \rightleftarrows {}^{13}CO + C^+ \qquad (35)$$

(Watson, Anicich, and Huntress 1976) and on differing photodissociation rates as functions of depth (cf. Glassgold, Huggins, and Langer 1985). In the central zones of the diffuse cloud models, the ion-exchange reaction occurs at a rate comparable to the adopted photodissociation rate, and contributes as source and sink for both CO and ^{13}CO. Our calculations indicate that the $N(^{13}CO)/N(CO)$ ratio is enhanced by a factor of approximately 2 in relation to the overall isotope abundance ratio $[^{13}C/^{12}C]$. The measured value for the ζ Oph cloud, $N(^{13}CO)/N(CO) = 1/(55 \pm 11)$ (Wannier, Penzias, and Jenkins 1982) could then most easily be explained if the carbon isotope abundance is near its value in the solar system, $[^{13}C/^{12}C] = 1/90$. On the other hand, this would conflict with the recent accurate measurement of $N(^{12}CH^+)/N(^{13}CH^+) = 43 \pm 6$ (Hawkins, Jura, and Meyer

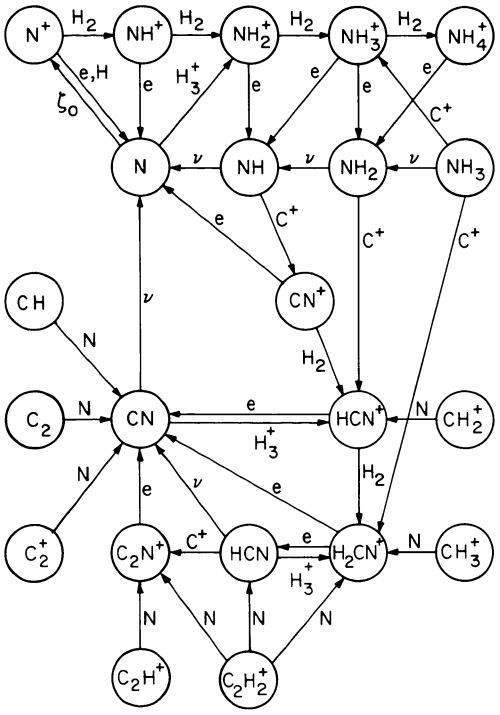

FIG. 7.—Same as Fig. 4, but for the nitrogen-bearing molecules

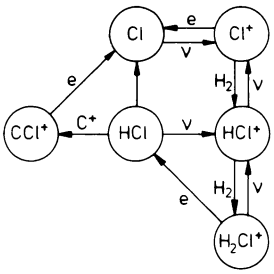

FIG. 8.—Same as Fig. 4, but for the chlorine-bearing molecules

1985), unless fractionation of carbon isotopes also occurs in CH^+. The $C^{18}O$ isotope is not fractionated in our models.

g) *Nitrogen-bearing Species*

The principal observational constraints on the nitrogen chemistry are provided by the measured amounts of CN and upper limits on NH. The reaction sequence leading to NH (see Fig. 7) is presumed to be initiated by an unusual reaction (Huntress 1977),

$$H_3^+ + N \rightarrow NH_2^+ + H, \qquad (36)$$

because the more typical proton abstraction channel is endoergic. The rate of reaction (36) is very uncertain; however, as long as the rate is not extremely small, the large abundance of H_3^+ will ensure a significant source of nitrogen-bearing molecules. The principal sources of CN in our models are dissociative recombination of HCN^+ and H_2CN^+, and an assumed reaction

$$C^+ + NH \rightarrow CN + H^+. \qquad (37)$$

The neutral-neutral reactions of CH and C_2 with N are found to be only minor sources of CN, contrary to the conclusions of Federman, Danks, and Lambert (1984). This difference results from our use of a smaller C_2 column density, a larger CN photodissociation rate, and more intense ultraviolet radiation fields. Also, the density in our models is generally less than $n_H = 500$ cm^{-3} assumed by Federman, Danks, and Lambert (1984). Reactions of carbon hydride ions and C^+ with nitrogen hydrides also lead to CN. The predicted abundances of NH and CN are thus coupled. The reaction network easily produces too much NH and too little CN compared with observations. In order to approach the observational constraints, we adopted $k_{36} = 2\times10^{-10}$ cm^3 s^{-1}, and assumed a rate of photodissociation of NH twice that of OH. In addition, NH is assumed to be a relatively unlikely product channel for $NH_m^+ + e$ reactions. The calculated CN abundances in the ζ Per and ζ Oph models are still a factor of 2 too small. It is a common feature of our models that N(NH) lies very near the current upper limits; therefore, further sensitive searches for this molecule in thick diffuse clouds are encouraged. Among the other nitrogen-bearing species, NH_2 is predicted to have a column density near 10^{12} cm^{-2}. In thicker clouds, NH_2 may also be worthy of observational investigations through its absorption lines in the visible region.

h) *Chlorine-bearing Molecules*

The low abundance of the HCl molecule in diffuse interstellar clouds has been a puzzle for some time. The chlorine chemistry, as outlined in Figure 8, has been discussed by Jura (1974) and Dalgarno *et al.* (1974), but previous models tended to produce too much HCl and too little Cl^+ (BD) compared with observations. In order to remove this discrepancy, it has been suggested that both reactions

$$Cl^+ + H_2 \rightarrow HCl^+ + H, \qquad (38)$$

$$HCl^+ + H_2 \rightarrow H_2Cl^+ + H, \qquad (39)$$

proceed with a small barrier, which would reduce their rates at low temperatures (Black and Smith 1980; Smith, Yoshino, and Parkinson 1980; Smith *et al.* 1980; Johnson, Black, and Jura 1981). Subsequent experiments (Smith and Adams 1981; Cates, Bowers, and Huntress 1981) have obtained conflicting results for reaction (38), but indicate that reaction (39) remains rapid at low temperatures. In the present scheme, we have adopted the rate of Smith and Adams (1981), $k_{38} = 1.0 \times 10^{-9}$ s^{-1}, for reaction (38), as well as a fast rate, $k_{39} = 1.3 \times 10^{-9}$ s^{-1}, for reaction (39). The fast rate of reaction (38) mainly affects the abundance of Cl^+, but not that of HCl. We also assumed that the dissociative recombination of H_2Cl^+ produces mostly H_2 and Cl, and in only 10% of the cases HCl and H, as suggested by Smith and Adams (1981). With these assumptions, and with the improved photodissociation rate of HCl, which is a factor of 3 larger than used previously (van

Dishoeck, van Hemert, and Dalgarno 1982), the calculated column density of HCl in the ζ Oph cloud is slightly below the observational upper limit (Smith, Yoshino, and Parkinson 1980; Smith *et al.* 1980). Further searches for HCl in diffuse clouds would be valuable. HCl has recently been detected in emission at submillimeter wavelengths in molecular clouds (Blake, Keene, and Phillips 1985). The abundance of Cl^+ is, with $\delta_{Cl} \approx 0.6$, an order of magnitude below observations, although in many cases there may be a significant contribution from ionized regions associated with the observed background stars. If a slow rate for reaction (38) is used, its abundance is increased by a factor of about 5.

The calculated abundances of other chlorine-bearing molecules such as CCl and HCCl are very small in the models, because the reaction of CCl^+ with H_2 is evidently slow (Blake, Anicich, and Huntress 1985; Smith and Adams 1985).

i) *Metal-bearing Species*

Elements such as magnesium and sodium exist primarily as singly charged atomic ions in diffuse clouds. In thick molecular clouds these ions may play a significant role in the overall ionization balance, because, once formed—either by photoionization or by charge transfer—they are much slower to recombine than most molecular ions. Whether such elements form gas-phase molecules readily is not known. In order to place some limits on expected abundances, we have assumed that a generic metal hydride molecule MH is formed by the recombination of M^+ on grain surfaces at a rate $10^{-16} n_H$ cm^{-3} s^{-1} per ion. Radiative association in the gas phase, $M^+ + H_2 \rightarrow MH_2^+ + h\nu$, followed by dissociative recombination, $MH_2^+ + e \rightarrow MH + H$, even if possible, is not likely to be substantially more efficient. A metal hydride like NaH is quite vulnerable to photodissociation (Kirby and Dalgarno 1978), and its maximum abundance is likely to be undetectable. It is possible to place quite stringent observational limits on the abundances of the magnesium-bearing species MgH and MgO, both of which have potential interstellar absorption lines of large oscillator strength near 5000 Å (Bernath, Black, and Brault 1985). If the rate of photodissociation of MgH (Kirby, Saxon, and Liu 1979; van Dishoeck 1986) is no higher than the rate of photoionization of Mg, then MgH could be detectable even in diffuse clouds. The few existing upper limits suggest that it is not formed efficiently.

VIII. CONCLUDING REMARKS

Techniques have been developed to compute detailed models of interstellar clouds which can be compared directly with measurable properties. A critical model analysis has been carried out to assess how accurately local parameters such as density, temperature, cosmic-ray flux, and ultraviolet radiation field can be determined from the available data on the best studied diffuse clouds.

The improved cloud models have been constructed to reproduce the observed H and $H_2(J)$ column densities for several lines of sight. The main difference from previous models is the treatment of the self-shielding in the H_2 lines, which had been underestimated substantially. The models assume that the H and H_2 abundances are in steady state, and that no strong shock has passed through the interstellar cloud. In that case, the observed H_2 rotational population and abundance may provide powerful constraints on the physical conditions in the clouds. Compared with earlier models, the new models generally have lower central densities and more intense ultraviolet radiation fields. Also, the differences in physical conditions between the individual lines of sight are considerably smaller than was previously thought for the four clouds studied in this work. The strength of the ultraviolet radiation field could be better constrained through observations of lines arising from the higher rotational levels $J > 5$, and from vibrationally excited levels. The central density is the least well determined parameter in the models. It is uncertain by a factor of about 2, owing to uncertainties in the formation rate of H_2 on grains, the population distribution of H_2 upon formation, and the turbulence in the cloud. For example, it will usually be impossible to distinguish solutions of high density and low formation rate from solutions of lower density and proportionally higher formation rate, on the basis of H_2 observations alone. New high-resolution ultraviolet observations of various species may provide more information on the appropriate Doppler parameters in the clouds. Whether significant improvements in our knowledge of the H_2 formation processes on grains will be possible in the near future remains questionable. At present, the uncertainties in this respect considerably reduce the value of the H/H_2 abundance ratio as a diagnostic probe of the density in the cloud.

It is evident that a single type of observational data cannot provide a unique description of the physical conditions in a diffuse cloud. However, if enough complementary data of high quality on other atoms and molecules can be assembled, the range of allowable parameters may be narrowed. If the collisional rates for the C_2 molecule were better determined, this molecule would be a more powerful probe of the density than the H/H_2 abundance ratio. In addition, the observational data on C_2 may be obtained conveniently from Earth. The rotational population of CO and the fine-structure populations of the C, C^+, and O atoms are sensitive to the density as well, but observational data are still limited or uncertain. Ultraviolet spectra of CO with sufficient resolution to show the rotational structure of the bands will be of great value. For CO column densities larger than 10^{15} cm^{-2}, its population distribution may also be observed by infrared absorption-line techniques (Black and Willner 1984). Sensitive observations of C^+ in the weak intersystem transition near 2325 Å are needed.

For the ζ Per and χ Oph clouds, the various diagnostic species indicate densities that are consistent with the analysis of the H and $H_2(J)$ abundances, but the uncertainties both in the molecular parameters and in the observational data do not allow further constraints. For the ζ Oph and o Per clouds, the C_2 and CO rotational excitation indicate lower densities than the H/H_2 abundance ratio. Compared with earlier models, it is encouraging to note that the discrepancies between the various diagnostics have been reduced from an order of magnitude to a factor of about 2. Several possible explanations for the remaining differences for these two clouds have been presented in § V*g*.

The four clouds studied in this work are the only clouds for which extensive observations for both C_2 and H_2 are available. The fact that the observed C_2 excitation is remarkably similar in the four directions, whereas the observed H_2 excitation differs considerably, may provide an important clue to the structure of diffuse clouds, and to the presence of interstellar shocks. It is interesting to note that magnetohydrodynamic shock models have now been constructed which, together with the quiescent cloud models, can reproduce the observed H_2 rotational populations quite well. If such a shocked region is taken into account, the quiescent parts of the four clouds studied in this work may be similar to the present models of the ζ Per cloud. Sensitive searches for vibrationally excited H_2 are likely to be fruitful and will be useful in constraining further the contribution of the ultraviolet pumping in the quiescent region to the excitation of H_2. Further combined C_2 and H_2 observations, for clouds with both smaller and larger total visual extinctions, will be very valuable.

The polytropic models, although convenient, may not provide realistic temperature and density gradients in the outer parts of the cloud. The gradients in the temperature and density are constrained in the present models by the observed column densities of H_2 in $J = 2$ and $J = 3$. They could be better determined if both the observed column densities for these levels and the H–H_2 collisional rates were better known. In principal, the requirement of thermal balance, which has been neglected in the present models, provides the relation between the temperature and the density as a function of depth into the cloud. Calculations of the heating and cooling processes *a posteriori* in our models indicate that in the center of the cloud the corresponding rates balance, within the factor of 2 uncertainty in the processes. However, in the outer part of the models the cooling rates exceed the presently known heating sources by a factor of about 5. Also, the C fine-structure excitation indicates that the density and temperature have been overestimated in the outer regions of some of the clouds. Such low boundary densities with relatively low boundary temperatures, and a high central density and low central temperature cannot be represented by the present polytropic structures. Nevertheless, the polytropic models provide a reasonable approximation to the temperature and density variations with depth for the major part of the cloud. If the temperature in the outer part of the cloud were reduced, the calculated H_2 populations in $J = 2$ and $J = 3$ would be low compared with observations for most of the clouds studied in this work. Unless the observed values have been overestimated or the collisional rates underestimated, this would be another indication that an additional heated or shocked region needs to be present in the cloud.

The abundances of the oxygen-bearing molecules are considerably reduced in the new models, as a result of the reduction of both the warm zone and the H–H_2 transition region compared with earlier models, the enhanced strength of the interstellar radiation field, and increased photodissociation rates. If most of the OH molecules are formed in the quiescent clouds, the calculations of the OH abundance suggest that an increase in the cosmic-ray ionization rate is needed to bring the models into harmony with observations. The magnitude of the increase depends on the rate of the H_3^+ dissociative recombination reaction, which is uncertain. If this rate is indeed very low at interstellar temperatures, only a modest increase in the cosmic-ray ionization rate to $\zeta_0 \approx 7 \times 10^{-17}\ s^{-1}$ is needed. If part of the OH molecules are formed in a shocked region of the cloud, no significant variations in the cosmic-ray ionization rate from cloud to cloud are required to reproduce the OH observations for the four lines of sight. The observed abundances of the HD molecule are found to be consistent with the average deuterium abundance in the interstellar medium. The observed abundances of other simple molecules, such as CH, C_2, and HCl, can be reproduced by reasonable, although ad hoc, adjustments of the molecular reaction rates. Still, it is unfortunate that the lingering uncertainties in some of the most crucial rates, such as the radiative association rate for $C^+ + H_2$, several photodissociation rates, and the branching ratios for dissociative recombination, preclude at present the use of, e.g., the CH and C_2 abundances as indicators of the density in the cloud. The chemical scheme leading to the formation of the nitrogen-bearing molecules is still subject to great uncertainties, and it is difficult to satisfy simultaneously the low upper limit on the NH abundance and the relatively large CN abundance. The abundance determination of the ubiquitous CO molecule has been shown to be much more complicated than thought previously if the photodissociation of this molecule is dominated by line absorption. It is difficult to understand the large abundance of CO in diffuse clouds if the photodissociation of CO is as rapid as suggested by experiments. Since the ^{12}CO abundance influences that of ^{13}CO in a complicated way, care must be taken to interpret the observed $^{12}CO/^{13}CO$ abundance ratios.

Apart from further observational and theoretical studies of the present four diffuse clouds, it will be interesting to perform a similarly extensive study of denser clouds with $A_V^{tot} \approx 3$ mag. These clouds form the bridge between the classical diffuse and dark interstellar clouds, and they may reveal new insights into the proposed molecular formation schemes. Also, the study of fractionation processes in these clouds will be of great interest. Much can still be learned about the physical structures of interstellar clouds and the formation of molecules by a combination of observational, theoretical, and experimental studies of the smallest such molecules.

The authors are indebted to A. Dalgarno, H. J. Habing, M. C. van Hemert, T. de Jong, and P. T. de Zeeuw for comments on an earlier version of the manuscript, and to B. T. Draine for useful discussions concerning shock models. They thank J. Schaefer, R. Schinke, and B. T. Draine for communicating their results prior to publication. The hospitality of the Institute for Advanced Study and the Princeton University Observatory, where part of this work was performed, and support through the Visiting Scientists Program of the Smithsonian Institution are gratefully acknowledged. Partial support was provided by the National Aeronautics and Space Administration through Theoretical Astrophysics grant NAGW-763 to the University of Arizona.

REFERENCES

Aannestad, P. A., and Field, G. B. 1973, *Ap. J.* (*Letters*), **186**, L29.
Adams, N. G., and Smith, D. 1986, in *IAU Symposium 120, Astrochemistry*, ed. M. S. Vardya and S. P. Tarafdar (Dordrecht: Reidel), in press.
Albritton, D. L. 1976, quoted in R. L. Kurucz, *Smithsonian Ap. Obs. Spec. Rept.*, No. 374.
Allen, M., and Robinson, G. W. 1976, *Ap. J.*, **207**, 745.
Allison, A. C., and Dalgarno, A. 1967, *Proc. Phys. Soc. London*, **90**, 609.
_____. 1970, *Atomic Data*, **1**, 289.
Bally, J., and Langer, W. D. 1982, *Ap. J.*, **255**, 143; **261**, 747.
Barsuhn, J., and Nesbet, R. K. 1978, *J. Chem. Phys.*, **68**, 2783.
Barsuhn, J., and Walmsley, C. M. 1977, *Astr. Ap.*, **54**, 345.
Bauer, W., Becker, K. H., Hubrich, C., Meuser, R., and Wildt, J. 1985, *Ap. J.*, **296**, 758.
Bernath, P. F., Black, J. H., and Brault, J. W. 1985, *Ap. J.*, **298**, 375.
Blaauw, A. 1961, *Bull. Astr. Inst. Netherlands*, **15**, 265.
Black, J. H., and Dalgarno, A. 1973*a*, *Ap. J.* (*Letters*), **184**, L101.
_____. 1973*b*, *Ap. Letters*, **15**, 79.
_____. 1976, *Ap. J.*, **203**, 132.
_____. 1977, *Ap. J. Suppl.*, **34**, 405 (BD).
Black, J. H., Hartquist, T. W., and Dalgarno, A. 1978, *Ap. J.*, **224**, 448 (BHD).
Black, J. H., and Smith, P. L. 1980, in *IAU Symposium 87, Interstellar Molecules*, ed. B. H. Andrew (Dordrecht: Reidel), p. 271.
_____. 1984, *Ap. J.*, **277**, 562.
Black, J. H., and van Dishoeck, E. F. 1986, in preparation.
Black, J. H., and Willner, S. P. 1984, *Ap. J.*, **279**, 673.
Blake, G. A., Anicich, V. G., and Huntress, W. T. 1986, *Ap. J.*, **300**, 415.
Blake, G. A., Keene, J., and Phillips, T. G. 1985, *Ap. J.*, **295**, 501.
Bohlin, R. C., Hill, J. K., Jenkins, E. B., Savage, B. D., Snow, T. P., Spitzer, L., and York, D. G. 1983, *Ap. J. Suppl.*, **51**, 277.
Boland, W., and de Jong, T. 1984, *Astr. Ap.*, **134**, 87.
Brzozowski, J., Bunker, P., Elander, N., and Erman, P. 1976, *Ap. J.*, **207**, 414.
Burke, P. G., and Taylor, K. T. 1979, *J. Phys. B*, **12**, 2971.
Cates, R. D., Bowers, M. T., and Huntress, W. T. 1981, *J. Phys. Chem.*, **85**, 313.
Chaffee, F. H. 1974, *Ap. J*, **189**, 427.
Chaffee, F. H., and Lutz, B. L. 1977, *Ap. J.*, **213**, 394.
Chaffee, F. H., Lutz, B. L., Black, J. H., Vanden Bout, P. A., and Snell, R. L. 1980, *Ap. J.*, **236**, 474.
Chambaud, G., Launay, J. M., Levy, B., Millie, P., Roueff, E., and Tran Minh, F. 1980, *J. Phys. B*, **13**, 4205.
Chlewicki, G., and Greenberg, J. M. 1984*a*, *M.N.R.A.S.*, **210**, 791.
_____. 1984*b*, *M.N.R.A.S.*, **211**, 719.
Chu, Y.-H., and Watson, W. D. 1983, *Ap. J.*, **267**, 151.
Clavel, J., Viala, Y. P., and Bel, N. 1978, *Astr. Ap.*, **65**, 435.
Clegg, R. E. S., and Lambert, D. L. 1982, *M.N.R.A.S.*, **201**, 723.
Cooper, D. M., and Langhoff, S. R. 1981, *J. Chem. Phys.*, **74**, 1200.
Cravens, T. E., and Dalgarno, A. 1978, *Ap. J.*, **219**, 750.
Croswell, K., and Dalgarno, A. 1985, *Ap. J.*, **289**, 618.
Crutcher, R. M. 1975, *Ap. J.*, **202**, 634.
_____. 1979, *Ap. J.* (*Letters*), **231**, L151.
Crutcher, R. M., and Watson, W. D. 1976, *Ap. J.*, **209**, 778.
_____. 1981, *Ap. J.*, **244**, 855 (CW).
Curl, R. F., Carrick, P. G., and Merer, A. J. 1985, *J. Chem. Phys.*, **82**, 3479.
Curtis, L. J., and Erman, P. 1977, *J. Opt. Soc. Am.*, **67**, 1218.
Dabrowski, I. 1984, *Canadian J. Phys.*, **62**, 1639.
Dalgarno, A., and Black, J. H. 1976, *Rept. Progr. Phys.*, **39**, 573.
Dalgarno, A., Black, J. H., and Weisheit, J. C. 1973, *Ap. Letters*, **14**, 77.
Dalgarno, A., de Jong, T., Oppenheimer, M., and Black, J. H. 1974, *Ap. J.* (*Letters*), **192**, L37.
Dalgarno, A., and Stephens, T. L. 1970, *Ap. J.* (*Letters*), **160**, L107.
Danks, A. C., Federman, S. R., and Lambert, D. L. 1984, *Astr. Ap.*, **130**, 62.
Danks, A. C., and Lambert, D. L. 1983, *Astr. Ap.*, **124**, 188.
Davis, S. P., Smith, W. H., Brault, J. W., Pecyner, R., and Wagner, J. 1984, *Ap. J.*, **287**, 455.
de Boer, K. S. 1979, *Ap. J.*, **229**, 132.
_____. 1981, *Ap. J.*, **244**, 848.
de Boer, K. S., and Morton, D. C. 1974, *Astr. Ap.*, **37**, 305.
_____. 1979, *Astr. Ap.*, **71**, 141.
de Jong, T. 1980, in *Proc. 21st Liège Colloquium, Les Spectres des Molécules simples au laboratoire et en astrophysique* (Liège: Institut d'Astrophysique, Université de Liège), p. 117.
de Jong, T., Dalgarno, A., and Boland, W. 1980, *Astr. Ap.*, **91**, 68.
Diffenderfer, R. N., Yarkony, D. R., and Dagdigian, P. J. 1983, *J. Quant. Spectrosc. Rad. Transf.*, **29**, 329.
Draine, B. T. 1978, *Ap. J. Suppl.*, **36**, 595.
_____. 1986, *Ap. J.*, in press.
Draine, B. T., and Katz, N. S., 1986*a*, *Ap. J.*, **306**, 655.
_____. 1986*b*, *Ap. J.*, in press.
Draine, B. T., and Lee, H. M. 1984, *Ap. J.*, **285**, 89.
Elitzur, M., and Watson, W. D. 1980, *Ap. J.*, **236**, 172.
Fairchild, P. W., Smith, G. P., Crosley, D. K., and Jeffries, J. B. 1984, *Chem. Phys. Letters*, **107**, 181.
Federman, S. R. 1982, *Ap. J.*, **257**, 125.
Federman, S. R., Danks, A. C., and Lambert, D. L. 1984, *Ap. J.*, **287**, 219.
Federman, S. R., and Glassgold, A. E. 1980, *Astr. Ap.*, **89**, 113.
Federman, S. R., Glassgold, A. E., and Kwan, J. 1979, *Ap. J.*, **227**, 466.
Fehsenfeld, F. C. 1980, in *IAU Symposium 87, Interstellar Molecules*, ed. B. H. Andrew (Dordrecht: Reidel), p. 291.
Field, G. B., Somerville, W. B., and Dressler, K. 1966, *Ann. Rev. Astr. Ap.*, **4**, 207.
Field, R. W., Benoist d'Azy, O., Lavollée, M., Lopez-Delgado, R., and Tramer, A. 1983, *J. Chem. Phys.*, **78**, 2838.
Flannery, B. P., Roberge, W., and Rybicki, G. B. 1980, *Ap. J.*, **236**, 598.
Flower, D. R., and Launay, J. M. 1977, *J. Phys. B.*, **10**, 3673.
_____. 1985, *M.N.R.A.S.*, **214**, 271.
Fock, J.-H., Gürtler, P., and Koch, E. E. 1980, *Chem. Phys.*, **47**, 87.
Frisch, P. C. 1979, *Ap. J.*, **227**, 474.
_____. 1980, *Ap. J.*, **241**, 697.
Gerlich, D., and Bohli, H. J. 1981, in *Abstrs. European Conf. on Atomic Physics*, ed. J. Kowalski, G. zu Putlitz, and H. G. Weber (Heidelberg: European Physical Society), **5A** (Ser. II), 930.
Gerola, H., and Glassgold, A. E. 1978, *Ap. J. Suppl.*, **37**, 1.
Glassgold, A. E., Huggins, P. J., and Langer, W. D. 1985, *Ap. J.*, **290**, 615.
Glassgold, A. E., and Langer, W. D. 1974, *Ap. J.*, **193**, 73.
_____. 1976, *Ap. J.*, **206**, 85.
Graedel, T. E., Langer, W. D., and Frerking, M. A. 1982, *Ap. J. Suppl.*, **48**, 321.
Graff, M., and Dalgarno, A. 1986, private communication.
Green, S., and Chapman, S. 1978, *Ap. J. Suppl.*, **37**, 169.
Green, S., and Truhlar, D. G. 1979, *Ap. J.* (*Letters*), **231**, L101.
Harrison, E. R., and Lake, R. G. 1972, *Ap. J.*, **171**, 323.
Hartquist, T. W., Black, J. H., and Dalgarno, A. 1978, *M.N.R.A.S.*, **185**, 643.
Hawkins, I., Jura, M., and Meyer, D. M. 1985, *Ap. J.* (*Letters*), **294**, L131.
Hayashi, M., Hasegawa, T., Gatley, I., Garden, R., and Kaifu, N. 1985, *M.N.R.A.S.*, **215**, 31P.
Hayes, M. A., and Nussbaumer, H. 1984*a*, *Astr. Ap.*, **134**, 193.
_____. 1984*b*, *Astr. Ap.*, **139**, 233.
Henning, K. 1981, *Astr. Ap. Suppl.*, **44**, 405.
Herbig, G. H. 1968, *Zs. Ap.*, **68**, 243.
Herbst, E. 1979, *J. Chem. Phys.*, **70**, 2201.
_____. 1982, *Ap. J.*, **252**, 810.
Herbst, E., and Klemperer, W. 1973, *Ap. J.*, **185**, 505.
Hibbert, A., Dufton, P. L., and Keenan, F. P. 1985, *M.N.R.A.S.*, **213**, 721.
Hobbs, L. M. 1973*a*, *Ap. J.*, **181**, 79.
_____. 1973*b*, *Ap. J.*, **181**, 795.
_____. 1978, *Ap. J. Suppl.*, **38**, 129.
_____. 1979, *Ap. J.* (*Letters*), **232**, L135.
_____. 1981, *Ap. J.*, **243**, 485.
Hobbs, L. M., and Campbell, B. 1982, *Ap. J.*, **254**, 108.
Hobbs, L. M., York, D. G., and Oegerle, W. 1982, *Ap. J.* (*Letters*), **252**, L21.
Hofzumahaus, A., and Stuhl, F. 1985, *J. Chem. Phys.*, **82**, 3152.
Holland, R. F., and Maier, W. B. 1972, *J. Chem. Phys.*, **56**, 5229.
Hollenbach, D., and Salpeter, E. E. 1970, *J. Chem. Phys.*, **53**, 79.
_____. 1971, *Ap. J.*, **163**, 155.
Hollenbach, D. J., Werner, M. W., and Salpeter, E. E. 1971, *Ap. J.*, **163**, 165.
Hunter, D. A., and Watson, W. D. 1978, *Ap. J.*, **226**, 477.
Huntress, W. T. 1977, *Ap. J. Suppl.*, **33**, 495.
Iglesias, E. 1977, *Ap. J.*, **218**, 697.
Jenkins, E. B., Jura, M., and Loewenstein, M. 1983, *Ap. J.*, **270**, 88.
Jenkins, E. B., Savage, B. D., and Spitzer, L. 1986, *Ap. J.*, **301**, 355.
Jenkins, E. B., and Shaya, E. J. 1979, *Ap. J.*, **231**, 55.
Johnson, C., Black, J. H., and Jura, M. 1981, private communication.
Jura, M. 1974, *Ap. J.* (*Letters*), **190**, L33.
_____. 1975, *Ap. J.*, **197**, 581.
Jura, M., and Meyer, D. M. 1985, *Ap. J.*, **294**, 238.
Kirby, K., and Dalgarno, A. 1978, *Ap. J.*, **224**, 444.
Kirby, K., Roberge, W. G., Saxon, R. P., and Liu, B. 1980, *Ap. J.*, **239**, 855.
Kirby, K., Saxon, R. P., and Liu, B. 1979, *Ap. J.*, **231**, 637.

Lambert, D. L., and Danks, A. C. 1986, *Ap. J.*, **303**, 401.
Larsson, M., and Siegbahn, P. E. M. 1983*a*, *J. Chem. Phys.*, **79**, 2270.
_____. 1983*b*, *Chem. Phys.*, **76**, 175.
Larsson, M., Siegbahn, P. E. M., and Ågren, H. 1983, *Ap. J.*, **272**, 369.
Launay, J. M., and Roueff, E. 1977*a*, *Astr. Ap.*, **56**, 289.
_____. 1977*b*, *J. Phys. B*, **10**, 879.
Lavendy, H., Gandara, G., and Robbe, J. M. 1984, *J. Molec. Spectrosc.*, **106**, 395.
Le Dourneuf, M., and Nesbet, R. K. 1976, *J. Phys. B*, **9**, L241.
Lee, L. C. 1984, *Ap. J.*, **282**, 172.
Lee, L. C., and Guest, J. A. 1981, *J. Phys. B*, **14**, 3415.
Leonas, V. B., and Pjarnpuu, A. A. 1981, *Soviet Astr. Letters*, **7**, 19.
Liszt, H. S. 1979, *Ap. J.* (*Letters*), **233**, L147.
_____. 1981, *Ap. J.* (*Letters*), **246**, L147.
Lugger, P. M., York, D. G., Blanchard, R., and Morton, D. C. 1978, *Ap. J.*, **224**, 1059.
Luine, J. A., and Dunn, G. H. 1985, *Ap. J.* (*Letters*), **299**, L67.
Mahan, B. H., and O'Keefe, A. 1981, *Ap. J.*, **248**, 1209.
Mann, A. P. C., and Williams, D. A. 1985, *M.N.R.A.S.*, **214**, 279.
Mathis, J. S., Mezger, P. G., and Panagia, N. 1983, *Astr. Ap.*, **128**, 212.
Mendoza, C. 1983, in *IAU Symposium 103*, *Planetary Nebulae*, ed. D. R. Flower (Dordrecht: Reidel), p. 143.
Meyer, D. M., and Jura, M. 1985, *Ap. J.*, **297**, 119.
Michels, H. H., and Hobbs, R. H. 1984, *Ap. J.* (*Letters*), **286**, L27.
Millar, T. J., and Freeman, A. 1984, *M.N.R.A.S.*, **207**, 405.
_____. 1984, *M.N.R.A.S.*, **207**, 425.
Mitchell, G. F., and Deveau, T. J. 1983, *Ap. J.*, **266**, 646.
Mitchell, G. F., Ginsburg, J. L, and Kuntz, P. J. 1978, *Ap. J. Suppl.*, **38**, 39.
Mitchell, G. F., and Watt, G. D. 1985, *Astr. Ap.*, **151**, 121.
Möhlmann, G. R., Bhutani, K. K., de Heer, F. J., and Tsurubuchi, S. 1978, *Chem. Phys.*, **31**, 273.
Morton, D. C. 1974, *Ap. J.* (*Letters*), **193**, L35.
_____. 1975, *Ap. J.*, **197**, 85.
Mul, P. M., Mitchell, J. B. A., D'Angelo, V. S., Defrance, P., McGowan, J. W., and Froelich, H. R. 1981, *J. Phys. B*, **14**, 1353.
Nishimura, S., and Takayanagi, K. 1969, *Pub. Astr. Soc. Japan*, **21**, 111.
Nussbaumer, H., and Rusca, C. 1979, *Astr. Ap.*, **72**, 129.
Nussbaumer, H., and Storey, P. J. 1981, *Astr. Ap.*, **96**, 91.
O'Donnell, E. J., and Watson, W. D. 1974, *Ap. J.*, **191**, 89.
Oka, T. 1981, *Phil. Trans. Roy. Soc. London*, *A*, **303**, 543.
Pineau-des-Forêts, G., Flower, D. R., Hartquist, T. W., and Dalgarno, A. 1986, *M.N.R.A.S.*, submitted.
Pitts, W. M., Pasternack, L., and McDonald, J. R. 1982, *Chem. Phys.*, **68**, 417.
Pouilly, B., Robbe, J. M., Schamps, J., and Roueff, E. 1983, *J. Phys. B*, **16**, 437.
Pradhan, A. K., and Saraph, H. E. 1977, *J. Phys. B*, **10**, 3365.
Prasad, S. S., and Huntress, W. T. 1980, *Ap. J. Suppl.*, **43**, 1.
Reimers, J. R., Wilson, K. R., Heller, E. J., and Langhoff, S. R. 1985, *J. Chem. Phys.*, **82**, 5064.
Roberge, W. G. 1981, Ph.D. thesis, Harvard University.
Roberge, W. G., Dalgarno, A., and Flannery, B. P. 1981, *Ap. J.*, **243**, 817.
Rostas, F. 1985, private communication.
Roueff, E. 1981, *Astr. Ap.*, **99**, 394; also extensive preliminary version.
Sancisi, R., Goss, W. M., Anderson, C., Johansson, L. E. B., and Winnberg, A. 1974, *Astr. Ap.*, **35**, 445.
Savage, B. D., Bohlin, R. C., Drake, J. F., and Budich, W. 1977, *Ap. J.*, **216**, 291.
Schaefer, J. 1985, private communication.
Schinke, R., Engel, V., Buck, U., Meyer, H., and Diercksen, G. H. F. 1985, *Ap. J.*, **299**, 939.
Shu, F. H., Milione, V., Gebel, W., Yuan, C., Goldsmith, D. W., and Roberts, W. W. 1972, *Ap. J.*, **173**, 557.
Shull, J. M. 1978, *Ap. J.*, **219**, 877.
Smith, A. M., Krishna Swamy, K. S., and Stecher, T. P. 1978, *Ap. J.*, **220**, 138.
Smith, D., and Adams, N. G. 1981, *M.N.R.A.S.*, **197**, 377.
_____. 1984, *Ap. J.* (*Letters*), **284**, L13.
_____. 1985, *Ap. J.*, **298**, 827.
Smith, G. P., and Crosley, D. R. 1981, in *Proc. 18th Internat. Symposium on Combustion* (Pittsburgh: Combustion Institute), p. 1511.
Smith, P. L., Griesinger, H. E., Black, J. H., Yoshino, K., and Freeman, D. E. 1984, *Ap. J.*, **277**, 569.
Smith, P. L., Yoshino, K., and Parkinson, W. H. 1980, in *IAU Symposium 87*, *Interstellar Molecules*, ed. B. H. Andrew (Dordrecht: Reidel), p. 269.
Smith, P. L., Yoshino, K., Black, J. H., and Parkinson, W. H. 1980, *Ap. J.*, **238**, 874.
Smith, P. L., Yoshino, K., Griesinger, H. E., and Black, J. H. 1981, *Ap. J.*, **250**, 166.
Smith, W. H. 1978, *Phys. Scripta*, **17**, 513.
Smith, W. H., Schempp, W. V., and Federman, S. R. 1984, *Ap. J.*, **277**, 196.
Smith, W. H., and Snow, T. P. 1979, *Ap. J.*, **228**, 435.
Snow, T. P. 1975, *Ap. J.* (*Letters*), **201**, L21.
_____. 1976, *Ap. J.*, **204**, 759.
_____. 1977, *Ap. J.*, **216**, 724.
_____. 1983, *Ap. J.* (*Letters*), **269**, L57.
Snow, T. P., and Smith, W. H. 1977, *Ap. J.*, **217**, 68.
_____. 1981, *Ap. J.*, **250**, 163.
Solomon, P. M., and Klemperer, W. 1972, *Ap. J.*, **178**, 389.
Spitzer, L. 1942, *Ap. J.*, **95**, 329.
_____. 1978, *Physical Processes in the Interstellar Medium* (New York: Wiley Interscience).
Spitzer, L., and Cochran, W. D. 1973, *Ap. J.* (*Letters*), **186**, L23.
Spitzer, L., Cochran, W. D., and Hirschfeld, A. 1974, *Ap. J. Suppl.*, **28**, 373.
Spitzer, L., and Jenkins, E. B. 1975, *Ann. Rev. Astr. Ap.*, **13**, 133.
Spitzer, L., and Morton, W. A. 1976, *Ap. J.*, **204**, 731.
Spitzer, L., and Zweibel, E. G. 1974, *Ap. J.* (*Letters*), **191**, L127.
Stecher, T. P., and Williams, D. A. 1967, *Ap. J.* (*Letters*), **149**, L29.
Stephens, T. L., and Dalgarno, A. 1972, *J. Quant. Spectrosc. Rad. Transf.*, **12**, 569.
Tielens, A. G. G. M., and Hollenbach, D. 1985*a*, *Ap. J.*, **291**, 722.
_____. 1985*b*, *Ap. J.*, **291**, 747.
Turner, J., Kirby-Docken, K., and Dalgarno, A. 1977, *Ap. J. Suppl.*, **35**, 281.
van de Hulst, H. C. 1949, *Rech. Astr. Obs. Utrecht*, **11** (Part 2), 1.
van Dishoeck, E. F. 1983, *Chem. Phys.*, **77**, 277.
_____. 1984, Ph.D. thesis, University of Leiden.
_____. 1986, in *IAU Symposium 120*, *Astrochemistry*, ed. M. S. Vardya and S. P. Tarafdar (Dordrecht: Reidel), in press.
van Dishoeck, E. F., and Black, J. H. 1982, *Ap. J.*, **258**, 533.
_____. 1984, *Messenger*, **38**, 16.
_____. 1986*a*, *Ap. J.*, **307**, 332.
_____. 1986*b*, in preparation.
van Dishoeck, E. F., and Dalgarno, A. 1983, *J. Chem. Phys.*, **79**, 873.
_____. 1984, *Ap. J*, **277**, 576.
van Dishoeck, E. F., and de Zeeuw, T. 1984, *M.N.R.A.S.*, **206**, 383.
van Dishoeck, E. F., van Hemert, M. C., and Dalgarno, A. 1982, *J. Chem. Phys.*, **77**, 3693.
Viala, Y. P. 1972, *C.R. Acad. Sci., Paris*, **275B**, 117.
Viala, Y. P., and Horedt, Gp. 1974*a*, *Astr. Ap.*, **33**, 195.
_____. 1974*b*, *Astr. Ap. Suppl.*, **16**, 173.
Viala, Y. P., and Walmsley, C. M. 1976, *Astr. Ap.*, **50**, 1.
Vidal-Madjar, A., and Gry, C. 1984, *Astr. Ap.*, **138**, 285.
Villinger, H., Henchman, M. J., and Lindinger, W. 1982, *J. Chem. Phys.*, **76**, 1590.
Wang, C. C., and Huang, C. M. 1980, *Phys. Rev. A*, **21**, 1235.
Wannier, P. G., Penzias, A. A., and Jenkins, E. B. 1982, *Ap. J.*, **254**, 100.
Watson, W. D. 1974, *Ap. J.*, **188**, 35.
_____. 1976, *Rev. Mod. Phys.*, **48**, 413.
_____. 1978, *Ann. Rev. Astr. Ap.*, **16**, 585.
Watson, W. D., Anicich, V. G., and Huntress, W. J. 1976, *Ap. J.* (*Letters*), **205**, L165.
Watt, G. D. 1983, *M.N.R.A.S.*, **205**, 321.
Wolken, G., Miller, W. H., and Karplus, M. 1972, *J. Chem. Phys.*, **56**, 4930.
Wright, E. L., and Morton, D. C. 1979, *Ap. J.*, **227**, 483.
York, D. G., Spitzer, L., Bohlin, R. C., Hill, J., Jenkins, E. B., Savage, B. D., and Snow, T. P. 1983, *Ap. J.* (*Letters*), **266**, L55.

J. H. BLACK: Steward Observatory, University of Arizona, Tucson, AZ 85721

E. F. VAN DISHOECK: Center for Astrophysics, 60 Garden Street, Cambridge, MA 02138